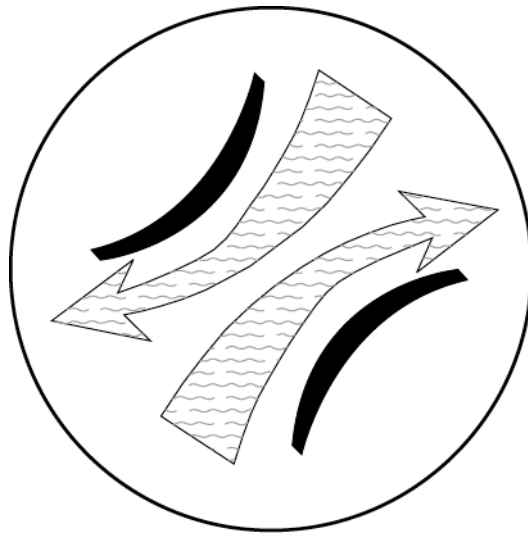


**Short-term climate variability  
in the North Atlantic  
during the onset of northern hemisphere glaciation  
and the final closure of the Panamanian seaways,  
3.3-2.5 Ma.**



**Dissertation  
zur Erlangung des Doktorgrades  
der Mathematisch-Naturwissenschaftlichen Fakultät  
der Christian-Albrechts-Universität  
zu Kiel**

Vorgelegt von

**Gretta Bartoli**

**Kiel 2005**

Referent: Prof. Emer. Michael Sarnthein

Korreferentin: Dr. Habil. Mara Weinelt

Tag der Disputation: 6 Juli 2005

Zum Druck genehmigt: Kiel, den

Der Dekan:

## Contents

Abstract	5
Kurzfassung	7
Acknowledgements	9
Chapter 1: Objectives and Oceanographic setting	11
Chapter 2: Methods and Strategy	15
Chapter 3: Age models	21
Chapter 4: <i>Final closure of the Isthmus of Panama and the onset of northern hemisphere glaciation</i>	23
Chapter 5: <i>Late Pliocene millennial-scale climate variability in the northern North Atlantic prior and after the onset of northern hemisphere glaciation</i>	35
Chapter 6: <i>Gateway-controlled decline of primary production in the northern North Atlantic at 2.74 Ma ?</i>	55
Chapter 7: IOPD Expedition 303 Preliminary Report. North Atlantic Climate. <i>Ice sheet-ocean atmosphere interactions on millennial timescales during the Neogene-Quaternary using a paleointensity-assisted chronology for the North Atlantic. 25 September-16 November 2004, Shipboard Scientific Party</i>	71
Chapter 8: <i>IODP Expedition 303: Northern Atlantic Climate I</i>	109
Chapter 9: Summary and Conclusions	115
Appendices: Curriculum and “Eidesstattliche Erklärung”	117



## Abstract

Long- and short-term Late Pliocene climate variations were studied at North Atlantic Sites (S.) ODP 984 and DSDP 609, supplemented by published records from S. 907 and S. 610. Foraminiferal  $\delta^{18}\text{O}$  records provided the base for stable-isotope stratigraphy. Deepwater and sea surface temperatures (SST) were reconstructed from Mg/Ca values of benthic and planktic foraminifera. Epibenthic  $\delta^{13}\text{C}$  variations were used as tracers of deepwater ventilation. Counts of ice rafted detritus served to trace back the initiation of the Greenland ice-sheet. In addition, counts of benthic foraminifera (M. Weinelt) served as tracer for primary production.

**Chapter 1** shows that the onset of northern hemisphere glaciation (NHG), in particular on Greenland occurred only slightly after, hence as a result of the final closure of the Central American Seaways, which led to an increase in Caribbean sea surface salinity by up to 0.9‰. A first step occurred 2.95-2.82 Ma (marine isotope stage – MIS – G16-11), a second step 2.75-2.73 Ma (MIS G6), in total amounting to ~90 m of glacial sea-level fall. The first step was coeval with an intensified Atlantic thermohaline circulation (0.2-0.3‰ increase in benthic  $\delta^{13}\text{C}$ ; 2-3°C increase in SST), leading to enhanced snow precipitation in northern high-latitudes.

**Chapter 2** documents millennial-scale climate variations prior and after the onset of NHG at Site 984 to test the hypothesis that Dansgaard-Oeschger (DO) cycles of 1470 yr (and their multiples) are linked to ice-breakouts and meltwater incursions from northern hemisphere ice-sheets. On the long term, periodicities of 1300, 950, and 450 yr prevail, which closely resemble solar cycles of the Holocene. The same applies to selected glacial stages prior to the onset of NHG and to interglacial stages in general. However, glacial stages after the onset of NHG (MIS G14, G6, and 104) show periodicities near 1.47, 2.9 and 4.4 kyr, DO-like periodicities which thus occur in the presence of large northern hemisphere ice-sheets only, and as result of ice breakouts.

**Chapter 3** (with M. Weinelt as first author) reports on changes in surface productivity prior and after the onset of NHG. A distinct benthic faunal turnover started at ~2.75 Ma and culminated at 2.70 Ma (MIS G6), precisely coeval with a 0.6‰ drop in  $\delta^{18}\text{O}$  and a cooling of Upper North Atlantic Deep Water. Prior to MIS G6, the benthic fauna at Site 984 was characteristic of high nutrient fluxes as recorded by *Bolivina pacifica*, a benthic taxa that abruptly disappeared during early MIS G6, being replaced by *Cassidulina teretis*, a fauna adapted to low and irregular food supply. This faunal turnover may record a drop in North Atlantic primary production, resulting from enhanced seasonality and/or surface water stratification.

**Chapter 4** and **5** summarize the results of IODP Expedition 303 “North Atlantic Climate I” in which I participated as sedimentologist to supplement the results on the onset of NHG outlined above with high-quality sediment cores from the Northwest Atlantic, in particular, from Site U1307 off the southern tip of Greenland. It will provide new insights into the history of the East Greenland Current and deepwater sources in the Labrador Sea with a time resolution of 300 years.



## Kurzfassung

Langfristige und kurzfristige Klimaveränderungen im Spätpliozän wurden an den ODP Site 984 und DSDP 609 im Nordatlantik untersucht, die durch die bereits veröffentlichten Daten der Sites 907 und 610 ergänzt wurden. Die Bestimmungen von stabilen Sauerstoffisotopen an Foraminiferen dienten als Grundlage für die Stratigraphie. Die Temperaturen des Oberflächen- und des Tiefenwassers wurden aus den Mg/Ca Werten von planktischen und benthischen Foraminiferen rekonstruiert. Die Veränderungen der  $\delta^{13}\text{C}$  Werte der epibenthischen Foraminiferen stellen einen Tracer für die Belüftung im Tiefenwasser dar und die Menge des Eisbergschutts gibt Auskunft über das Einsetzen der Grönlandvereisung. Die Zählungen von benthischen Foraminiferen (M. Weinelt) wurden als Anzeiger für die Primärproduktion herangezogen.

Das **Chapter 1** beschreibt den Beginn der Vereisung der Nordhemisphäre (NHG), speziell das späte Einsetzen der Vereisung auf Grönland. Als Ursache wird die endgültige Schließung des Zentralamerikanischen Seeweges gesehen, was auch zu einer Erhöhung der Salinitäten des Oberflächenwassers in der Karibik von bis zu 0.9‰ führte. Die Schließung setzte zwischen 2.95-2.82 Ma (marines Isotopenstadium- MIS- G16-11) ein und endete in einem weiteren Schritt zwischen 2.75-2.73 Ma. Dabei kam es zu einem Absinken des glazialen Meeresspiegels von bis zu ~90m. Der erste Schließungsschritt ging zeitgleich mit einer Verstärkung der thermohalinen Zirkulation im Atlantik einher (Anstieg der benthischen  $\delta^{13}\text{C}$ -Werte von 0.2-0.3‰ und der Meeresoberflächentemperaturen um 2-3°C), was zu einem erhöhten Schneefall in den nördlichen Breiten führte.

Das **Chapter 2** beschreibt die klimatischen Veränderungen auf Zeitskalen von Jahrhunderten bis Jahrtausenden vor und nach dem Einsetzen der Nordhemisphären Vereisung in Site 984, um die Hypothese zu überprüfen, ob die Eisberg - und Schmelzwassereinträge von dem Eisschild der nördlichen Hemisphäre an die Dansgaard-Oeschger (DO) Zyklen von 1470 Jahren (und ihre Vielfachen) gekoppelt waren. Langzeitlich betrachtet, herrschten Frequenzen von 1300, 950 und 450 Jahren vor, die den Sonnenzyklen aus dem Holozän sehr stark ähneln. Diese Frequenzen konnten auch bei ausgewählten glazialen Stadien vor dem Einsetzen der Nordhemisphären Vereisung und generell für die interglazialen Stadien beobachtet werden. Die glazialen Stadien zeigen aber nach dem Einsetzen der Nordhemisphären Vereisung (MIS G14, G6 und 104) Frequenzen von ungefähr 1.47, 2.9 und 4.4 tausend Jahren auf also DO-ähnliche Frequenzen, die nur mit dem Vorhandensein von großen Eisschilden in der nördlichen Hemisphäre auftreten und aus dem Eintrag von Eisbergen resultieren.

Die Veränderungen der Oberflächenproduktion vor und nach der Nordhemisphären Vereisung werden im **Chapter 3** (M. Weinelt als Erstautor) behandelt. Eine deutliche benthische Faunenveränderung begann um ~2.75 Ma und gipfelte bei 2.70 Ma (MIS G6), was exakt zeitgleich mit einem Rückgang der  $\delta^{18}\text{O}$  – Werte von 0.6‰ und einer Abkühlung des oberen Nordatlantischen Tiefenwassers zusammenfällt. Vor MIS G6 war die benthische Fauna von Site 984 charakterisiert durch einen hohen Nährstofffluß nachweisbar an *Bolivina pacifica*, einer benthischen Art, die während des frühen MIS G6 plötzlich verschwand und durch die Faunenart *Cassidulina teretis* ersetzt wurde, die an ein geringes und unregelmäßiges Nahrungsangebot angepasst ist. Dieser Faunenumschwung dokumentiert eine Senkung in der Primärproduktion des Atlantiks durch eine verstärkte Saisonalität und/oder einer ausgeprägteren Oberflächenwasserstratifizierung.

Die **Chapter 4 und 5** fassen die Ergebnisse der IODP Expedition 303 "North Atlantic Climate I", auf der ich als Sedimentologin teilnahm, zusammen. Die dabei gewonnenen hochqualitativen Sedimentkerne aus dem Nordwestatlantik, besonders der Site U1307 vor der südlichen Spitze Grönlands, sollen die Ergebnisse des Beginns der NHG stützen. Es werden neue Erkenntnisse zur Geschichte der Ostgrönlandströmung und über die Quellen des Tiefenwassers in der Labradorsee mit einer zeitlichen Auflösung von 300 Jahren erwartet.





## Acknowledgements

At first, I would like to thank the person who enables me to pass my doctor degree, Professor Michael Samthein, responsible for the "Ocean Gateways" project, for giving me this PhD position, and supporting me until the end. Without him, nothing I would not be here today.

Of course, I owe a lot to my second supervisor as well, my "Doktormutti" Mara Weinelt, who provided me her motherly support during three and a half (long) years.

Vielen Dank, mille grazie, thanks and arigato to the visitors and employees of the Institut für Geowissenschaften who helped me in my work and in getting accustomed to my new "kieler" life: Claudia Sieler, Daniela Crudeli, Andrea Lorenz, Hiroshi Kawamura, Hanno Kinkel, Holger Gebhardt, Christian Millo, Thorsten Kiefer, Christian Bühring, and Bettina Kaste. I am very grateful to Helmut Erlenkeuser and Nils Andersen for the stable-isotope analysis and to Dieter Garbe-Schönberg, Karin Kißling, and Nadine Gehre for the Mg/Ca analysis. David Lea, Dorothy Pak, and George Paradis are thanked for kindly welcoming me in Santa Barbara and training me in the Mg/Ca analysis techniques. I also want to acknowledge the work of my numerous Hi-Wis, especially Christian Sievert and Claudia Geier, who spent a great amount of time processing some samples.

Vielen Dank to Ralf Tiedemann for teaching me the orbital tuning technique and for sharing with us some unpublished results. Vielen Dank to Dirk Nürnberg for his help with the Mg/Ca-paleothermometry and to Michael Schulz for teaching me the use of the programs SPECTRUM and REDFIT. Gerald Haug is thanked for thoughtful discussions about the "Panama story".

I also would like to thank the heads of the German and European IODP offices, Hermann Kudraß and Jeroen Kenter, for letting me participate to IODP Expedition 303. Jim Channell, Toki Sato and the Exp. 303 shipboard party are acknowledged for their assistance in collecting cores and for sharing with me their knowledge. It was an unforgettable experience. My thanks go also to the participants of the PRV *Polarstern* RV ARK XVIII/1a cruise, in which I acquired my first experience at sea.

This thesis in the frame of the Research Unit "Ocean gateways" was supported by the Deutsche Forschungsgemeinschaft, project FOR 451. The samples for this study were obtained by the Deep Sea Drilling Program and Ocean Drilling Project.

Bien sûr, il me faut remercier mes parents qui m'ont supportée financièrement et moralement pendant de longues années et qui m'ont permis d'aller si loin (jusqu'à la thèse mais aussi jusqu'à Kiel, qui est un peu le bout du bout du monde). Je remercie aussi mon petit frère et ma petite soeur qui se sont gentiment moqués de moi pendant toutes mes années d'étude et à qui je demande pardon de leur avoir volés la "bosse des sciences" avant leur naissance. I am also thankful to my friends in Kiel, Vero & Matt, and to my boyfriend Javier, who provided me with their thoughtful support.



## Chapter 1

### Objectives and Oceanographic setting

#### Objectives:

The long term cooling trend of the Earth's climate over the last ~50 Myr is related to opening and closure of ocean gateways (Lear et al., 2000) that play a major role in the evolution of ocean circulation, global climate, and marine biota (Hay, 1996).

In particular, the final onset of northern hemisphere glaciations (NHG) at ~2.73 Ma (Jansen et al., 2000) is considered as possibly linked to the final closure of the Central American Seaway (CAS; many studies starting from Keigwin et al., 1982) at ~2.73 Ma (Kameo & Sato, 2002). As inferred from both modeling experiments (Maier-Reimer et al., 1990; Mikolajewicz & Crowley, 1997) and sediment-based reconstructions (Dowsett et al., 1992, Haug & Tiedemann 1998), it appears highly likely that the CAS closure resulted in an intensified North Atlantic thermohaline circulation (THC).

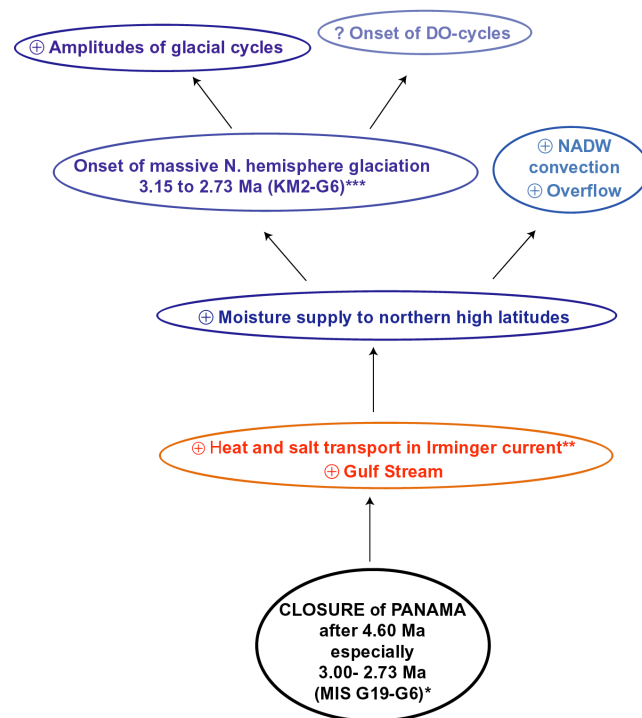
**Fig. 1-1.** Flow-chart presenting the scenario for onset of NHG as it is tested in this study.

⊕ stands for "increased"

\* Kameo & Sato (2000)

\*\* Dowsett et al. (1992)

\*\*\* Shackleton & Hall (1984), Jansen & Sjøholm (1991), Tiedemann et al. (1994), Maslin et al. (1996), Jansen et al. (2000), Kleiven et al. (2002).



In this study we tried to test the following scenario for the onset of NHG (Fig. 1-1). The increased heat and salt transport toward the northern high-latitudes has resulted from the final closure of the CAS, and has enhanced North Atlantic evaporation and deepwater formation, and in turn, precipitation / snowfall in northern high latitudes, especially so in Greenland and Eurasia (Haug & Tiedemann, 1998). Once major ice-sheets were established in the northern hemisphere, the climate variability during glacial times may have greatly increased, perhaps, with the apparition of millennial-scale Dansgaard-Oeschger (DO) oscillations. In case DO stadials have been triggered by ice breakouts from the Greenland ice-sheet (Ganopolski & Rahmstorf, 2001), one may expect that they indeed can be traced back until the first major glaciations of Greenland during Marine Isotope Stage (MIS) G6 (~2.73 Ma) or MIS G10 (~2.82 Ma) but not prior to this date.

However, apart from IRD records (Jansen et al., 2000, Kleiven et al., 2002), only few records are yet available on short-term climate variability in the subpolar North Atlantic for the Late Pliocene. In particular, no paleosea surface temperature (SST) estimates as primary expression of meridional heat transport to the high latitudes and THC strength have been published yet. Accordingly, major aims of this study have been:

- To generate surface and deepwater records of the subpolar and North Atlantic oceanic circulation for the time interval 2.5-3.3 Ma; in particular, records of foraminiferal Mg/Ca-based sea surface and deepwater temperatures (SST, DWT), planktic and benthic foraminiferal stable isotopes, and of ice rafted detritus (IRD).
- To achieve a consistent stratigraphic time frame sufficient to compare with millennial-scale resolution paleoceanographic records from different areas in the northern and tropical Atlantic and worldwide.
- To examine the potential links between the final closure of the CAS and the onset of NHG.
- To study the impact of the closure of the CAS on the evolution of planktic primary production in the subpolar North Atlantic.
- To compare the submillennial-scale climate evolution prior and after the onset of NHG and to test whether the Late Pliocene melting of the Greenland ice-sheet has triggered DO cycles.
- To record the full amplitudes of Pliocene climatic changes by generating paleoclimate records with an unprecedented time resolution of several hundred to thousand years.

#### **Oceanographic setting and selection of site locations:**

The evolution of the Gulf Stream current system and of the North Atlantic deep-water (NADW) formation in the northern North Atlantic and Nordic Seas monitor past changes in North Atlantic meridional overturn circulation. At the sea surface, the North Atlantic and Irminger Currents advect warm and saline waters into the Nordic Seas through the eastern Denmark Strait and across the Iceland-Farø-Ridge (Fig. 1-2). On the other hand, NADW formed in the northern Nordic Seas and Icelandic Sea is passing through the same gateways in the deep and forms the onset of the global “conveyor belt”.

However, Late Pliocene paleoceanographic changes are difficult to reconstruct in the Nordic Seas, since carbonate preservation is very low or zero in sediments older than 1.8 Ma (Heinrich et al., 2002). For this reason, most benthic and planktic  $\delta^{18}\text{O}$  records published for the Plio-Pleistocene from northern North Atlantic sites do not extend further back than 2.2 Ma such as at Site (S.) 983 (Channell et al., 2002) or 1.6 Ma at S. 907 (Jansen et al., 2000).

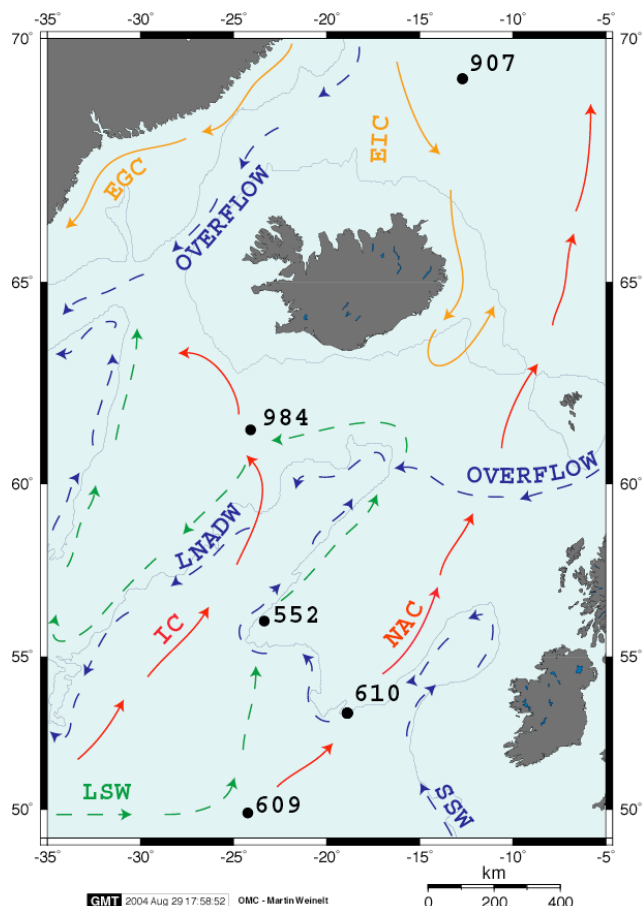
For this reason, we selected the shallow ODP S. 984 which is located off southern Iceland and contains sufficient carbonate for our study. In addition, a much deeper site was selected further south, DSDP S. 609, from the eastern flank of the mid-Atlantic Ridge to obtain a second surface water record from the southern part of the North Atlantic Current (NAC) system, moreover, a North Atlantic deepwater transect. Both sites record the northward heat transport with the NAC system. However, S. 984 on the Björn Drift documents the history of the Irminger Current and, at the seafloor, that of Labrador Sea Water (LSW, Upper NADW), while S. 609 (eastern flank of the Mid-Atlantic Ridge) records changes in NAC and in the deep, that of Southern Source Water (SSW), and, alternating, that of Lower NADW (Fig. 1-2).

In addition, various previously published records from ODP and DSDP Sites 607, 610, and in particular, the IRD record of S.907, were included to form a broader basis for the interpretations (Table 1-1, Fig 1-2).

**Table 1-1.** Sites location and water depth of cores studied.

<b>Core</b>	<b>Location</b>	<b>water depth</b>	
984	61.25°N, 24.04°W	1648 m	this study
609	49.52°N, 24.14°W	3883 m	this study
610	53.13°N, 18.53°W	2433 m	Kleiven et al. (2002)
607	41.00°N, 35.57°W	3427 m	Dwyer et al. (1995)
907	69.14°N, 12.42°W	1802 m	Jansen et al. (2000)

**Fig. 1-2.** North Atlantic Ocean with site locations discussed in this study and modern surface (solid lines) and deep-water currents (broken lines) in the Northeast Atlantic. IC stands for Irminger Current, NAC for North Atlantic Current, EGC for East Greenland Current, EIC for East Iceland Current LSW for Labrador Sea Water, SSW for Southern Source Water, and NADW for North Atlantic Deep Water.



The backbone of this study is formed by stable-isotope and temperature reconstructions that may serve to decipher past changes in Atlantic meridional overturning circulation on time scale that permit precise assessment of millennial-scale climate variability in the time and frequency domains.

Within the Kiel research unit “Ocean Gateways”, results of the modeling group of A. Schmittner were incorporated to arrive to a better understanding of the causal links between the closure of the CAS and the onset of NHG. For example, the UVic ocean-atmosphere coupled General Circulation Model (GCM) documented successive changes in SST and nutrient availability for different sill depths of the rising Panama Isthmus, results that are discussed in Chapter 4 and 6.

## References

- Channell, J.E.T., Mazaud, A., Sullivan, P., Turner, S. and Raymo, M.E. Geomagnetic excursions and paleointensities in the Matuyama Chron at Ocean Drilling Program Sites 983 and 984 (Iceland Basin). *Journal of Geophysical Research*, **107** (B6), (2002).
- Dowsett, H.J. et al. Micropaleontological evidence for increased meridional heat transport in the North Atlantic Ocean during the Pliocene. *Science*, **258**, 1133-1135 (1992).
- Ganopolski, A. and Rahmstorf, S. Rapid changes of glacial climate simulated in a coupled climate model. *Nature*, **409**, 153-158 (2001).
- Haug, G.H. and Tiedemann, R. Effect of the formation of the Isthmus of Panama on Atlantic Ocean thermohaline circulation. *Nature*, **393**, 673-676 (1998).
- Hay, W.W. Tectonics and climate. *Geol Rundsch*, **85**, 409-437 (1996).
- Henrich, R., Baumann, K.-H., Huber, R. and Meggers, H. Carbonate preservation records of the past 3 Myr in the Norwegian-Greenland Sea and the northern North Atlantic: implications for the history of NADW production. *Marine Geology*, **184**, 17-39 (2002).
- Jansen, E. and Sjolholm, J. Reconstruction of glaciation over the past 6 Myr from ice-borne deposits in the Norwegian Sea. *Nature*, **349**, 600-603 (1991).

Jansen, E., Fronval, T., Ranck, F. and Channell, J.E.T. Pliocene-Pleistocene ice rafting history and cyclicity in the Nordic Seas during the last 3.5 Myr. *Paleoceanography*, **15** (6), 709-721 (2000).

Kameo, K. and Sato, T. Biogeography of Neogene calcareous nannofossils in the Caribbean and eastern equatorial Pacific-floral response to the emergence of the Isthmus of Panama. *Marine Micropaleontology*, **39**, 201-218 (2000).

Keigwin, L. Isotopic Paleocyanography of the Caribbean and East Pacific: Role of Panama Uplift in Late Neogene Time. *Science*, **217**, 350-352 (1982).

Kleiven, H.F., Jansen, E., Fronval, T. and Smith, T.M. Intensification of Northern Hemisphere glaciations in the circum Atlantic region (3.5-2.4 Ma) - ice-rafted detritus evidence. *Paleogeogr. Paleoclim. Paleocol.*, **184**, 213-223 (2002).

Lear, C.H., Elderfield, H. and Wilson, P.A. Cenozoic Deep-Sea temperatures and global ice volumes from Mg/Ca in benthic foraminiferal calcite. *Science*, **287**, 269-272 (2000).

Maier-Reimer, E., Mikolajewicz, U. and Crowley, T.J. Ocean general circulation model sensitivity experiment with an open Central American isthmus. *Paleoceanography*, **5**, 349 (1990).

Maslin, M.A., Haug, G.H., Sarnthein, M. and Tiedemann, R. The progressive intensification of northern hemisphere glaciation as seen from the North Pacific. *Geol Rundsch*, **85**, 452-465 (1996).

Mikolajewicz, U. and Crowley, T.J. Response of a coupled ocean/energy balance model to restricted flow through the central American isthmus. *Paleoceanography*, **12** (3), 429-441 (1997).

Shackleton, N.J. et al. Oxygen isotope calibration of the onset of ice-rafting and history of glaciation in the North Atlantic region. *Nature*, **307**, 620-623 (1984).

Tiedemann, R., Sarnthein, M. and Shackleton, N.J. Astronomic timescale for the Pliocene Atlantic  $\delta^{18}\text{O}$  and dust flux records of Ocean drilling Program site 659. *Paleoceanography*, **9** (4), 619-638 (1994).

## Chapter 2

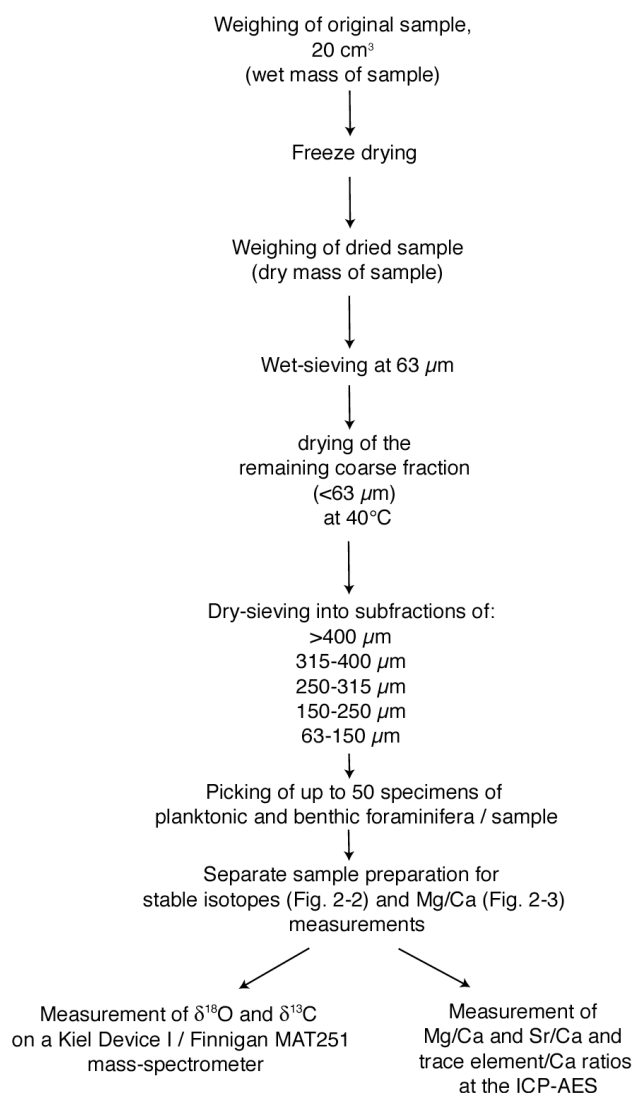
### Methods and Strategy

Each single paper presented in Chapter 4-6 contains its own methods chapter. In this chapter, however, all analytical techniques are summarized in greater detail.

#### 1. Sediment sample processing

Cores were sampled at the East Coast and Bremen DSDP and ODP Core Repositories with the help of the local technical staff. Sampling resolution was chosen so as to reach a centennial-to-millennial time resolution (i.e., 10 cm for S. 984, 20 cm for S. 609). Sediment samples are 2 cm-wide and amount to 20 cm<sup>3</sup>. Fig. 2-1 provides a flow chart of sample processing.

**Fig. 2-1.** Flow-chart of sample processing.



At S. 984, foraminifera species mainly consist of planktic *Globigerina bulloides* and *Neogloboquadrina atlantica*, the latter being more abundant during glacial periods. For stable-isotope and trace metal analyses, *G. bulloides* was picked in the 315-400 μm size-fraction. *N. atlantica* was picked in the 250-315 μm size-fraction, in case not sufficient specimens of *G. bulloides* were available, that is mainly during coldest glacial stages. *G. bulloides* is known to calcify in spring and lives in the top first 50-200 m of the water column in the North Atlantic and thus contains an average signal of surface and subsurface waters. Benthic foraminifera

specimens, such as *Cibicides wuellerstorfi*, were rare at this site. Thus new species were tested for their ability to record seawater  $\delta^{18}\text{O}$  changes (*Elphidium excavatum* and *Cassidulina teretis*), see chapter 6. Table 2-1 lists the benthic species used in this study.

**Table 2-1.** Benthic foraminifera species used for stable isotopes measurements and correction applied for species-specific offsets relative to *U. peregrina* and *C. wuellerstorfi* considered to represent equilibrium  $\delta^{18}\text{O}$  and  $\delta^{13}\text{C}$ , respectively.

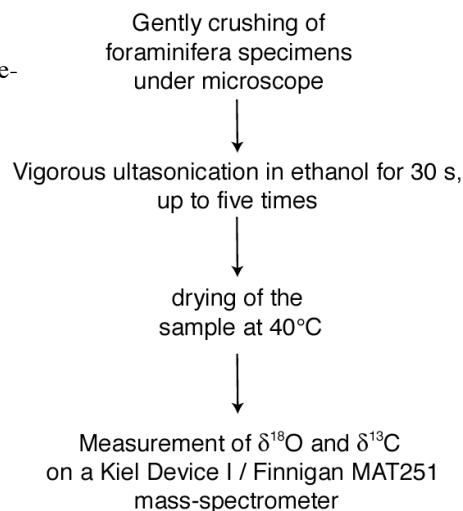
	$\delta^{18}\text{O}$	$\delta^{13}\text{C}$	References
<i>Cibicides wuellerstorfi</i>	+0.64	0.00	Duplessy et al. (1984)
<i>Cibicides pachyderma</i>	+0.64	0.00	Duplessy et al. (1984)
<i>Uvigerina peregrina</i>	0.00	not used	Duplessy et al. (1984)
<i>Oridorsalis tener</i>	0.00	not used	Duplessy et al. (1984)
<i>Elphidium excavatum</i>	+0.64	not used	Weinelt et al. (subm.) See Chapter 6
<i>Cassidulina teretis</i>	0.00	not used	Jansen et al. (1988)
<i>Melonis barleeanum</i>	+0.36	not used	Graham et al. (1981)

At S. 609, planktic warm water species (subtropical to temperate) dominate the assemblages including *G. bulloides*, *Globigerinoides ruber* (white), *Gobigerinoides sacculifer*, *Globorotalia truncatulinoides*, and *Globorotalia menardii*. To enable direct comparison with the data obtained from S. 984, we measured Mg/Ca and  $\delta^{18}\text{O}$  also on *G. bulloides*. Benthic foraminifera specimens are more abundant than at S. 984 and mainly comprise *Cibicides wuellerstorfi*, *C. pachyderma*, *Oridorsalis umbonatus*, *Uvigerina peregrina*, *Melonis barleeanum* and *Melonis pompilioides*.

## 2. Stable isotopes

Benthic and planktic stable isotopes are measured to assess the changes in global ice volume (benthic  $\delta^{18}\text{O}$ ), changes in deepwater ventilation (benthic  $\delta^{13}\text{C}$ ), and changes in sea surface salinity (planktic  $\delta^{18}\text{O}$ ).

**Fig. 2-2.** Flow-chart of sample preparation for stable-isotope analysis.



Monospecific samples for stable isotopes analyses usually consist of 1 to 5 benthic foraminifers (Table 2-1) and 1 to 30 *G. bulloides* or *N. atlantica* specimens. They were sonicated in ethanol for 5-10 s, oven dried at 40°C (see Fig. 2-2), and measured on the Kiel Device I/Finnigan MAT251 system with an analytical precision of 0.07‰ for  $\delta^{18}\text{O}$  and 0.05‰ for  $\delta^{13}\text{C}$  at the Leibniz Laboratory in Kiel. Benthic  $\delta^{18}\text{O}$  and  $\delta^{13}\text{C}$  values were corrected for species-specific offsets relative to *Uvigerina peregrina* and *Cibicides wuellerstorfi*, considered to represent equilibrium  $\delta^{18}\text{O}$  and  $\delta^{13}\text{C}$ , respectively, listed in Table 2-1.



### 3. Mg/Ca, Sr/Ca and trace elements

#### 3.1 Mg/Ca-paleothermometry technique

To estimate seawater paleotemperatures, foraminiferal Mg/Ca-paleothermometry was employed. Mg/Ca ratios of carbonate shells vary exponentially with the temperature at which the carbonate was secreted. The incorporation of Mg into carbonated shells of various (planktic and benthic) foraminifer, ostracod, and bivalve taxa has been calibrated against modern temperatures (Nürnberg et al., 1996, Toyofuku et al., 2000, Dwyer et al., 1995, Freitas et al., 2005). Accordingly Mg/Ca ratios are considered adequate for calculating paleotemperatures for surface and deep-waters. In contrast to  $\delta^{18}\text{O}$ , Mg/Ca is supposed to be widely independent of salinity effects (Nürnberg et al., 1996, Lea et al., 1999, Toyofuku et al., 2000), at least outside basins with prevailing evaporation (Groeneveld et al., *subm.*). Mg/Ca-based temperature estimates have an accuracy of  $\pm 1^\circ\text{C}$ .

Recently much effort has been made towards a multi-species calibration of Mg/Ca ratios. Elderfield & Ganssen (2000) first provided a calibration valid for 8 planktic species from the North Atlantic. Later, Anand et al. (2003) reviewed most of the calibrations existing for planktic foraminifers and inferred from sediment trap time series a single calibration based on 14 different species. Applying one single calibration to different species is less accurate than applying a specific calibration to each single species, calculated for a specific season and/or epoch, for a well-defined location, a specific size-fraction and a specific cleaning method. However the use of a general calibration formula for different species has the advantage to allow reconstruction of long-term SST records over several Myr that can only be obtained from analysings multiple and/or extinct species (Tripathi et al., 2003).

Major advantages of Mg/Ca-paleothermometry versus other SST proxies are: 1) It renders a direct quantitative estimate of SST. 2) In principle, it can be applied to species today extinct. Tripathi & Elderfield (2004) measured Mg/Ca ratio on species as old as 55 Ma. 3) By combining both Mg/Ca and  $\delta^{18}\text{O}$  data measured on the same sample, one can derive the  $\delta^{18}\text{O}$  signature of the seawater in which the foraminifers have calcified (Mashiotta et al., 1999, Rosenthal et al., 1999). This  $\delta^{18}\text{O}_{\text{seawater}}$  reflects both changes in global ice volume and local salinity.

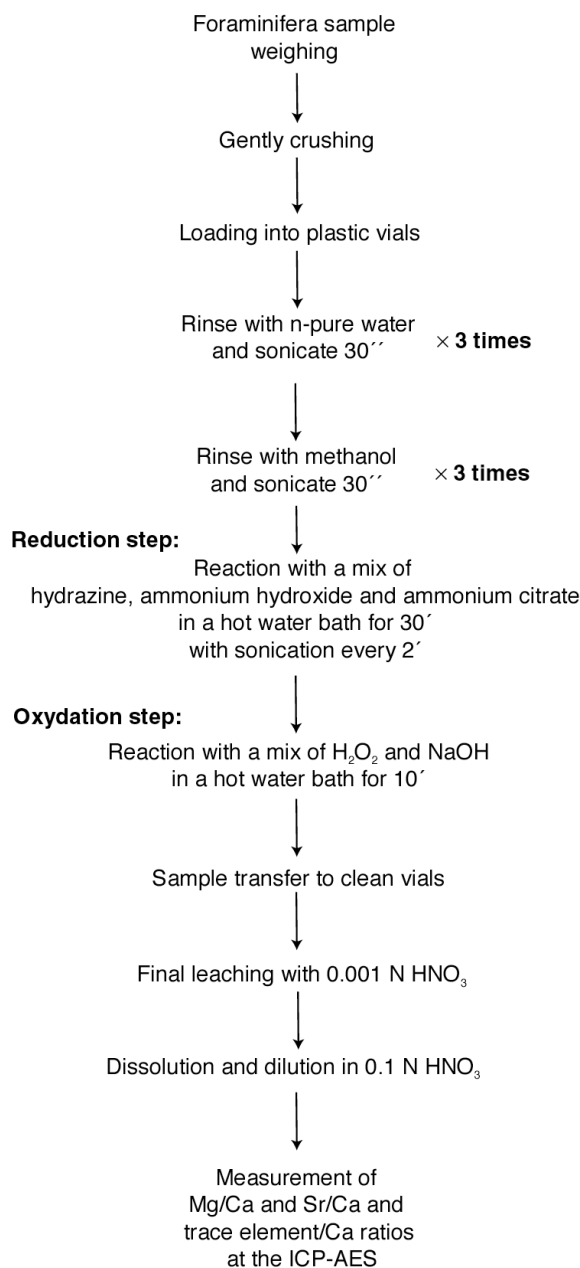
#### 3.2 Cleaning protocol

Foraminifera samples were prepared prior to Mg/Ca, Sr/Ca and trace metal element analyses according to the methods described by Martin & Lea (2002) (see Fig. 2-3). Controversies exist about whether or not to include a reduction step, which is thought to be highly aggressive to the carbonate sample but necessary to remove coatings of metal oxides from the shell. In this context, Barker et al. (2003) published a precise study of the necessity or not of each single step included in different existing protocols. However, these authors do not clearly conclude on the reduction step.

A simple test has also been made in collaboration with the Leibniz Labor für Meereskunde (Nürnberg, Groeneveld, Regenber, Koch). We obtained a temperature offset of less than  $1^\circ\text{C}$  when either including or not including the reduction step for the analysis of *G. bulloides* and *Globigerinoides sacculifer*. This offset is of same order of the accuracy the current paleo-SST equations ( $\pm 1^\circ\text{C}$ ).

During a recent Mg/Ca workshop at the ICP-8 (Biarritz, 2004) it was agreed that the choice of the cleaning method should depend on the preservation degree of the samples, the kind of contamination they may be submitted to, and on the kind of benthic and planktonic species, whether they are easily “contaminable” or not. It was also commonly agreed to publish with each foraminiferal Mg/Ca-record, the offsets from applying the different two cleaning methods for this particular record.

**Fig. 2-3.** Individual steps of the cleaning protocol prior to Mg/Ca analysis according to Martin & Lea (2002).



### 3.3 Analysis with an ICP-AES

The analysis method of the ICP-Absorption-Emission-Spectrometer (ICP-AES) is described in Garbe-Schönberg et al. (subm.) and follows the techniques described in de Villiers et al. (2002), that are needed to produce direct estimates of Mg/Ca ratios. Interlaboratory comparisons were necessary to ensure of the compatibility of Mg/Ca paleo-thermometry within the paleoceanographic community. Rosenthal et al. (2004) presented the first intercomparison study between 14 laboratories worldwide, concluding that the reproducibility between the different group is better than 8% relative standard deviation (RSD) that translates in  $\pm 2\text{-}3^\circ\text{C}$ . A second interlaboratory comparison study gathering more labs including the Institute für Geowissenschaften in Kiel is in progress (coordinated by N. Caillon, Gif-sur-Yvette & M. Greaves, Cambridge).

Despite rigorous cleaning, sometimes contaminants are not completely removed. Thus, the signal of these contaminant are mixed with those of the samples. Therefore, trace elements including Fe, Al, and Mn are measured to monitor the degree of possible contamination in each sample measured, as described in Schmidt et al. (2004).

### 3.4 Mg/Ca-temperature calibrations

Table 2-2 lists all equations used to derive SST estimates from Mg/Ca ratios for the various planktic and benthic foraminifera taxa analyzed. Calibrations generally yield temperatures with an uncertainty of  $\pm 1^\circ\text{C}$ .

**Table 2-2.** Paleo-temperature equations of studied species.

<i>Species</i>	calibrations Mg/Ca =	References
<i>G. bulloides</i>	0.474 exp (0.107 $\times$ SST)	Mashiotta et al. (1999)
<i>N. atlantica</i>	0.5 exp (0.1 $\times$ SST)	Elderfield & Ganssen (2000)
<i>C. wuellerstofi</i> and <i>C. pachyderma</i>	0.867 exp (0.109 $\times$ SST)	Lear et al. (2002)
<i>U. peregrina</i>	0.85 exp (0.15 $\times$ SST)	Martin et al. (2002)
<i>O. umbonatus</i>	1.06 exp (0.1 $\times$ SST)	Lear et al. (2002)
<i>M. pompilioides</i> and <i>M. barleeaanum</i>	0.982 exp (0.101 $\times$ SST)	Lear et al. (2002)

As Mg-rich calcite is dissolved preferentially to Mg-poor calcite (Lorens et al., 1977), the degree of dissolution of foraminiferal tests has been checked carefully prior to measuring Mg/Ca ratios. The degree of dissolution strongly depends on the water depth of sediment deposition as most dissolution occurs while foraminifera tests lie on the sea floor (Adelseck Jr & Berger, 1975). Rosenthal & Lohmann (2002) produced a dissolution-corrected calibration of Mg/Ca ratios versus temperatures by integrating the shell weight for a specific test size into the paleo-temperature equation. On the other hand, Dekens et al. (2002) integrated the water depth into the paleo-temperature equation to correct for dissolution effect.

### 3.5 IRD and benthic foraminifera counts and Spectral analysis.

To study the history of iceberg discharge, up to 300 lithic grains of ice-rafted debris (IRD) were counted in the size fraction  $>150 \mu\text{m}$ . Values are given as number of grains/g dry sediment. In addition, census counts of benthic foraminifera species characteristic of primary production changes such as *Uvigerina peregrina*, *Elphidium excavatum*, *Cassidulina teretis* and *Bolivina* spp were performed on the same size fraction. Since many samples contain very low specimen numbers, only raw census data (individuals per 10 g dry sediment) are shown.

To study the short-term climate variability, we performed spectral analysis on the paleoclimate records at S. 984. The REDFIT program (Schulz & Mudelsee, 2002) permitted the use of non-evenly spaced data and to define the red-noise level. In addition, we used the Blackman-Tukey method from AnalySeries 1.2 software (Paillard et al., 1996) for which the times series were interpolated to obtain evenly spaced data.

## References

- Adelseck Jr, C.G. and Berger, W.H. On the dissolution of planktonic foraminifera and associated microfossil during settling and on the sea floor. *Cushman Foundation for Foraminiferal Research, special publication NO. 13, Dissolution of deep-sea carbonates* (edited by W. V. Sliter, A. W. H. Bé, and W. H. Berger), (1975).
- Anand, P., Elderfield, H. and Conte, M.H. Calibration of Mg/Ca thermometry in planktonic foraminifera from a sediment trap time series. *Paleoceanography*, **18** (2), 1050 (2003).
- Barker, S., Greaves, M. and Elderfield, H. A study of cleaning procedures used for foraminiferal Mg/Ca paleothermometry. *Geochem. Geophys. Geosys.*, **4** (9), 8407, doi:10.1029/2003GC000559 (2003).
- Dekens, P.S., Lea, D.W., Pak, D.K. and Spero, H.J. Core top calibration of Mg/Ca in tropical foraminifera: Refining paleotemperature estimation. *Geochem. Geophys. Geosys.*, **3** (4), (2002).
- Duplessy, J.-C. et al.  $^{13}\text{C}$  record of benthic foraminifer in the last interglacial ocean: implications for the carbon cycle and the global deep water circulation. *Quat. Res.*, **21**, 225-243 (1984).
- Dwyer, G.S. et al. North Atlantic deepwater temperature change during the Late Pliocene and Late Quaternary climatic cycles. *Science*, **270**, 1347-1350 (1995).
- Elderfield, H. and Ganssen, G. Past temperature and  $\delta^{18}\text{O}$  of surface ocean waters inferred from Mg/Ca ratios. *Nature*, **405**, 442-445 (2000).

Freitas, P., Clarke, L.J., Kennedy, H., Richardson, C. and Abrantes, F. Mg/Ca, Sr/Ca, and stable-isotope ( $\delta^{18}\text{O}$  and  $\delta^{13}\text{C}$ ) ratio profiles from the fan mussel *Pinna nobilis*: Seasonal records and temperatures relationships. *Geochem. Geophys. Geosys.*, **6** (4), Q04D14 (2005).

Garbe-Schönberg, D., J. Groeneveld, G. Bartoli, M. Sarnthein, C. Dullo. High-precision Mg/Ca and Sr/Ca ratios of biogenic carbonate and seawater by simultaneous ICP-OES. submitted to *Geochem. Geophys. Geophys.*

Graham D. W., B. H. Corliss, M. L. Bender, L. D. Keigwin Jr. Carbon and oxygen isotopic disequilibria of recent deep-sea benthic foraminifera, *Mar. Micropaleo.*, **6**, 483-497 (1981).

Groeneveld, J., Nürnberg, D., Steph, S., Tiedemann, R., Reichart, G. J., Reuning, L., Crudeli, D. The Pliocene Mg/Ca SST increase in the Caribbean: Western Atlantic Warm Pool formation, salinity influence or diagenetical overprint? submitted to *Geochem. Geophys. Geophys.*

Jansen, E. U. Bleil, R. Henrich, L. Kringstad, B. Slettemark. Paleoenvironmental changes in the Norwegian Sea and the Northwest Atlantic during the last 2.8 m.y.: Deep Sea Drilling Project/Ocean Drilling Program sites 610, 642, 643 and 644. *Paleoceanography*, **3** 563–581 (1988).

Lea, D.W., Mashiotto, T.A. and Spero, H.J. Controls on magnesium and strontium uptake in planktonic foraminifera determined by live culturing. *Geochim. Cosmochim. Acta*, **63** (16), 2369-2379 (1999).

Lorens, R.B., Williams, D.F. and Bender, M.L. The early nonstructural chemical diagenesis of foraminiferal calcite. *J. Sediment. petrol.*, **47**, 1602-1609 (1977).

Martin, P.A. and Lea, D.W. A simple evaluation of cleaning procedures on fossil benthic foraminiferal Mg/Ca. *Geochem. Geophys. Geophys.*, **3** , 8401 (2002).

Mashiotto, T.A., Lea, D.W. and Spero, H.J. Glacial-interglacial changes in Subantarctic sea surface temperature and  $\delta^{18}\text{O}$ -water using foraminiferal Mg. *Earth Planet. Sci. Lett.*, **170** , 417-432 (1999).

Nürnberg, D., Bijma, J. and Hemleben, C. Assessing the reliability of magnesium in foraminiferal calcite as a proxy for water mass temperatures. *Geochim. Cosmochim. Acta*, **60** (5), 803-814 (1996).

Paillard D., Labeyrie L., and Yiou P. Macintosh program performs time-series analysis. *EOS Trans*, AGU **77**, 379 (1996).

Rosenthal, Y. and Lohmann, G.P. Accurate estimation of sea surface temperatures using dissolution-corrected calibrations for Mg/Ca paleothermometry. *Paleoceanography*, **17** (3), 1044-1050 (2002).

Rosenthal, Y. et al. Interlaboratory comparison study of Mg/Ca and Sr/Ca measurements in planktonic foraminifera for paleoceanographic research. *Geochem. Geophys. Geosyst.*, **5** (4), (2004).

Rosenthal, Y., Lohmann, G.P., Lohmann, K.C. and Sherrell, R.M. Incorporation and preservation of Mg in *Globigerinoides sacculifer*: Implications for reconstructing the temperature and  $^{18}\text{O}/^{16}\text{O}$  of seawater. *Paleoceanography*, **15**, 135-145 (2000).

Schmidt, M.W., Spero, H.J. and Lea, D.W. Links between salinity variation in the Caribbean and North Atlantic thermohaline circulation. *Nature*, **428**, 160-163 (2004).

Schulz M. and Mudelsee M. REDFIT: Estimating red-noise spectra directly from unevenly spaced paleoclimatic time series. *Computers and Geosciences* **25** (3), 421-426 (2002).

Toyofuku, T., Kitazato, H., Kawahata, H., Tsuchiya, M. and Nohara, M. Evaluation of Mg/Ca thermometry in foraminifera: comparison of experimental results and measurements in nature. *Paleoceanography*, **15** (4), 456-464 (2000).

Tripathi, A.K. and Elderfield, H. Abrupt hydrographic changes in the equatorial Pacific and subtropical Atlantic from foraminiferal Mg/Ca indicate greenhouse origin for the thermal maximum at the Paleocene-Eocene Boundary. *Geochem. Geophys. Geosyst.*, **5** (2), Q02006 (2004).

Tripathi, A.K. et al. Tropical sea-surface temperature reconstruction for the early Paleogene using Mg/Ca ratios of planktonic foraminifera. *Paleoceanography*, **18** (4), 1101 (2003).

de Villiers, S., Greaves, M. and Elderfield, H. An intensity ratio calibration method for the accurate determination of Mg/Ca and Sr/Ca of marine carbonates by ICP-AES. *Geochem. Geophys. Geophys.*, **3**, (2002).

Weinelt, M., G. Bartoli M. Sarnthein, H. Erlenkeuser, Abrupt reorganization of northern North Atlantic productivity provinces during the initiation of NHG. Submitted to *Mar. Micropal.* see also Chapter 6.

## Chapter 3

### Age models

#### 1. S. 984 age control points

Magnetic stratigraphy suffered from drilling disturbance below 260 mbsf, at the base of the advanced hydraulic piston corer (APC) section (Channell & Lehman, 1999) and thus, was only measured back to 2.2 Ma (Reunion Event). Further back, biostratigraphic control was only established by the last occurrence (LO) datum of *Ebriopsis cornuta* between 359.74 to 369.06 mbsf (2.61 Ma; Jansen et al., 1996). In absence of any benthic  $\delta^{18}\text{O}$  record, Raymo tried to deduce marine isotope stages from the magnetic susceptibility record (in Austin & Evans, 2000). Proceeding from her estimates we established a revised stable-isotope stratigraphy using our new planktic isotope record of *G. bulloides* and *N. atlantica*, and a composite record of several benthic species, as explained in Chapter 2, § 2. Direct orbital tuning was not employed because of major glacial-to-interglacial changes in sedimentation rate and various gaps in the record because of samples barren of foraminifers.

#### 2. S. 609 age control points

Such as with S. 984, the age model at S. 609 was obtained from tuning the benthic  $\delta^{18}\text{O}$  record to the orbitally tuned  $\delta^{18}\text{O}$  record of ODP S. 659 and S. 846 with geomagnetic age control points (provided by DSDP shipboard party) listed in Table 3-1 according to Berggren et al. (1995).

**Table 3-1.** Geomagnetic events measured at S. 609.

Geomagnetic events	Depth interval (m)	Age (Ma)	
		Berggren et al. (1995)	Lisiecki & Raymo (2005)
Matuyama/Gauss	169.69-171.19	2.58	2.608
Kaena Top	209.59-211.69	3.04	3.045
Kaena Bottom	216.19-217.77	3.11	3.127
Mammoth Top	227.33-228.84	3.22	3.210
Mammoth Bottom	235.51-237.02	3.33	3.319

#### 3. Orbital tuning

The orbital timescale for both sites was indirectly derived from tuning the planktic  $\delta^{18}\text{O}$  (S. 984) or the benthic  $\delta^{18}\text{O}$  (S. 609) records to the orbitally tuned standard benthic  $\delta^{18}\text{O}$  stratigraphy of S. 846 (Shackleton et al., 1995) by graphical correlation of peaks and stage edges using the AnalySeries 1.2 software (Paillard et al., 1996). Between the stratigraphic tie points the sedimentation-rate is assumed to be constant and linear interpolation was applied. At S. 984, MIS 99 to G22 were identified and at S. 609, MIS 103 to M2.

Recently, Lisiecki & Raymo (2005) published a new stacked benthic  $\delta^{18}\text{O}$  record for the Pliocene-Pleistocene, named LR04. This  $\delta^{18}\text{O}$  stack integrates 57 benthic  $\delta^{18}\text{O}$  records from the global ocean including 25 records over the time span 1-3 Ma, and 12 over 3-5 Ma and thus appears more reliable than a single benthic  $\delta^{18}\text{O}$  record, since the noise-to-signal ratio is greatly reduced.

Therefore, we corrected the timescale at S. 984 by tuning the planktic  $\delta^{18}\text{O}$  record to the LR04 record (see Chapter 5) to study millennial-scale climate variability in the frequency domain. The differences between the initial and final age model amount to 5-10 kyr but no more than 20 kyr. In our new age model for S. 984, the lower part of the initial stage G3 has become G5 and stages 101 and 102 have been better defined, in order to be more accurate with the LR04 stack. This new age scale for S. 984 is discussed in greater detail in Chapter 5.

## References

- Austin, W.E.N. and Evans, J.R. Benthic foraminifera and sediment grain size variability at intermediate water depths in the Northeast Atlantic during the late Pliocene-early Pleistocene. *Marine Geology*, **170**, 423-441 (2000).
- Berggren, W.A. et al. Late Neogene chronology: new perspectives in high-resolution stratigraphy. *GSA Bulletin*, **107** (11), 1272-1287 (1995).
- Channell, J. E. T. and Lehman B. Magnetic stratigraphy of North Atlantic Sites 980-984. In: Raymo, M.E., Jansen, E., Blum, P., and Herbert, T.D. (Eds.), 1999. *Proc. ODP, Sci. Results*, **162**: College Station, TX (Ocean Drilling Program).
- Jansen, E., Raymo, M.E., Blum, P., and Herbert, T.D. (Eds.), 1996. *Proc. ODP, Init. Results*, **162**: College Station, TX (Ocean Drilling Program).
- Lisiecki, L.E. and Raymo, M.E. A Pliocene-Pleistocene stack of 57 globally distributed benthic  $\delta^{18}\text{O}$  records. *Paleoceanography*, **20**, PA1003 (2005).
- Paillard, D., Labeyrie, L. and Yiou, P. Macintosh program performs time-series analysis. *EOS Trans, AGU*, **77**, 379 (1996).
- Shackleton, N.J., Hall, M.A. and Pate, D. Pliocene Stable Isotope stratigraphy of Site 846. *Proceedings of the Ocean Drilling Program, Scientific Results*, **138**, 337-353 (1995).



ELSEVIER

Available online at [www.sciencedirect.com](http://www.sciencedirect.com)

SCIENCE @ DIRECT®

Earth and Planetary Science Letters 237 (2005) 33–44

EPSL

[www.elsevier.com/locate/epsl](http://www.elsevier.com/locate/epsl)

## Final closure of Panama and the onset of northern hemisphere glaciation

G. Bartoli <sup>a,\*</sup>, M. Sarnthein <sup>a</sup>, M. Weinelt <sup>a</sup>, H. Erlenkeuser <sup>b</sup>,  
D. Garbe-Schönberg <sup>a</sup>, D.W. Lea <sup>c</sup>

<sup>a</sup>Kiel University, Institute for Geosciences, Olshausenstr. 40, D-24118 Kiel, Germany

<sup>b</sup>Leibniz-Laboratory for Radiometric Dating and Stable Isotope Research, Kiel University,  
Max-Eyth-Str. 11, D-24118 Kiel, Germany

<sup>c</sup>Department of Geological Sciences, University of California, Santa Barbara, CA 93106, USA

Received 26 November 2004; received in revised form 10 May 2005; accepted 10 June 2005

Available online 21 July 2005

Editor: E. Boyle

### Abstract

The Greenland ice sheet is accepted as a key factor controlling the Quaternary “glacial scenario”. However, the origin and mechanisms of major Arctic glaciation starting at 3.15 Ma and culminating at 2.74 Ma are still controversial. For this phase of intense cooling Ravelo et al. [1] [A.C. Ravelo, D.H. Andreasen, M. Lyle, A.O. Lyle, M.W. Wara, Regional climate shifts caused by gradual global cooling in the Pliocene epoch. *Nature* 429 (2004) 263–267.] proposed a complex gradual forcing mechanism. In contrast, our new submillennial-scale paleoceanographic records from the Pliocene North Atlantic suggest a far more precise timing and forcing for the initiation of northern hemisphere glaciation (NHG), since it was linked to a 2–3 °C surface water warming during warm stages from 2.95 to 2.82 Ma. These records support previous models [G.H. Haug, R. Tiedemann, Effect of the formation of the Isthmus of Panama on Atlantic Ocean thermohaline circulation, *Nature* 393 (1998) 673–676.[2]] claiming that the final closure of the Panama Isthmus (3.0–~2.5 Ma [J. Groeneveld S. Steph, R. Tiedemann, D. Nürnberg, D. Garbe-Schönberg, The final closure of the Central American Seaway, *Geology*, in prep. [3]]) induced an increased poleward salt and heat transport. Associated strengthening of North Atlantic Thermohaline Circulation and in turn, an intensified moisture supply to northern high latitudes resulted in the build-up of NHG, finally culminating in the great, irreversible “climate crash” at marine isotope stage G6 (2.74 Ma). In summary, there was a two-step threshold mechanism that marked the onset of NHG with glacial-to-interglacial cycles quasi-persistent until today.

© 2005 Elsevier B.V. All rights reserved.

*Keywords:* Late Pliocene; onset of NHG; foraminiferal Mg/Ca; Panama closure

\* Corresponding author. Tel.: +49 4318802884; fax: +49 4318804376.

E-mail address: [gb@gpi.uni-kiel.de](mailto:gb@gpi.uni-kiel.de) (G. Bartoli).

## 1. Introduction

Pleistocene climate is characterized by a persistent succession of glacial-to-interglacial cycles driven by orbital forcing. However, these northern hemisphere glaciations (NHG) and large-scale Arctic sea ice have only appeared since the Late Pliocene (~3.2 Ma), a time, when a major reorganization of the ocean-climate system took place. This event appears approximately coeval with the final closure of the Central American Seaways (CAS) ending the advection of Pacific surface water into the Atlantic Ocean [3,4]. In this context, two questions are still controversial, (1) the precise timing of the final closure of the CAS and (2), whether a causal relationship exists between this closure and the onset of NHG and to which physical processes it may be ascribed [1].

Whereas intermediate-water circulation through the Panama Strait was gradually barred as early as 4.5–4.0 Ma with short-lasting re-openings near 3.8 and 3.4–3.3 Ma [2,5], a shallow-water connection continued far beyond 3.0 Ma [6]. This gateway ensured the advection of Pacific low-salinity surface water into the southern Caribbean, here weakening the North Atlantic salt transport. Combined  $\delta^{18}\text{O}$  and Mg/Ca records of *Globigerinoides sacculifer* used as proxy of surface water salinity at south Caribbean Site 999 [3,7] depict a first weak divergence of 0.0–0.4‰  $\delta^{18}\text{O}$  between Caribbean and Pacific sea surface salinity (SSS) records at 4.0–3.8 Ma. However, this minor offset remained constant further on, with a significant short-term convergence near 3.3 Ma. Only thereafter, we observe a second, renewed divergence with a  $\delta^{18}\text{O}$  offset, finally reaching 1‰ at 2.5 Ma, a divergence that is crucial for question (2), the potential processes in the ocean and atmosphere, that have led to NHG.

One model [8] suggests that the closure of the CAS has enhanced the advection of warm and saline water to northern high-latitudes which, in turn, increased North Atlantic Deep Water (NADW) production. This process led to higher evaporation and hence to more moisture supply to high latitudes, fueling the build-up of northern hemisphere ice-sheets. Increasing amplitude variations of Earth obliquity leading to periods with colder summers may have transformed the additional moisture into a permanent snow cover [2]. The orbital trend, however, has been reversed

after 2.2 Ma, whereas the Greenland ice sheet remained in place ever since and has acted as key albedo factor for the enhanced climate sensitivity to orbital forcing, characteristic of the Quaternary. Driscoll and Haug [9] postulate a different suite of processes, proposing that increased delivery of freshwater to the Arctic Ocean via the Siberian rivers has promoted formation of sea ice, enhancing the albedo thus cooling the North Polar region. However, pertinent records are still lacking.

To trace back potential changes in THC between 3.2 to 2.5 Ma, that may have served as trigger for NHG, we now present new submillennial-scale records of Mg/Ca-paleothermometry and stable isotopes from planktic and benthic foraminifers in the northern North Atlantic, a region crucial for the understanding of NHG (Fig. 1).

## 2. Study area and methods

ODP 984 (61.25°N, 24.04°W, 1648 m, Bjorn Drift) records the history of the Irminger Current (IC) and LSW (Labrador Sea Water, Upper NADW). DSDP 609 (49.52°N, 24.14°W, 3883 m, eastern flank of the Mid-Atlantic Ridge) records changes in NAC (North Atlantic Current), SSW (Southern Source Water), and in Lower NADW (LNADW).

### 2.1. Age control

At Site 984, magnetic stratigraphy suffered from drilling disturbance below 260 mbsf, at the base of the advanced hydraulic piston corer (APC) section [10] and thus was only measured back to 2.2 Ma (Reunion). Further back, biostratigraphic control was established by the last occurrence (LO) of *Ebriopsis cornuta* between 359.74 to 369.06 mbsf (2.61 Ma). In absence of any benthic  $\delta^{18}\text{O}$  record, Raymo tried to deduce a succession of marine isotope stages from the magnetic susceptibility record [11]. Proceeding from her estimates we established a revised stable-isotope stratigraphy using our new isotopic records of *Globigerina bulloides* and *Neogloboquadrina atlantica* and mixed benthic species (Fig. 2). This stratigraphic framework is compared with planktic and benthic isotopic records from Site 610 on the Rockall Plateau [12], much farther south, records



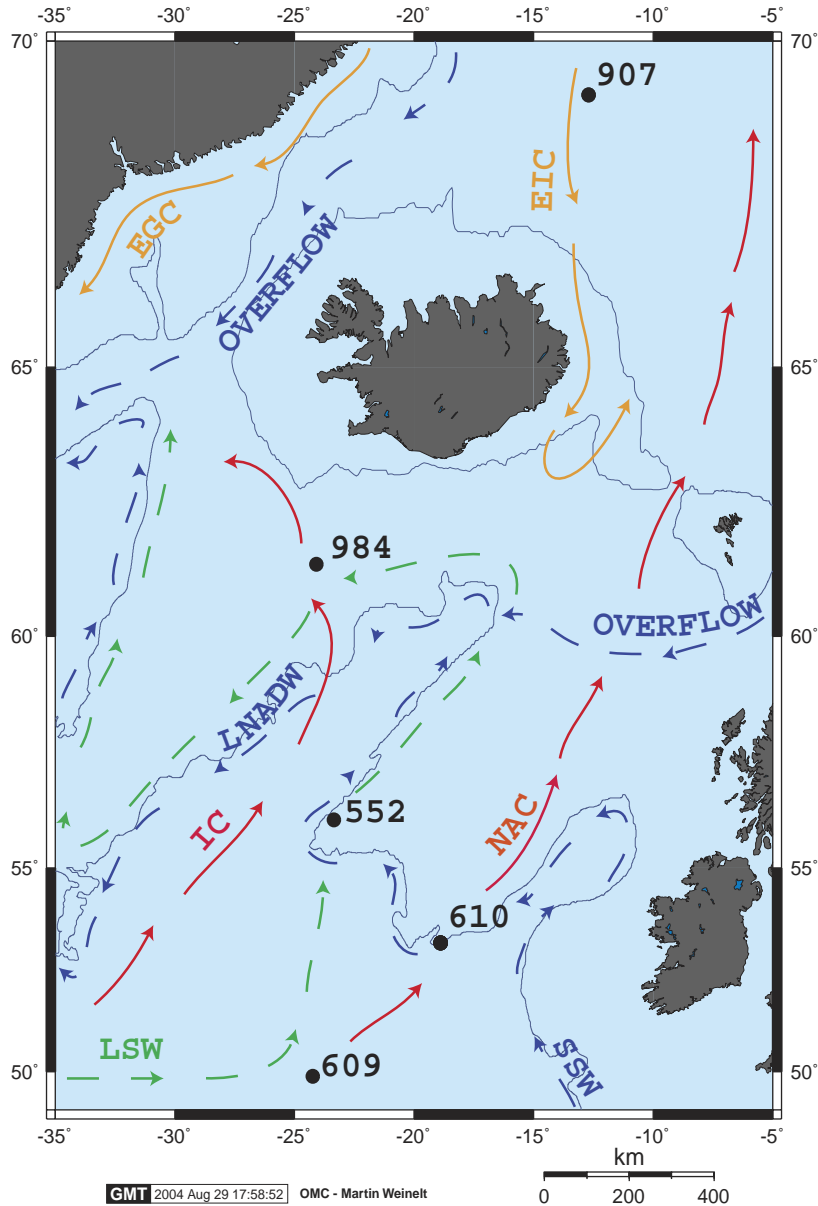


Fig. 1. Site locations (numbers) and modern surface (solid lines) and deep-water currents (broken lines) in the Northeast Atlantic. IC stands for Irminger Current, NAC for North Atlantic Current, EGC for East Greenland Current, EIC for East Iceland Current LSW for Labrador Sea Water, SSW for Southern Source Water, and NADW for North Atlantic Deep Water.

that extend back to MG6 (3.5 Ma), however, with a much lower resolution.

Direct orbital tuning could not be employed because of glacial-to-interglacial changes in sedimentation rate and various gaps in the records because of samples barren of foraminifers. Instead, age models of

ODP 984 and DSDP 609 are based on magneto- and biostratigraphic control points defined by the DSDP/ODP shipboard parties and on detailed tuning of the planktic  $\delta^{18}\text{O}$  (ODP 984) and benthic  $\delta^{18}\text{O}$  (DSDP 609) records to the standard benthic  $\delta^{18}\text{O}$  stratigraphy of ODP 846 [13]. Time resolution at ODP 984 gen-

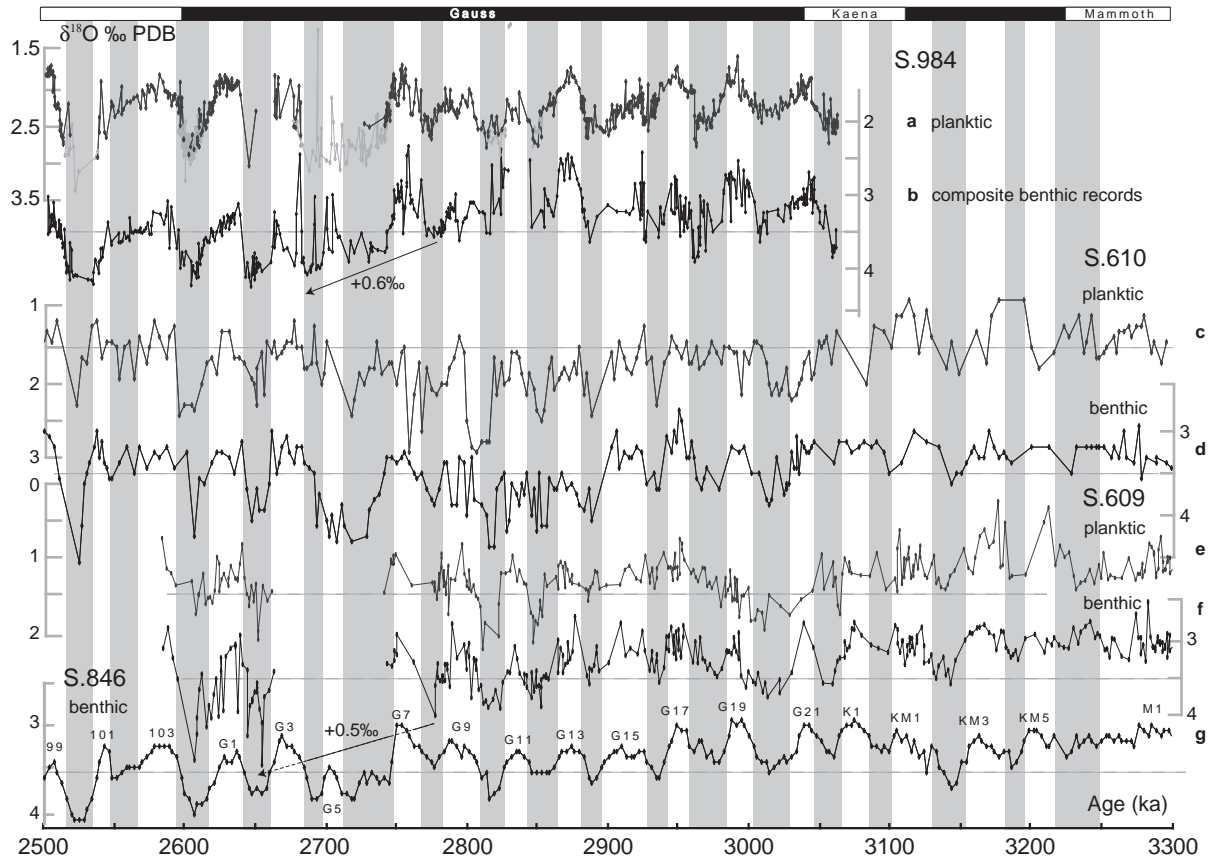


Fig. 2. Age control based on planktic and benthic  $\delta^{18}\text{O}$  records fitted to the orbitally tuned benthic record [13] of ODP 846. (a) Planktic  $\delta^{18}\text{O}$  record from ODP 984. Dark grey diamonds present data based on *G. bulloides* and light grey diamonds data based on *N. atlantica*. (b) Benthic  $\delta^{18}\text{O}$  from ODP 984 based on multiple foraminiferal species (see Methods). Arrows indicate long-term shift in glacial  $\delta^{18}\text{O}$  level from MIS G8 to MIS G4. (c) Planktic  $\delta^{18}\text{O}$  record from DSDP 610 [12]. (d) Benthic  $\delta^{18}\text{O}$  record from DSDP 610 [12]. (e) Planktic  $\delta^{18}\text{O}$  record from DSDP 609, based on *G. bulloides*. (f) Benthic  $\delta^{18}\text{O}$  from DSDP 609 based on multiple foraminiferal species (see Methods). Data for MIS G17 to M2 from R. Tiedemann (unpubl.). (g) Composite benthic  $\delta^{18}\text{O}$  from ODP 846 [13]. Numbers 101, 103, G1, etc., indicate interglacial Marine Isotope Stages.

erally amounts to 300–600 yrs. This unprecedented sampling resolution for Late Pliocene records enables us to compare millennial-scale climate changes prior and after the onset of NHG.

## 2.2. Stable isotope and Mg/Ca analysis

Monospecific samples for stable isotopes analyses usually consist of 1 to 5 benthic foraminifers (Table 1) and 1 to 30 *G. bulloides* specimens. They were sonicated in ethanol for 5–10 s, oven dried at 40 °C, and measured on the Kiel Device I/Finnigan MAT251 system with an analytical precision of 0.07‰ for

$\delta^{18}\text{O}$  and 0.05‰ for  $\delta^{13}\text{C}$  at the Leibniz Laboratory in Kiel. Benthic  $\delta^{18}\text{O}$  and  $\delta^{13}\text{C}$  values were corrected for species-specific offsets relative to *Uvigerina peregrina* and *Cibicides wuellerstorfi*, considered to represent equilibrium  $\delta^{18}\text{O}$  and  $\delta^{13}\text{C}$ , respectively, listed in Table 1.

Foraminiferal samples for Mg/Ca analyses were cleaned according to the protocol of Martin and Lea [18]. Analyses were partly performed at University of California in Santa Barbara (UCSB) on an ICP-SF-MS instrument (Thermo Finnigan Element). Most samples were analyzed at the Institute of Geosciences of Kiel University [19], using a simultaneous ICP-

Table 1

Benthic foraminifer species used for stable isotopes measurements and correction applied for species-specific offsets relative to *U. peregrina* and *C. wuellerstorfi* considered to represent equilibrium  $\delta^{18}\text{O}$  and  $\delta^{13}\text{C}$ , respectively

	$\delta^{18}\text{O}$	$\delta^{13}\text{C}$	References
<i>Cibicides wuellerstorfi</i>	+0.64	0.00	[14]
<i>Cibicides pachyderma</i>	+0.64	0.00	[14]
<i>Uvigerina peregrina</i>	0.00	not used	[14]
<i>Oridorsalis tener</i>	0.00	not used	[14]
<i>Elphidium excavatum</i>	+0.64	not used	[15]
<i>Cassidulina teretis</i>	0.00	not used	[16]
<i>Melonis barleeanum</i>	+0.36	not used	[17]

OES instrument (Spectro Ciros SOP) with cooled cyclonic spraychamber and microconcentric nebulization ( $200 \mu\text{l}\cdot\text{min}^{-1}$ ). Intensity ratio calibration followed the method of de Villiers et al. [20]. Internal analytical precision at Kiel and UCSB labs was estimated from replicate measurements and is better than 0.1–0.2% RSD corresponding to  $\pm 0.02$  °C. Replicate analyses on the same samples (cleaned and re-analyzed) showed a standard deviation of 0.09 mmol/mol, equivalent to a temperature error of 0.5 °C. Accuracy was checked by analyzing sets of consistency standards obtained from M. Greaves, University of Cambridge, and D. Lea, UCSB. Differences in molar Mg/Ca between the labs were  $\pm 1\%$ <sub>rel</sub>.

Paleo-sea surface temperatures (SST) were derived from the Mg/Ca ratio using the calibration curves of Mashiotta et al. [21] for *G. bulloides* ( $\pm 0.8$  °C). Since no specific calibration exists for *N. atlantica*, a species that became extinct at 1.8 Ma, and since using the calibration for its potential descendant *N. pachyderma* sin. may introduce some bias [22], we used the multispecies calibration of Elderfield and Ganssen [23] calculated for eight North Atlantic planktic species (including *N. pachyderma* sin.) as suggested by Anand et al. [24], where the overall calibration accuracy is  $\pm 0.7$  °C.

Deepwater temperatures (DWT) were obtained from five benthic foraminiferal species. Large parts of the DWT record employ the average of Mg/Ca-based temperature values measured on up to five different species with the intent to overcome the calibration uncertainties of single-species records. Individual calibration curves were used from Martin et al. [25] for *U. peregrina*, and from Lear et al. [26] for *Melonis barleeanum*, *C. wuellerstorfi*, *Oridorsalis*

*umbonatus*, and *C. pachyderma*. Calibration accuracy is  $\pm 1.4$  °C and  $\pm 1$  °C, respectively.

Ice volume was deduced from benthic  $\delta^{18}\text{O}$  after correction for DWT assuming constant deepwater salinity, with 0.1‰ seawater  $\delta^{18}\text{O}$  set equal to 10 m sea level [27].

In addition, census counts of selected benthic foraminifera species indicating environmental change were performed on the size fraction larger than 150 microns. Since many samples contain very low specimen numbers, only raw census data (individuals per 10 g dry sediment) are shown.

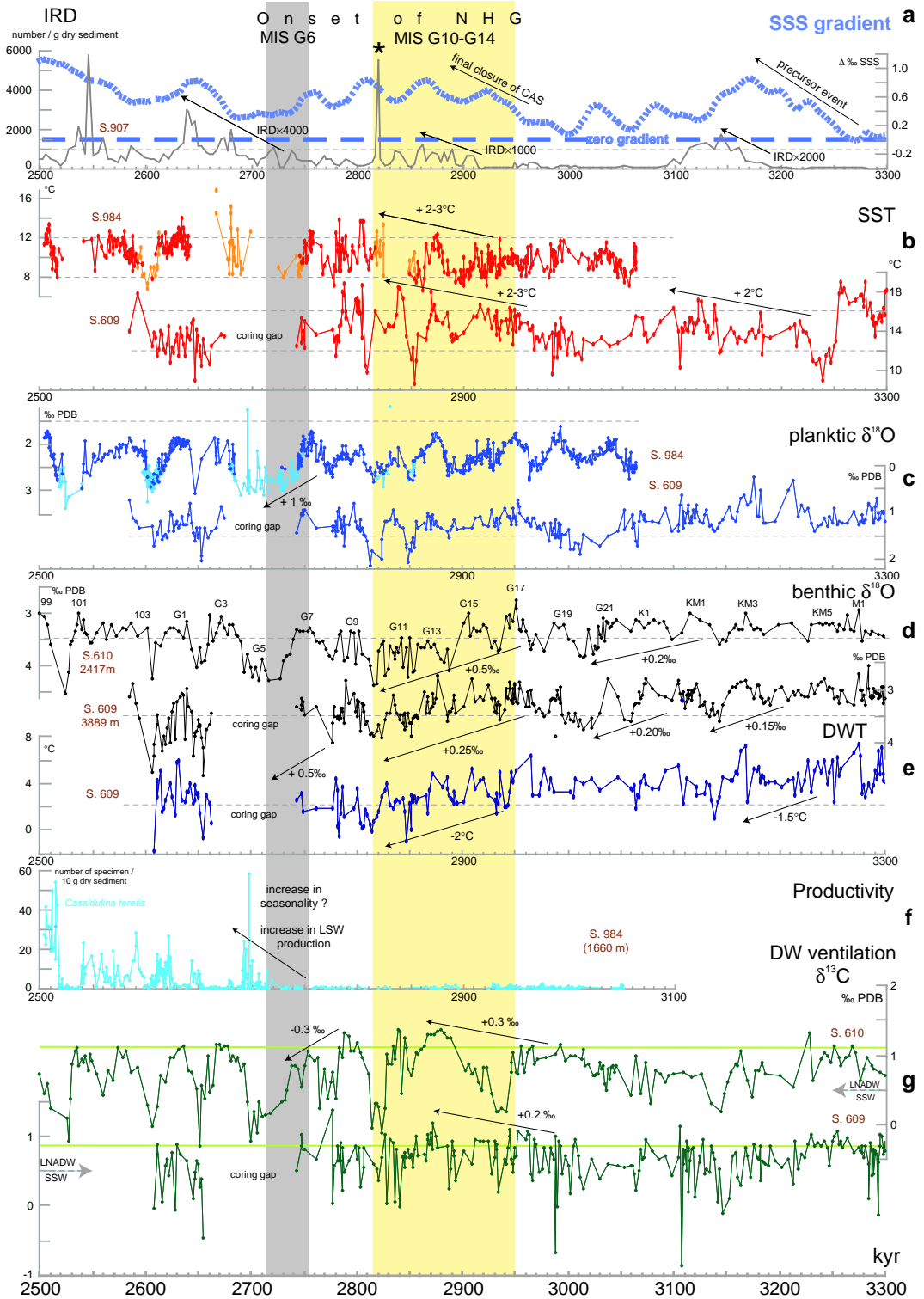
### 3. Results and discussion

#### 3.1. The Late Pliocene “climate crash”

The first occurrence of continental-scale ice sheets, especially on Greenland, is recorded as ice-rafted detritus (IRD) released from drifting icebergs into sediments of the mid- and high-latitude ocean. After a transient precursor event at 3.2 Ma, signals of large-scale glaciations suddenly started in the subpolar North Atlantic in two steps, at 2.92–2.82 and 2.74–2.64 Ma, that are Marine Isotopes Stages (MIS) G16-G10 and G6-G2 (e.g [28–30,12]) (Fig. 3a). The latter interval is also recorded for the onset of IRD deposition in the North Pacific [31].

This largely irreversible “climate crash” is also reflected by a profound and rapid reorganization of the northern high-latitude faunal provinces. For example, Atlantic planktic foraminiferal high-latitude provinces shifted dramatically southward while low-latitude provinces contracted [32]. In the Northwest Pacific, the proportion of *Coccolithus pelagicus*, today a typical cold-water phytoplankton species, jumped to 80% at 2.74 Ma [33]. This event is linked to the onset of NHG and precisely coeval with the separation of Pacific and Caribbean coccolithophorid assemblages, which results from the final closure of the Panama Isthmus [34].

The benthic foraminifer *Cassidulina teretis* which is adapted to low nutrients, harsher over-all conditions, and perhaps to higher seasonality became dominant at Rockall Plateau (DSDP 552) along with the first occurrence of IRD and cold-water planktic foraminifers [35]. Our new centennial-scale record of



ODP 984 now defines the sudden dominance of *C. teretis* in the Upper NADW level and the rapid reorganization of the North Atlantic THC at precisely 2.74 Ma (Fig. 3f).

The major expansion of global ice volume over MIS G16–G10 (2.93–2.82 Ma) is widely reflected in paleoceanographic records by a benthic 0.4‰  $\delta^{18}\text{O}$  increase [36,37]. In North Atlantic deepwater, the total increase from 3.2–2.8 Ma was stronger, amounting to 0.7‰ (Fig. 3d) which also documents a long-term cooling trend as deduced from ostracods [38] and from benthic foraminiferal Mg/Ca (Fig. 3e). Changes in North Atlantic DWT (DSDP 609) largely parallel the benthic  $\delta^{18}\text{O}$  variations and range from  $-1.8^\circ$  to  $7.4^\circ\text{C}$ , that is between temperatures as cold as in the modern Nordic Seas and temperatures that were  $\sim 4\text{--}5^\circ\text{C}$  warmer than today. Between 2.94 and 2.81 Ma, average DWT decreased by  $2^\circ\text{C}$  during both glacial and interglacials. This trend is consistent with a Late Pliocene  $\sim 4^\circ\text{C}$  cooling recorded at ODP 747 (Southern Ocean,  $\sim 1700\text{ m}$ ) [39] and a global average cooling of deepwater by  $\sim 3.5^\circ\text{C}$  from 5 Ma to today [40].

To better constrain the role of the THC over this critical time span, we employed three benthic  $\delta^{18}\text{O}$  records from different water depths in the northeastern Atlantic (Fig. 2). On the basis of coeval strong  $\delta^{13}\text{C}$  oscillations the benthic  $\delta^{18}\text{O}$  records at DSDP 609 (3900 m water depth) and DSDP 610 (2400 m water depth) [12] reveal an alternating glacial-to-interglacial influence of SSW and LNADW in addition to global ice volume and DWT changes.

In summary, Mg/Ca-based DWT record a coeval stepwise cooling by at least  $2^\circ\text{C}$ , equal to a 0.45–0.55‰  $\delta^{18}\text{O}$  increase (Fig. 3e). The remaining benthic  $\delta^{18}\text{O}$  increase by 0.2‰ suggests a growth of global ice volume during glacial stages equivalent to 20–25 m

sea level drop. A further drop by 20 m (equivalent to 0.2‰  $\delta^{18}\text{O}$ ) should be added to compensate for a slight salinity decrease because of increased admixture of SSW during glacial stages. Dwyer et al. [38] postulated a similar Late Pliocene ice volume increase by 0.4‰. For comparison, the present ice volume on Greenland corresponds to an equivalent of 0.06‰  $\delta^{18}\text{O}$  equal to  $\sim 7\text{ m}$  sea level [41]. At DSDP Sites 609 and 610 the  $\delta^{18}\text{O}$  increase from MIS G16–G10 matches the start of long-term IRD discharge in the northern North Atlantic, recording the general build-up of NHG, but precedes the final “climate crash” 2.74 Ma. Finally, at 2.82 Ma (immense IRD spike at MIS G10; Fig. 3a) the resulting sea level drop over glacial stages G16–G10 had progressed that far ( $\Delta 40\text{--}45\text{ m}$ ) that it produced a positive feedback on the closure of the CAS which then were very shallow.

During the transient glacial stages of sea level lowstand the Panama Isthmus probably dried up completely, but was breached once again during interglacial stages. Indeed this conceptual model is strongly supported by the antiphasing of glacial-to-interglacial SST oscillations on both sides of the Panama Isthmus, an anomaly that first appeared at 2.82 Ma (coeval with the sudden great American faunal interchange [42]), reappeared after 2.65 Ma, and continued beyond 2.5 Ma [3, Tiedemann, pers. comm.].

At intermediate depth (1700 m), ODP 984 records the evolution of LSW, a component of Upper NADW. Here, glacial benthic  $\delta^{18}\text{O}$  maxima jumped only once during MIS G8–G4, from 3.6‰ to 4.2‰ (Fig. 2b). This abrupt 0.6‰ increase matches a similar 0.5‰ shift at DSDP 609 at 3900 m depth, a shift that does not parallel a further DWT decrease (Fig. 3d and e) and thus documents a second major expansion of global ice volume by approximately 45 m sea level

Fig. 3. Paleoclimatic records for the Pliocene North Atlantic. (a) SSS anomaly (Caribbean– East Pacific) record of the final gradual closure of the CAS [3] and IRD record of NHG from ODP 907 (Iceland Plateau) [29] with new age model [30] based on tephra stratigraphy in number/g dry sediment. \*Marks first synglacial closure of CAS. (b) Mg/Ca-SST from ODP 984 and DSDP 609. Red dots are data obtained from *G. bulloides*, orange dots are data obtained from *N. atlantica*. (c) Planktic  $\delta^{18}\text{O}$  curves from ODP 984 and DSDP 609. Dark blue dots are data obtained from *G. bulloides*, light blue dots from *N. atlantica*. (d) Benthic  $\delta^{18}\text{O}$  records from DSDP 610 [12] (*Cibicides spp.*) and DSDP 609 (*C. wuellerstorfi*, *C. pachyderma*, *U. peregrina*, *O. tener* adjusted to *U. peregrina*). Numbers 101, 103, G1, etc. are interglacial Marine Isotope Stages. DSDP 609 data from MIS G17 to M2 were kindly provided by R. Tiedemann, Kiel. (e) Mg/Ca-based DWT record from S. 609, averaged values (see Methods). (f) Number of benthic foraminifera *Cassidulina teretis*/10 g dry sediment, a species characteristic of low nutrient input and high seasonality [59]. (g) Benthic  $\delta^{13}\text{C}$  records from ODP 984 (*C. wuellerstorfi* and *O. tener*), DSDP 610 [12] (*C. wuellerstorfi*), and from DSDP 609 (*C. wuellerstorfi* and *C. pachyderma*). Horizontal arrows mark Upper Pliocene water mass boundaries between SSW and LSW/LNADW [55]. Times of major change (2.95–2.82 Ma and 2.75–2.72 Ma) are highlighted. Labelled arrows outline major long-term trends (on top of glacial-to-interglacial variability).

equivalent, also recorded in the increase of IRD (Fig. 3a). In total, the sea level may have been lowered by 90 m with the onset of NHG. During MIS G6, the benthic  $\delta^{18}\text{O}$  signal at ODP 984 may provide a striking new insight into the scenario of the great “climate crash”. It appears to be linked to a major southward shift of the sites of NADW formation per analogy to that of the Last Glacial Maximum [43,44], that is from the Nordic Seas to the south of Iceland. Due to a lack of benthic foraminifers glacial MIS G16 to G10 are insufficiently recovered at ODP 984 to pick the first expansion of global ice volume between MIS G16 and G10.

### 3.2. Increase in poleward heat and salt transport in the North Atlantic

A long-term warming of the North Atlantic and accordingly, an increased poleward heat transport by the Gulf Stream–NAC system around 3 Ma along with the final closure of the CAS was first suggested by means of ostracodes and planktic foraminiferal assemblages from coastal deposits of the eastern U.S. and northern Iceland [45]. This conclusion was supported by various recent GCM models [46,47] which independently predict a SST rise of 2–3 °C for the northern North Atlantic.

With Mg/Ca-paleothermometry on the planktic foraminifera *G. bulloides* we now succeeded to generate two high-precision ( $\pm 0.5$ – $1.0$  °C) SST records of the NAC system with 300–600 yrs resolution. Accordingly, early Late Pliocene SST varied at ODP 984 (IC) during summer from 6.7–14.0 °C and further south-east, at DSDP 609 (NAC) from 8.5–19.1 °C (Fig. 2b), with Mg/Ca ratios ranging from 0.9–2.1 and 1.2–3.7 mmol/mol. In general, interglacial temperatures then were 7–8 °C warmer than today [48]. Pliocene glacial SST were as mild as interglacial SSTs today, i.e. ~4 °C warmer than during the last glacial [49].

Most striking is the pronounced interglacial SST rise by 2–3 °C from MIS G15 to G11 (2.95–2.83 Ma). The final high SST level persisted over all subsequent interglacial stages until at least 2.5 Ma (ODP 984; not yet analyzed at DSDP 609). At DSDP 609 short lasting SST maxima similar to those at 2.85 Ma were also recorded earlier, at MIS KM1 and M1 (3.12 Ma and >3.26 Ma; Fig. 3b). The outlined great warming around 2.85 Ma was felt as far north

as 80°N, as recorded by the warm-water dinoflagellate *Operculodinium centrocarpum* at ODP 911, northwest of Svålbard [50]. In the subarctic North Pacific (ODP 882) a 1‰ decrease in planktic  $\delta^{18}\text{O}$  suggests a similar 4 °C increase in SST from 2.85–2.77 Ma [31], prior to MIS G6, however, slightly subsequent to the great North Atlantic warming. The link to the North Atlantic is not yet understood.

Most likely, the great warming at 2.95–2.83 Ma and its precursors reflect an intensified poleward heat transport and meridional turnover of the ocean, events that went along with a significant increase in the discharge of IRD in the Greenland Sea (ODP 907) and a major cooling of deepwater during subsequent glacial stages. However, coeval interglacial planktic  $\delta^{18}\text{O}$  values at ODP 984 and DSDP 609 (Fig. 3c) did not get depleted by 0.45–0.70‰ during this time, as was expected from the 2–3 °C warming. This absent  $^{18}\text{O}$  depletion reflects a major increase in seawater  $\delta^{18}\text{O}$ , which in turn documents both a coeval amplification of the global  $\delta^{18}\text{O}$  ice effect (0.2–0.4‰ ?) plus an increase in SSS by 0.2–0.4 psu, resulting from an enhanced salt transport in the Gulf Stream–NAC system. This trend was predicted by the modelers for the final closure of the CAS.

In addition, our new evidence for a 100-ky long coeval increase in SST and IRD (Fig. 3a and b) suggests that the interglacial (but not glacial) warming of the North Atlantic has much enlarged the supply of atmospheric moisture to high altitudes at northern high latitudes to initiate NHG. Indeed, high-latitude vegetation patterns in Eurasia [51] reflect a distinct warming and moistening over this critical period. Accordingly, we follow the “snow gun hypothesis” [52] in assuming that this increase must have been large enough to overcome the opposed effect of the interglacial temperature rise that have enhanced ice melt, different from the reasoning of Berger and Wefer [53]. These processes occurred on top of a transient phase of increased Earth obliquity 3.0–2.3 Ma, which resulted in cooler summer climate.

However, the records of Atlantic THC do not reveal any particular (antecedent and/or coeval) events linked to the final “climate crash” of MIS G6, the second step of rapid climate deterioration. Since our records suffer from coring gaps and a lack of foraminifera tests in the pertinent glacial sections, we found no coeval, only a subsequent IRD rise and no increase

in SST, only an increase in benthic  $\delta^{18}\text{O}$  that correspond to an additional ice volume equivalent of >45-m sea level drop. Possibly, this second step of climate deterioration was linked to thermohaline events in the northern North Pacific (*sensu* [31,54]), which recently were also explained by GCM modeling as effects of the final closure of the CAS [55].

Unfortunately, present GCM models appear unsatisfactory to predict precisely the conditions of the atmospheric water cycle, necessary to build-up continental ice sheets in the Late Pliocene. They either show a Greenland ice sheet already prior to the great North Atlantic warming [47] and/or do not succeed to generate the proper preconditioning of the climate system to build up a new ice sheet specific for the times approx. 2.92–2.83 Ma—independent of short-term differential amplitudes of orbital forcing [46].

### 3.3. Replacement of NADW during glacials by SSW

After 2.85 Ma DWT cooled from  $\sim 2^\circ\text{C}$  almost down to the freezing point ( $-1.8^\circ\text{C}$ ) during glacial stages subsequent to MIS G12 at DSDP 609. This cooling either reflects an enhanced incursion of cold SSW and thus, a relative shoaling of NADW, or an increased contribution and/or cooling of northern high-latitude deepwater sources. Epibenthic  $\delta^{13}\text{C}$  records, a proxy for deepwater ventilation at DSDP 609 and DSDP 610 (Fig. 3g) show a gradual  $\delta^{13}\text{C}$  increase by 0.25–0.3‰ during interglacial stages G17 to G13, finally reaching 1.2–1.4‰. This high ventilation level forms a clear tracer of LNADW, whereas low  $\delta^{13}\text{C}$  values of 0.3‰ and less, which are confined to short-lasting glacial stages (KM2, G22, and from G18 onwards) record short-term incursions of SSW originating from the Antarctic Circumpolar Current [56,57]. Moreover, the gradual increase in NADW ventilation from  $\sim 2.95$  Ma to  $\sim 2.87$  Ma reflects an enhanced meridional turnover rate during interglacial stages, which is in harmony with the prominent surface warming of the northeast Atlantic (Fig. 3b). Enhanced interglacial velocities of LNADW were also reported from various sites along the West Atlantic margin from 3.20–2.75 Ma [58]. Moreover, enhanced NADW formation led to improved carbonate preservation in the Nordic Seas during this time [59]. Subsequent to MIS G9, interglacial epibenthic  $\delta^{13}\text{C}$

values at DSDP 610 again returned to the level prior to MIS G17, possibly reflecting a THC then slightly reduced.

Unfortunately, the highly fragmentary benthic  $\delta^{13}\text{C}$  record of ODP 984 (1660 m) (not shown) does not reveal any significant trend in the variations of LSW which today and during the last glacial constitutes most of the Upper NADW. However, increased abundance of *C. teretis* subsequent to MIS G7 (Fig. 3f), may serve as robust tracer of LSW/Upper NADW during glacial and stadial conditions [60]. This trend may document a shift of deepwater convection cells from the Nordic Seas to the south of Iceland, as we already deduced from the benthic  $\delta^{18}\text{O}$  record (Fig. 2b).

## 4. Conclusions

In summary, we find clear evidence based on IRD, SST, DWT, paleoproductivity, and deepwater ventilation records for an interglacial intensification of North Atlantic THC at 2.95–2.82 Ma (MIS G17–G11). This process has followed and probably accentuated the final closure of the CAS [3]. Moreover, it has promoted an increase in evaporation and poleward moisture transport from the North Atlantic as proposed by Haug and Tiedemann [2]. Beyond a short-term increase in Earth obliquity periods, increased moisture advection apparently has overcome the effects of interglacial warming and thus supported the fast build-up of continental ice sheets as documented by coeval IRD supply (Fig. 3a), as proposed by the “snow gun hypothesis” [52]. Finally, increased moisture advection to high latitudes has enhanced Siberian fluvial runoff and the formation of Arctic sea ice [9] and albedo, hence provided further support for the build-up of North Polar ice sheets. This conclusion neglects a potential global decrease in atmospheric  $\text{pCO}_2$  as potential factor driving the onset of NHG [61] because Pliocene changes in  $\text{pCO}_2$  actually observed are insignificant [62,63].

Subsequent to the major interglacial North Atlantic warming and first build-up of NHG 2.82 Ma (MIS G10), it took about 80,000 yrs (approximately two obliquity cycles) to arrive at the final “climate crash” during glacial MIS G6, when Quaternary-style [64] climate cycles were fully established,

sea level dropped further by 45 m, and floral and faunal provinces were rapidly reorganized on a global scale.

## Acknowledgments

We gratefully acknowledge D. Pak and G. L. Paradis who helped with Mg/Ca analyses in Santa Barbara, moreover N. Gehre and K. Kießling in Kiel. H. Gebhardt contributed to our species taxonomy at DSDP 609. N. Andersen, H. Heckt and H.H. Cordt helped with stable-isotope analyses. We thank many Kiel students for tedious but careful sample preparation. The IODP Bremen and East Coast Repositories are acknowledged for sampling assistance. The DSDP 609 isotopic record in part was kindly provided by R. Tiedemann, Kiel. A. Schmittner helped commenting on an early manuscript version; G. Haug contributed a lot to the quality of this paper by his critical review; A. Holbourn improved on our English wording. This work was supported by the Deutsche Forschungsgemeinschaft (DFG) within the Kiel Research Unit “Ocean Gateways”.

Data available on [www.pangaea.de/PangaVista?query=@Ref26496](http://www.pangaea.de/PangaVista?query=@Ref26496).

## References

- [1] A.C. Ravelo, D.H. Andreasen, M. Lyle, A.O. Lyle, M.W. Wara, Regional climate shifts caused by gradual global cooling in the Pliocene epoch, *Nature* 429 (2004) 263–267.
- [2] G.H. Haug, R. Tiedemann, Effect of the formation of the Isthmus of Panama on Atlantic Ocean thermohaline circulation, *Nature* 393 (1998) 673–676.
- [3] J. Groeneveld, S. Steph, R. Tiedemann, D. Nürnberg, D. Garbe-Schönberg, G.H. Haug, The final closure of the Central American Seaway, *Geology*, in preparation.
- [4] E. Maier-Reimer, U. Mikolajewicz, T. Crowley, Ocean general circulation model sensitivity experiment with an open Central American isthmus, *Paleoceanography* 5 (3) (1990) 349–366.
- [5] S. Steph, Pliocene stratigraphy and the impact of Panama uplift on changes in Caribbean and tropical East Pacific upper ocean stratification (6–2.5 Ma). Thesis of Kiel University, 2005, 158 pp, 52 figs, 10 tables, 8 appendices.
- [6] A.G. Coates, J.A. Obando, The geological evolution of the Central American Isthmus, in: J.B.C. Jackson, A.F. Budd, A.G. Coates (Eds.), *Evolution and Environment in Tropical America*, University of Chicago Press, Chicago, Illinois, 1996, pp. 21–56.
- [7] G.H. Haug, R. Tiedemann, R. Zahn, A.C. Ravelo, Role of Panama Uplift on oceanic freshwater balance, *Geology* 29 (3) (2001) 207–210.
- [8] L.D. Keigwin, Isotopic paleoceanography of the Caribbean and East Pacific: role of Panama Uplift in Late Neogene time, *Science* 217 (1982) 350–352.
- [9] N.W. Driscoll, G.H. Haug, A short circuit in thermohaline circulation: a cause for Northern Hemisphere Glaciation? *Science* 282 (1998) 436–438.
- [10] J.E.T. Channell, B. Lehman, Magnetic stratigraphy of North Atlantic sites 980–984, *Proc. ODP, Sci. Res.* 162 (1999) 113–130.
- [11] W.E.N. Austin, J.R. Evans, Benthic foraminifera and sediment grain size variability at intermediate water depths in the Northeast Atlantic during the late Pliocene–early Pleistocene, *Mar. Geol.* 170 (2000) 423–441.
- [12] H.F. Kleiven, E. Jansen, T. Fronval, T.M. Smith, Intensification of Northern Hemisphere glaciations in the circum Atlantic region (3.5–2.4 Ma) — ice-rafted detritus evidence, *Paleogeogr. Paleoclimatol. Paleoecol.* 184 (2002) 213–223.
- [13] R. Tiedemann, M. Sarnthein, N.J. Shackleton, Astronomic timescale for the Pliocene Atlantic  $\delta^{18}\text{O}$  and dust flux records of Ocean drilling Program site 659, *Paleoceanography* 9 (4) (1994) 619–638.
- [14] J.-C. Duplessy, et al.,  $^{13}\text{C}$  record of benthic foraminifer in the last interglacial ocean: implications for the carbon cycle and the global deep water circulation, *Quat. Res.* 21 (1984) 225–243.
- [15] M. Weinelt, G. Bartoli, H. Erlenkeuser, M. Sarnthein, Gateway-controlled decline of primary production in the northern North Atlantic at 2.74 Ma?, *Mar. Micropaleontol.* (submitted for publication).
- [16] E. Jansen, U. Bleil, R. Henrich, L. Kringstad, B. Slettemark, Paleoenvironmental changes in the Norwegian Sea and the Northwest Atlantic during the last 2.8 m.y.: deep sea drilling project/ocean drilling program sites 610, 642, 643 and 644, *Paleoceanography* 3 (1988) 563–581.
- [17] D.W. Graham, B.H. Corliss, M.L. Bender, L.D. Keigwin Jr., Carbon and oxygen isotopic disequilibria of recent deep-sea benthic foraminifera, *Mar. Micropaleontol.* 6 (1981) 483–497.
- [18] P.A. Martin, D.W. Lea, A simple evaluation of cleaning procedures on fossil benthic foraminiferal Mg/Ca, *Geochem. Geophys. Geophys.* 3 (2002) 8401.
- [19] D. Garbe-Schönberg, J. Groeneveld, G. Bartoli, M. Sarnthein, C. Dullo. High-precision Mg/Ca and Sr/Ca ratios of biogenic carbonate and seawater by simultaneous ICP-OES, *Geochem. Geophys. Geophys.*, in preparation.
- [20] S. de Villiers, M. Greaves, H. Elderfield, An intensity ratio calibration method for the accurate determination of Mg/Ca and Sr/Ca of marine carbonates by ICP-AES, *Geochem. Geophys. Geophys.* 3 (2002).
- [21] T.A. Mashiotta, D.W. Lea, H.J. Spero, Glacial-interglacial changes in Subantarctic sea surface temperature and  $\delta^{18}\text{O}$ -water using foraminiferal Mg, *Earth Planet. Sci. Lett.* 170 (1999) 417–432.



- [22] M. Kucera, J.P. Kennett, Causes and consequences of a middle Pleistocene origin of the modern planktonic foraminifer *Neogloboquadrina pachyderma* sinistral, *GSA Bull.* 30 (6) (2002) 539–542.
- [23] H. Elderfield, G. Ganssen, Past temperature and  $\delta^{18}\text{O}$  of surface ocean waters inferred from Mg/Ca ratios, *Nature* 405 (2000) 442–445.
- [24] P. Anand, H. Elderfield, M.H. Conte, Calibration of Mg/Ca thermometry in planktonic foraminifera from a sediment trap time series, *Paleoceanography* 18 (2) (2003) 1050.
- [25] P.A. Martin, et al., Quaternary deep sea temperature histories derived from benthic foraminiferal Mg/Ca, *Earth Planet. Sci. Lett.* 198 (2002) 193–209.
- [26] C.H. Lear, Y. Rosenthal, N. Slowey, Benthic foraminiferal Mg/Ca-paleothermometry: a revised core-top calibration, *Geochim. Cosmochim. Acta* 66 (19) (2002) 3375–3387.
- [27] R.G.A. Fairbanks, 17,000-year glacio-eustatic sea level record: influence of glacial melting rates on the Younger Dryas event and deep-ocean circulation, *Nature* 342 (1989) 637–642.
- [28] E. Jansen, J. Sjøhølm, Reconstruction of glaciation over the past 6 Myr from ice-borne deposits in the Norwegian Sea, *Nature* 349 (1991) 600–603.
- [29] E. Jansen, T. Fronval, F. Ranck, J.E.T. Channell, Pliocene–Pleistocene ice rafting history and cyclicity in the Nordic Seas during the last 3.5 Myr, *Paleoceanography* 15 (2000) 709–721.
- [30] C. Lacasse, P. van den Bogaard, Enhanced airborne dispersal of silicic tephra during the onset of Northern Hemisphere glaciations, from 6 to 0 Ma records of explosive volcanism and climate change in the subpolar North Atlantic, *Geology* 30 (7) (2002) 623–626.
- [31] M.A. Maslin, G.H. Haug, M. Sarnthein, R. Tiedemann, The progressive intensification of northern hemisphere glaciation as seen from the North Pacific, *Geol. Rundsch.* 85 (1996) 452–465.
- [32] R.C. Thunell, P. Belyea, Neogene planktonic foraminiferal biogeography of the Atlantic Ocean, *Micropaleontology* 28 (4) (1982) 381–398.
- [33] T. Sato, S. Yuguchi, T. Takayama, K. Kameo, Drastic change in the geographical distribution of the cold-water nannofossil *Coccolithus pelagicus* (Wallich) Schiller at 2.74 Ma in the Late Pliocene, with special reference to glaciation in the Arctic Ocean, *Mar. Micropaleontol.* 52 (2004) 181–193.
- [34] K. Kameo, T. Sato, Biogeography of Neogene calcareous nannofossils in the Caribbean and eastern equatorial Pacific: floral response to the emergence of the Isthmus of Panama, *Mar. Micropaleontol.* 39 (2000) 201–218.
- [35] D. Schnitker, High resolution records of benthic foraminifera in the Late Neogene of the northeastern Atlantic, *DSDP Init. Rept.* 81 (1989) 611–622.
- [36] C.H. Lear, H. Elderfield, P.A. Wilson, Cenozoic Deep-Sea temperatures and global ice volumes from Mg/Ca in benthic foraminiferal calcite, *Science* 287 (2000) 269–272.
- [37] L.E. Lisiecki, M.E. Raymo, A Pliocene–Pleistocene stack of 57 globally distributed benthic  $\delta^{18}\text{O}$  records, *Paleoceanography* 20 (2005) PA1003.
- [38] G.S. Dwyer, et al., North Atlantic deepwater temperature change during the Late Pliocene and Late Quaternary climatic cycles, *Science* 270 (1995) 1347–1350.
- [39] K. Billups, D.P. Schrag, Paleotemperatures and ice volume of the past 27 Myr revisited with paired Mg/Ca and  $^{18}\text{O}/^{16}\text{O}$  measurements on benthic foraminifera, *Paleoceanography* 17 (2002) 1003–1014.
- [40] C.H. Lear, Y. Rosenthal, J.D. Wright, The closing of a seaway: ocean water masses and global climate change, *Earth Planet. Sci. Lett.* 210 (2003) 425–436.
- [41] J.M. Gregory, P. Huybrechts, S.C.B. Raper, Threatened loss of the Greenland ice-sheet, *Nature* 428 (2004) 616.
- [42] S.D. Webb, The great American faunal interchange, in: A.G. Coates (Ed.), *Central America: A Natural and Cultural History*, Yale University Press, New Haven, 1997, pp. 97–122.
- [43] J.-C. Duplessy, et al., Surface salinity reconstruction of the North Atlantic Ocean during the last glacial maximum, *Oceanol. Acta* 14 (4) (1991) 311–324.
- [44] U. Pflaumann, et al., Glacial North Atlantic: sea-surface conditions reconstructed by GLAMAP 2000, *Paleoceanography* 18 (3) (2003) 1065.
- [45] H.J. Dowsett, et al., Micropaleontological evidence for increased meridional heat transport in the North Atlantic Ocean during the Pliocene, *Science* 258 (1992) 1133–1135.
- [46] A. Klocker, M. Prange, M. Schulz, Testing the influence of the Central American Seaway on orbitally forced northern hemisphere glaciation, *Geophys. Res. Lett.* 32 (2005) L03703.
- [47] A. Schmittner, B. Schneider, Simulating the impact of the Panamanian seaway closure on ocean circulation, marine productivity and nutrient cycling, in preparation.
- [48] S. Levitus, T. Boyer, *World Ocean Atlas 1994, Temperatures*. NOAA Atlas NESDIS4, 4, US. Department of Commerce, Washington, D. C., 1994.
- [49] S. van Kreveld, et al., Potential links between surging ice sheets, circulation changes, and the Dansgaard–Oeschger cycles in the Irminger Sea, 60–18 kyr, *Paleoceanography* 15 (2000) 425–442.
- [50] J. Knies, J. Matthiessen, C. Vogt, R. Stein, Evidence of “Mid-Pliocene (~3 Ma) global warmth” in the eastern Arctic Ocean and implications for the Svålbard/Barents Sea ice sheet during the late Pliocene and early Pleistocene (~3–1.7 Ma), *Boreas* 31 (2002) 82–93.
- [51] Baikal Drilling project BDP-96 (Leg II) Members, Continuous paleoclimate record recovered for last 5 million years, *EOS* 78 (51) (1997) 597–601.
- [52] M.L. Prentice, R.K. Matthews, Tertiary Ice Sheet Dynamics: the snow gun hypothesis, *J. Geophys. Res.* 96 (1991) 6811–6827.
- [53] W. Berger, G. Wefer, *Expeditions into the Past: paleoceanographic studies in the South Atlantic*, in: G. Wefer, W. Berger, G. Siedler, D. Webb (Eds.), *The South Atlantic: Present and Past Circulation*, Springer-Verlag, Berlin, 1996, pp. 363–410.
- [54] G.H. Haug, et al., North Pacific seasonality and the glaciation of North America 2.7 million years ago, *Nature* 433 (2005) 821–825.

- [55] T. Motoi, W.-L. Chan, S. Minobe, H. Sumata, North Pacific halocline and cold climate induced by Panamanian Gateway closure in a coupled ocean-atmosphere GCM, *Geophys. Res. Lett.* 32 (2005) L10618, doi:10.1029/2005GL022844.
- [56] A.C. Ravelo, D.H. Andreasen, Enhanced circulation during a warm climate, *Geophys. Res. Lett.* 27 (7) (2000) 1001–1004.
- [57] M. Sarnthein, et al., Changes in east Atlantic deepwater circulation over the last 30,000 years: eight time slice reconstructions, *Paleoceanography* 9 (2) (1994) 209–267.
- [58] M. Gröger, R. Henrich, T. Bickert, Variability of silt grain size and planktic foraminiferal preservation in Plio/Pleistocene sediments from the western equatorial Atlantic and Caribbean, *Mar. Geol.* 201 (2003) 307–320.
- [59] R. Henrich, K.-H. Baumann, R. Huber, H. Meggers, Carbonate preservation records of the past 3 Myr in the Norwegian–Greenland Sea and the northern North Atlantic: implications for the history of NADW production, *Mar. Geol.* 184 (2002) 17–39.
- [60] A.E. Jennings, G. Helgadottir, Foraminiferal assemblages from the fjords and shelf of eastern Greenland, *J. Foraminiferal Res.* 24 (1994) 123–144.
- [61] T.J. Crowley, Modeling pliocene warmth, *Quat. Sci. Rev.* 10 (1991) 275–282.
- [62] M.E. Raymo, B. Grant, M. Horowitz, G.H. Rau, Mid-Pliocene warmth: stronger greenhouse and stronger conveyor, *Mar. Micropaleontol.* 27 (1996) 313–326.
- [63] J. Zachos, M. Pagani, L. Sloan, E. Thomas, K. Billups, Trends, rhythms, and aberrations in global climate 65 Ma to present, *Science* 292 (2001) 686–693.
- [64] B. Pillans, T. Naish, Defining the quaternary, *Quat. Sci. Rev.* 23 (2004) 2271–2282.

## Chapter 5

# Late Pliocene millennial-scale climate variability in the northern North Atlantic prior and after the onset of northern hemisphere glaciation.

Bartoli, G.\*, Sarnthein, M., Weinelt, M.  
Christian-Albrechts-Universität Kiel, Institute für Geowissenschaften,  
Olshausenstr. 40, D-24098 Kiel, Germany.  
\* corresponding author: gb@gpi.uni-kiel.de

*submitted to Paleoceanography*

## Abstract

Sediments recovered at ODP Site 984 on the Reykjanes Ridge provided multicentennial-scale records of Late Pliocene climate change over the onset of Northern Hemisphere glaciation (NHG), 2.95-2.82 Ma. Short-term climate variations prior and after the onset of continent-wide glaciation were compared to test the hypothesis, whether Dansgaard-Oeschger (DO) cycles may have been triggered by continental ice breakouts. During two selected interglacial stages prior to and after NHG (G15 and G1) climate variability resembled that found in the Holocene and the mid-Pliocene warm period. In contrast, DO-like periodicities of 1470, 2900, and 4400 yr indeed only occurred in glacial stages after the onset of NHG (G14, G6, and 104), but not in stage 20 prior to the onset. These results suggest a causal link between DO cycles and the Late Pliocene onset of ice breakouts in the North Atlantic.

**Keywords:** Late Pliocene, North Atlantic climate variability, millennial-scale climate variations, onset of Northern Hemisphere Glaciation

## 1 Introduction

During recent years a number of paleoceanographic reconstructions focused on the study of centennial-to-millennial-scale climate variability, with the aim to closer constrain future climate change through the discovery of cyclicities that may perpetuate into the next millennium. In particular, Dansgaard-Oeschger (DO) cycles, which follow a ~1470-yr periodicity (and multiples of 1470 yr) are characteristic of glacial and semiglacial periods. These cycles were described from numerous Late Pleistocene records world-wide (Voelker et al., 2002) and from glacial stages as far back as 1.86-1.93 Ma (McIntyre et al., 2001). However, their origin may still be assigned to various forcings.

The freshwater release of continental ice breakouts and melting icebergs in the North Atlantic form the main potential trigger for DO cycles as inferred from model experiments (Paillard & Labeyrie, 1994; Sakai & Peltier, 1997; Ganopolski & Rahmstorf, 2001) and paleoceanographic reconstructions (Bond & Lotti, 1995; van Kreveland et al., 2000). If so, the 1470-yr periodicity may only be expected for times after the onset of major Northern Hemisphere glaciation (NHG), 2.82-2.95 Ma, that is as far back as the Late Pliocene (Bartoli et al., 2005). In contrast, DO cycles won't be present in paleoclimatic records prior to the build-up of major ice-sheets on the Northern Hemisphere. This initial build-up has first been documented by increasing

sediment portions of ice-rafted debris (IRD) to the north of Iceland (Figs. 1 and 2A, Bartoli et al., 2005) and by subsequent IRD pulses starting with Marine Isotope Stages (MIS) G6 to 104 (2.74–2.6 Ma) at ODP Site 984 to the south of Iceland (Fig. 2A; this study).

On the other hand, there are a number of other forcing mechanisms proposed for the origin of DO cycles, including internal oscillations of the ocean (Schulz et al., 2002), which can hardly be validated by paleoceanographic records. Arbic et al. (2004) claimed that Heinrich events (extreme DO stadials) are released by exceptionally high tides in the Labrador Sea, freeing huge numbers of icebergs in this area. This mechanism would tie the DO periodicity to the 1.8-kyr lunar cycle (Keeling & Whorf, 2000).

Furthermore, changes in solar forcing, even if small in its contribution to the energy balance, may have a significant impact on millennial-scale climate variability (Hoyt & Schatten, 1993) and trigger pertinent cyclicities (Shindell et al., 1999; van Geel et al., 1999; Hyde & Crowley, 2002). In particular, solar forcing may be responsible for pulses in the discharge of IRD with a temporal spacing of ~900–1000 and 500-yr in the Holocene (Bond et al., 2001; Sarnthein et al., 2003; Hu et al., 2003).

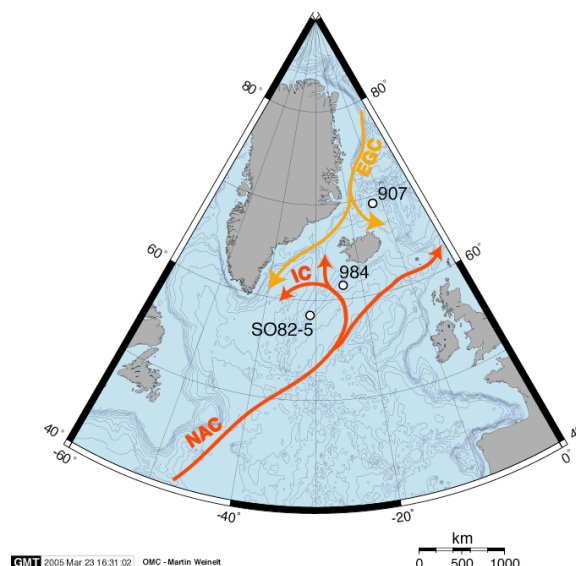
Muscheler & Beer (2004) demonstrated that the solar 208-yr de Vries cycle may be responsible for the 1456-yr cycle through a distinct cycle in amplitude variations comprising seven de Vries cycles each. Likewise, new results from an intermediate-complexity climate model suggest that DO events may be forced by periodic melt-/freshwater pulses following both the interfering (solar) 87-yr Gleissberg and 210-yr de Vries cycles (Braun et al., 2005).

On the basis of the U/Th dated  $\delta^{18}\text{O}$  record from the Hulu Cave speleothem (Wang et al., 2001; supplemented), Clemens (2005) suggested that the age model of the GISP2 record may be biased and that DO cycles may not follow a period of 1470-yr but rather periods of 1490-, 1190-, and 1667 years. These three periodicities may be heterodynes of potential solar cycles of 286, 352, 512 and 703 yr deduced from tree ring records. In case solar and/or lunar cycles have triggered the DO cycles, it should be possible to trace back DO cycles as a sort of pertinent feature beyond the times of NHG, in addition to shorter solar periodicities.

The present study reports of millennial-scale climate variability in the northern North Atlantic over Late Pliocene glacial and interglacial stages to better constrain the alternative models outlined above: (1) Whether DO cycles have been mainly triggered by meltwater pulses released by continental ice breakouts or (2) whether they present an ongoing cyclic process induced by solar forcing. Previous studies of Pliocene millennial-scale climate variability (Steenbrink et al., 2003; Draut et al., 2003; Niemitz & Billups, 2005; Becker et al., 2005) did not consider the role of the onset of NHG. Other studies which proposed a self-enhancing feedback mechanism between sub-Milankovitch cycles and NHG did not reach a time resolution sufficient to resolve DO cycles (Willis et al., 1999).

In this paper, we analyze paleoclimate records with multi-centennial-scale resolution for various selected glacial and interglacial stages at ODP Site 984 from the period 3.1–2.5 Ma both in the time and frequency domains to compare the climate variability prior and after the onset of NHG. In addition, we compare variations in Late Pliocene glacial stages subsequent to the onset of NHG with those in Pleistocene MIS 3, where DO cycles have originally been defined (Grootes et al., 1993).

**Fig. 1:** North Atlantic bathymetry, site locations, and modern surface water currents. EGC stands for East Greenland Current, IC for Irminger Current, and NAC for North Atlantic Current.



## 2 Methods and Core location

ODP Site 984 (Fig. 1) is located on the Reykjanes ridge (61°25 N, 24°04 W, 1648 m w. d.) and provides continuous high-resolution sediment records from 2.5 to 3.1 Ma, here documenting the Late Pliocene history of the warm Irminger Current and the Upper North Atlantic Deepwater (Fig. 2). Bartoli et al. (2005) presented the long-term paleoceanographic trends found at this site. The IRD record of Site 984 is compared with that from ODP Site 907 (Jansen et al., 2002) to the north of Iceland (69°15 N, 12°42 W, 1800 m w. d.).

Cores of Site 984 were sampled with 10-cm resolution of 2-cm thick sediment slices (i.e., 20 cc). This sampling resolution was increased to 3 cm for a special high-resolution study of glacial stage MIS 104.

For stable-isotope analyses, planktic foraminiferal tests of *Globigerina bulloides* and *Neogloboquadrina atlantica* were sonicated in ethanol for 5-10 s, oven-dried at 40°C, and measured on the Kiel Device I/Finnigan MAT251 system with an analytical precision of 0.07‰ for  $\delta^{18}\text{O}$  at the Leibniz Laboratory in Kiel. In larger samples containing >15 specimens, we measured stable isotopes on triplicates of 5 planktic specimens each to constrain the signal-to-noise ratio within a single isotope average value. The intra-sample variability varies between 0.68‰ within MIS G21 to 0.20‰ within MIS G1 (Fig. 2). In some glacial stages planktic foraminiferal specimens were extremely rare or absent. The benthic  $\delta^{18}\text{O}$  record is based on data of five different epibenthic species, corrected for species-specific offsets relative to *Uvigerina peregrina* considered to represent equilibrium  $\delta^{18}\text{O}$  as described in detail in Bartoli et al. (2005).

Planktic  $\delta^{18}\text{O}$  records reflect variations in local sea surface salinity (SSS), global ice volume, and SST. Combined with Mg/Ca-based SST, planktic  $\delta^{18}\text{O}$  should provide insights into SSS and ice volume changes.

10-25 planktic foraminiferal specimens each were cleaned for Mg/Ca analyses, following the protocol of Martin & Lea (2002). Samples were analyzed with a simultaneous ICP-OES instrument. The calibration of the Mg/Ca intensity ratio followed de Villiers et al. (2002). Internal analytical precision is better than 0.1-0.2 % relative standard deviation corresponding to  $\pm 0.02^\circ\text{C}$ . Replicate analyses on the same samples (cleaned and re-analyzed) showed a standard deviation of 0.09 mmol/mol, equivalent to a temperature error of 0.5°C. Paleosea surface temperatures (SST) were derived from the Mg/Ca ratio of *G. bulloides* with an accuracy of  $\pm$

0.8°C (Mashiotta et al., 1999) and from *N. atlantica* with an accuracy of  $\pm 0.7^\circ$  C (Elderfield & Ganssen, 2000) (details in Bartoli et al., 2005). The samples apparently did not suffer extensive carbonate dissolution.

To study the history of iceberg discharge, up to 300 lithic grains of IRD were counted in the size fraction  $>150 \mu\text{m}$ . Values are given as number of grains/g dry sediment.

The magnetic susceptibility at Site 984 during the Late Pliocene potentially records bottom current velocity changes, with interglacial lows in magnetic susceptibility corresponding to high velocity and improved carbonate preservation (Austin & Evans, 2000; *sensu* Kissel et al. 1999). An outstanding 1-cm sampling resolution (Jansen et al., 1996) may provide the best insights into submillennial-scale climate variability.

To study the short-term climate variability, we performed spectral analysis on planktic  $\delta^{18}\text{O}$ , Mg/Ca-based SST, and magnetic susceptibility records (for Nyquist frequencies see Fig. 2). The IRD record was not employed for spectral analysis because of the non-cyclic and highly discontinuous character of the IRD discharges. Also, the raw Mg/Ca data set was not employed here because of the offset between the signals of the two different species used.

The REDFIT program (Schulz & Mudelsee, 2002) permitted the use of non-evenly spaced data and to define the red-noise level. In addition, we analyzed our records using the Blackman-Tukey method from the AnalySeries 1.2 software (Paillard et al., 1996) for which the time series were interpolated to obtain evenly spaced data sets. Results from these two different techniques are compared to better constrain real and potentially “artificial” frequencies. Spectral analyses were employed to both the entire interval from 3.1 to 2.5 Ma and to six selected single glacial and interglacial stages, which display the highest and sufficient time-resolution sufficient to resolve sub-millennial-scale periodicities. In addition, we performed cross-spectral analyses on paleohydrographic signals (SST,  $\delta^{18}\text{O}$ ) versus IRD / magnetic susceptibility using the B-cross function of the AnalySeries 1.2 package. However, the results were not meaningful because of rather different sampling densities in the various records. AnalySeries was also employed for filtering selected periodicities out of paleoclimatic records.

All data (including the age models) are available on [www.pangaea.de/](http://www.pangaea.de/)

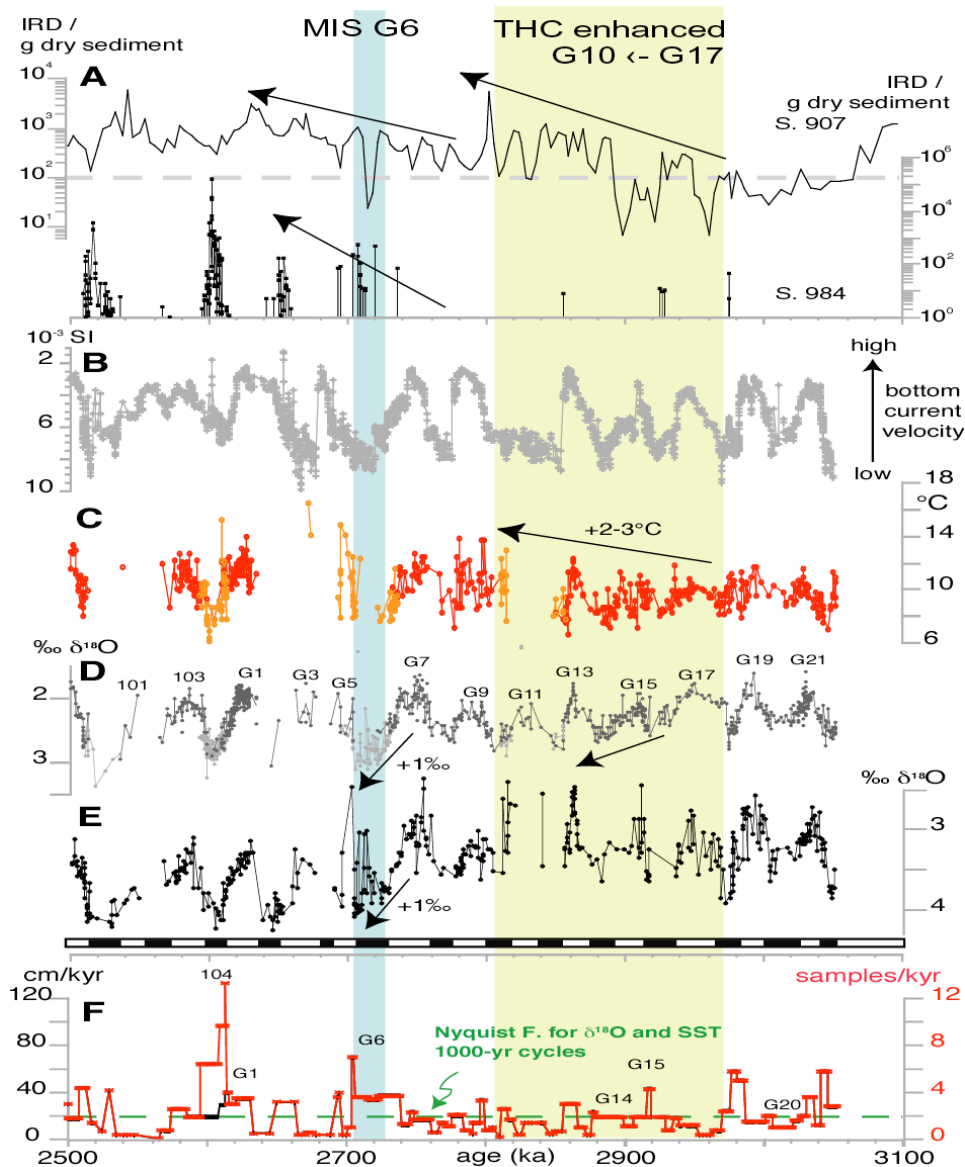


**Fig. 2:** Summary of paleoclimatic records from Site 984 (LR04 age model). **A.** IRD records are displayed on a log-scale in number / g dry sediment. IRD record from Site 907 is from Jansen et al. (2000), age control modified by Lacasse & van der Bogaard (2002). **B.** Magnetic susceptibility record in  $10^{-5}$  SI units (Jansen et al., 1996). **C.** Mg/Ca-based SST in °C measured on *N. atlantica* (orange dots) and on *G. bulloides* (red dots). **D.** Planktic  $\delta^{18}\text{O}$  record in ‰ PDB, with interglacial stages numbered and results of replicate samples measured on *N. atlantica* (grey) and *G. bulloides* (black). **E.** Benthic  $\delta^{18}\text{O}$  record in ‰ PDB. Black bars reflect glacial stages. **F.** Sedimentation rates in cm/kyr (left) and sampling resolution in number of samples/kyr (right) obtained from the LR04 age model. The dotted line represents a Nyquist Frequency (F.) of 1000 yr. Arrows outline long-term trends. Data points spaced by more than 10 kyr are not interconnected.

### 3 Age model

Initially, our age model (Bartoli et al., 2005) was obtained from tuning the planktic  $\delta^{18}\text{O}$  to the astronomically tuned benthic  $\delta^{18}\text{O}$  record of Pacific Site 846 (Tiedemann et al., 1994; Shackleton et al., 1995). A single biostratigraphic datum, Last Occurrence (LO) of *Ebriopsis cornuta*, was identified between 359.74 and 369.06 mbsf and provides an age of 2.61 Ma (Jansen et al., 1996) coeval with MIS 104.

However, Lisiecki & Raymo (2005) recently published a new stacked benthic  $\delta^{18}\text{O}$  record for the Pliocene-Pleistocene, named LR04. This stack integrates 25 benthic  $\delta^{18}\text{O}$  records over the time span 1-3 Ma and 12 records for the interval 3-5 Ma and thus appears more reliable than a single benthic  $\delta^{18}\text{O}$  record, since the noise-to-signal ratio is greatly reduced. Therefore, we also tuned the planktic  $\delta^{18}\text{O}$  record of Site 984 to the LR04 stack by graphical correlation of peaks and stage boundaries using the AnalySeries 1.2 software (Paillard et al., 1996). The differences between the two stratigraphies using (1) the benthic  $\delta^{18}\text{O}$  record at Site 846 and (2) the LR04 records are presented in Fig. 3A and B. In particular, the records disagree with regard to MIS G6. When based on LR04, this stage starts almost 20 kyr later, at 2.71 Ma, and hence is 10 kyr shorter than in the reference record of Site 846. Moreover, MIS G8 is much less accentuated in the LR04 stack than at Site 846. Likewise, MIS G7, G16 (ending ~15 kyr later), and G20 are getting much more expanded. MIS 102 is shifted back in time and is expanded by 10 kyr. On the other hand, MIS G22 is shifted forward by 10 kyr as are MIS G14, G12, G8, G4, and 102, so that the age differences of stage boundaries in total do not exceed 10 kyr.

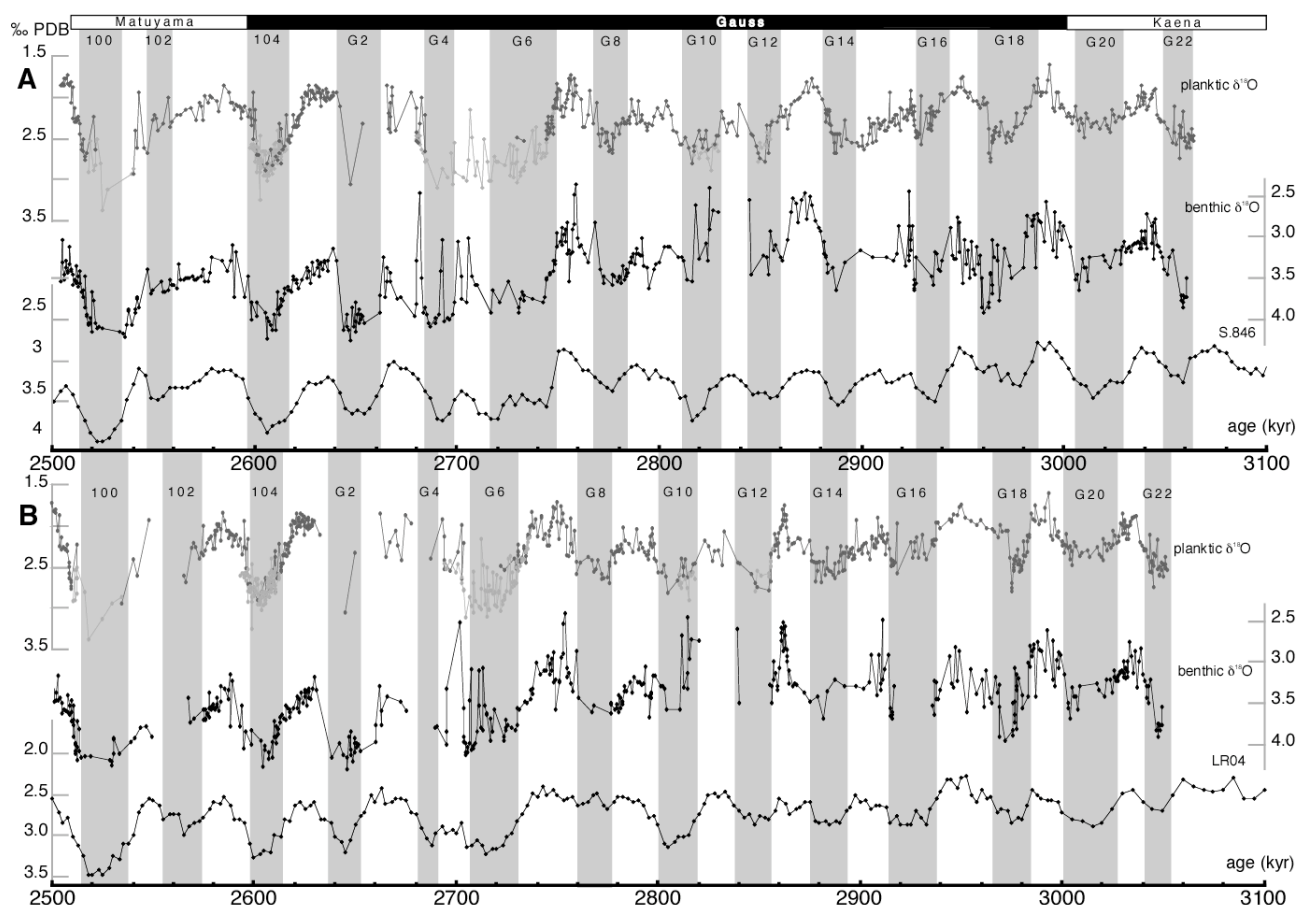
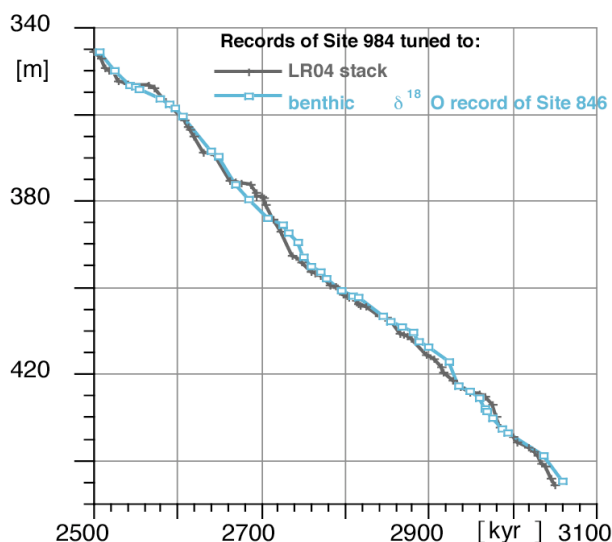


**Fig. 3:** Two different age models applied to Site 984. Glacial stages are numbered and indicated by grey bars, (A) tuned to benthic  $\delta^{18}\text{O}$  record of Pacific Site 846, (B) tuned to benthic  $\delta^{18}\text{O}$  stack LR04. Light grey dots are  $\delta^{18}\text{O}$  values obtained from *N. atlantica*, dark grey dots obtained from *G. bulloides*. Black dots figure composite benthic  $\delta^{18}\text{O}$  data obtained from 5 different epibenthic foraminifera taxa. Data points spaced by more than 10 kyr are not interconnected.



In the LR04 age model for Site 984, the initial lower part of stage G3 has been split off and attached to G5. Moreover, stages 101 and 102 are more clearly defined, in order to fit more accurately the structures of the LR04 stack. The age differences between the two age models are summarized in Fig. 4. The straight-line character of the age-depth curve suggests fairly continuous sedimentation rates.

**Fig. 4:** Depth-age plot for the two age models shown in Fig. 3 for Site 984.



The sedimentation rates resulting from the LR04 age model are ranging from 4 to 58 cm/kyr (average is 26 cm/kyr; Fig. 2F). In most cases the Nyquist frequency is sufficient to study millennial-scale climate fluctuations. In between the 76 stratigraphic tie points of the stage boundaries, sedimentation rates were assumed constant and the ages were deduced by linear interpolation. The resulting age model may be accurate within a range of 1-4 kyr in terms of absolute age. An age uncertainty of 1 kyr is based on the time resolution of the LR04 stack for the interval 2.5-3.1 Ma. The uncertainty of 4 kyr is derived from differences in core depth between the last occurrence of IRD and the position of the massive planktic  $\delta^{18}\text{O}$  decrease near the top of MIS 104.

With the new age model, each 2-cm thick sample represents a time slice of 55 to 500 yr (on the average 77 yr). At 10-cm sampling resolution, the spacings between the mid-points of two samples correspond to 172-2500 yr and average to 384 yr.

The alteration of paleoclimatic signals by bioturbation mixing can be regarded as insignificant since accumulation rates of organic carbon are as low as 0.5-1.0 g C m<sup>-2</sup> y<sup>-1</sup>, corresponding to a homogeneous mixing depth of 2 cm and less (Trauth et al., 1997).

In summary, the main uncertainty of the age model at Site 984 derives from the lack of sufficiently reliable absolute age control points to fix Late Pliocene glacial and interglacial stages boundaries. In contrast, the duration of single glacial and interglacial intervals may be more reliable and sufficient for an attempt of spectral analysis, although far from perfect.

To better constrain the sensitivity of cyclicities to the two different modes of age control, we calculated the response of frequency spectra to changes in the age model for MIS 104 (Fig. 5). In total, we obtained approximately the same number of cyclicities. However, the LR04 age model resulted in significant (and well familiar) periodicities at 1490 and 900-yr, while the Site 846 age model resulted in periodicities of 1180 and 800 yr. Similar variations were obtained for other stages (not shown).

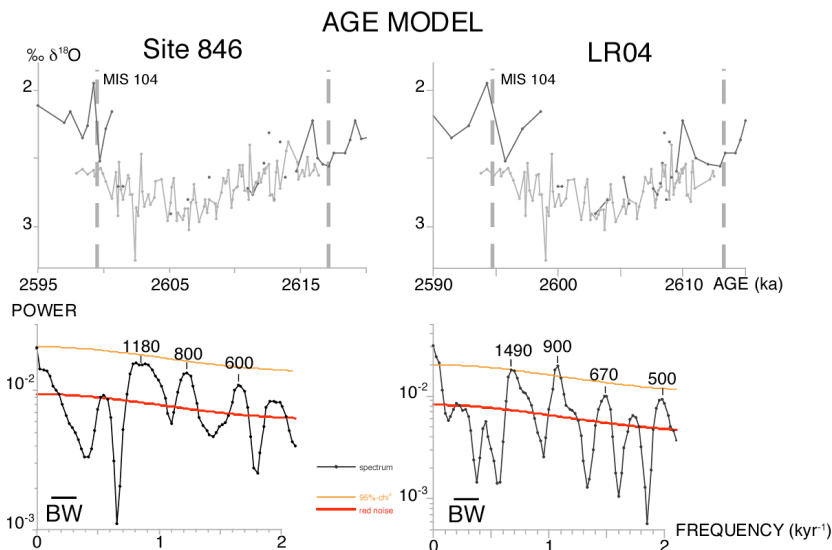


**Fig. 5:** Sensitivity-test of the frequency distributions obtained by REDFIT for the planktic  $\delta^{18}\text{O}$  record of MIS 104 for two different age models (Site 846 and LR04). Light grey diamonds are  $\delta^{18}\text{O}$  values obtained from *N. atlantica*, dark grey diamonds from *G. bulloides*. Onset and end of MIS 104 are marked by vertical broken lines. BW = bandwidth. Red-noise and the 95-% confidence levels are marked as bold red line and orange thin line, respectively.

## 4 Results

### 4.1 Summary of short-term variability between 3.1 and 2.5 Ma

At Site 984, to the south of Iceland, IRD deposition (Fig. 2A) is marking the onset of NHG after 2.74 Ma (MIS G6). In general, high IRD values parallel high magnetic susceptibility. However, magnetic susceptibility reveals distinct glacial-to-interglacial orbital cycles already much earlier than IRD deposition, that is throughout the whole Pliocene section (40/42-kyr periods in Fig. 6), with low values corresponding to interglacials and high values matching glacials, except for stages G11 and G5 (Fig. 2B). Amplitudes of glacial-to-interglacial shifts in magnetic susceptibility remained constant (100-1000  $10^{-5}$  SI units) from 3.1 to 2.5 Ma. This finding suggests that Late Pliocene magnetic susceptibility variations at Site 984 were hardly correlated with variations in IRD but rather with changes in bottom current velocity (Austin & Evans, 2000), as first proposed by Kissel et al. (1999) for the Late Pleistocene.

The 41-kyr obliquity cycle also dominates the planktic  $\delta^{18}\text{O}$ , SST, and benthic  $\delta^{18}\text{O}$  records (Fig. 6), as to be expected for high-latitude climate records (Ruddiman et al., 1986). In addition, SST reveal a weak 24-kyr precessional signal.

When averaging the ocean variability over 600 kyr (3.1-2.5 Ma), also some sub-Milankovitch-scale frequencies have been revealed (Table 1), although these results may suffer from the large uncertainties in absolute age control. Also most periodicities hardly reach the 95-% confidence level (Fig. 6). The spectra show some power near 15 kyr in the SST and benthic  $\delta^{18}\text{O}$  records. Benthic  $\delta^{18}\text{O}$  values also show a weak 7-kyr periodicity. Further periodicities occur near 2.3-2.5, 2.8-3.2, and 3.8-4.0 kyr. A 1.7/1.8-kyr period may occur in the planktic  $\delta^{18}\text{O}$  record. Shorter periodicities are possibly displayed in the magnetic susceptibility record near 1300, 900, and 450 yr (Fig. 6).

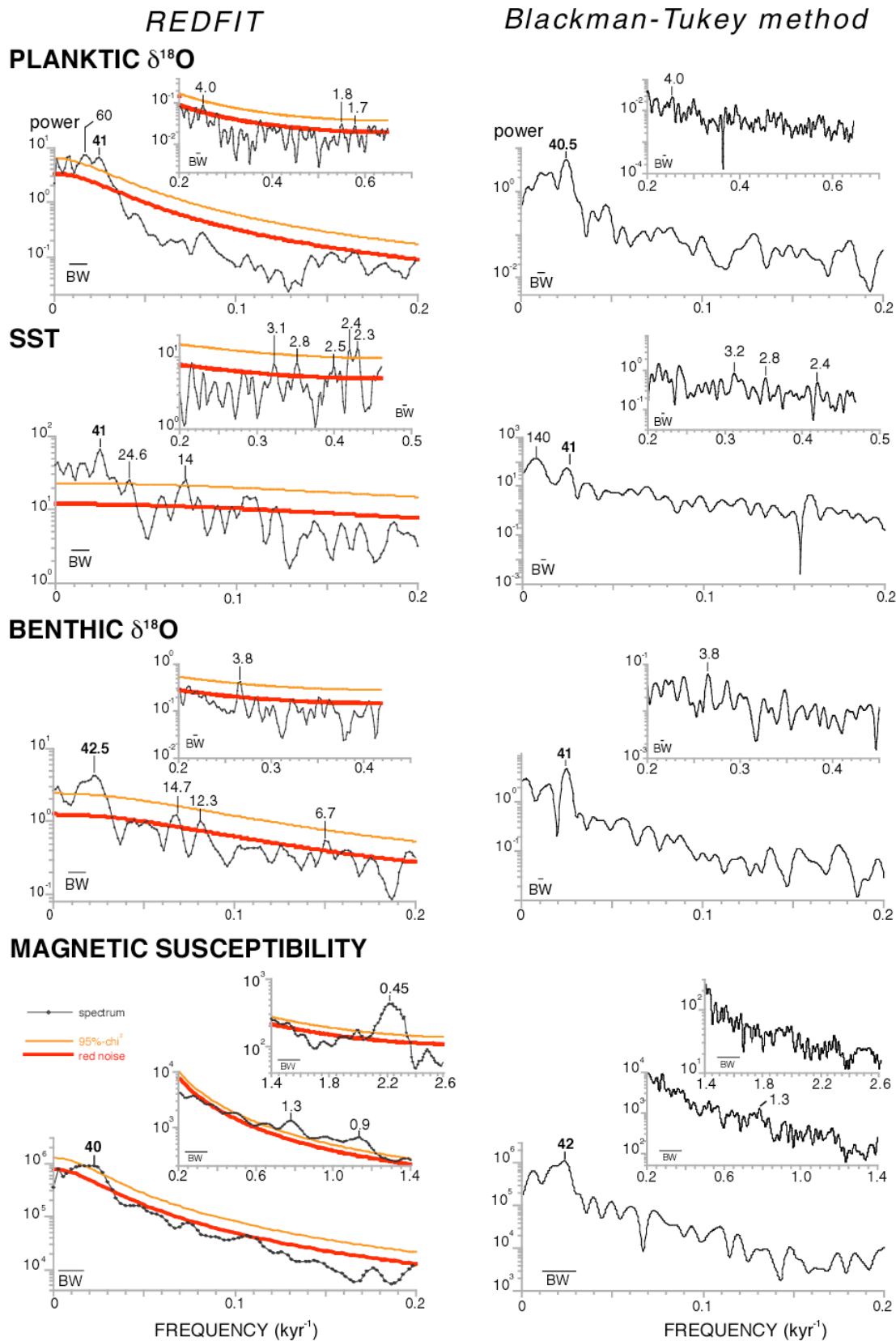


**Fig. 6:** Frequency spectra of Site 984 paleoclimatic records, summarizing the total interval 2.5–3.1 Ma, obtained with the REDFIT (left panel) and Blackman-Tukey (AnalySeries package; right panel) methods. Statistically most significant periods are indicated in kyr (41-kyr cycle in bold). BW = bandwidth. Red-noise and 95-% confidence levels are marked as bold red and orange thin lines, respectively. Graphs with frequencies  $>0.2 \text{ kyr}^{-1}$  are inserted.

**Table 1:** Periodicities displayed in various paleoclimatic records analyzed summarising the total interval 2.5-3.1 Ma (Fig. 6).

Periodicities	Planktic $\delta^{18}\text{O}$	SST	Benthic $\delta^{18}\text{O}$	Magnetic Susceptibility
41 kyr	x	x	x	x
24 kyr		x		
15 kyr		x		
12 kyr			x	
7 kyr			x	
ca. 4 kyr	x		x	
2.8-3 kyr		x		
2.4-2.5 kyr	x			
1.8 kyr	x			
1.3 kyr				x
900 yr				x
450 yr				x

#### 4.2 Millennial-scale variability during interglacial stages

Millennial-scale variability was analyzed in detail for interglacial MIS G1, and G15, where planktic  $\delta^{18}\text{O}$  and SST records have a time-resolution of 300 to 770 yr (Fig. 7, Table 2). Planktic  $\delta^{18}\text{O}$  values display short-term variations of 0.1-0.3‰ over intervals of ~300 to ~800 yr, subtle changes that exceed the analytical error ( $2\sigma = 0.14\text{‰ } \delta^{18}\text{O}$ ). Likewise SST varies by 1-3°C over intervals of ~300 to ~800 yr. Short-term variations in magnetic susceptibility (100-yr resolution) hardly exceed 20-70  $10^{-5}$  (Fig. 7). This variability is similar to that in a number of other interglacial stages, which, however, are in part less well sampled (Figs. 2, 3).

In the frequency domain (Fig. 8 and Table 3) planktic  $\delta^{18}\text{O}$  and magnetic susceptibility display a broad range of (mostly unknown) periodicities both prior (G15) and after (G1) the onset of NHG. Some spectral power occurs near 2500 and 1100/1200 yr, but also near better known periods of 1800 and 1540/1600 yr. In addition, magnetic susceptibility shows (significant) periodicities of 500 to 950 yr. Interglacial SST values vary at (inverse) frequencies of 1750 yr and its multiples of 3500 and 7000 yr before the onset of NHG (MIS G15). Subsequently (MIS G1) the SST signal is dominated by the 1470-yr DO cycle.

**Table 2:** Amplitudes of short-term variations in planktic  $\delta^{18}\text{O}$  and SST, specified for selected isotopic stages (Fig. 7). Glacial stages are in italics.

MIS	Planktic $\delta^{18}\text{O}$ ( $\Delta\text{‰}$ )	SST ( $\Delta^\circ\text{C}$ )
G1	0.1-0.2	1-3
G15	0.2-0.3	1-3
<i>104</i>	<i>0.3-0.4</i>	<i>2.6-3</i>
<i>G6</i>	<i>0.4</i>	--
<i>G14</i>	<i>0.3</i>	<i>1-3</i>
<i>G20</i>	<i>0.2-0.3</i>	<i>1-1.6</i>

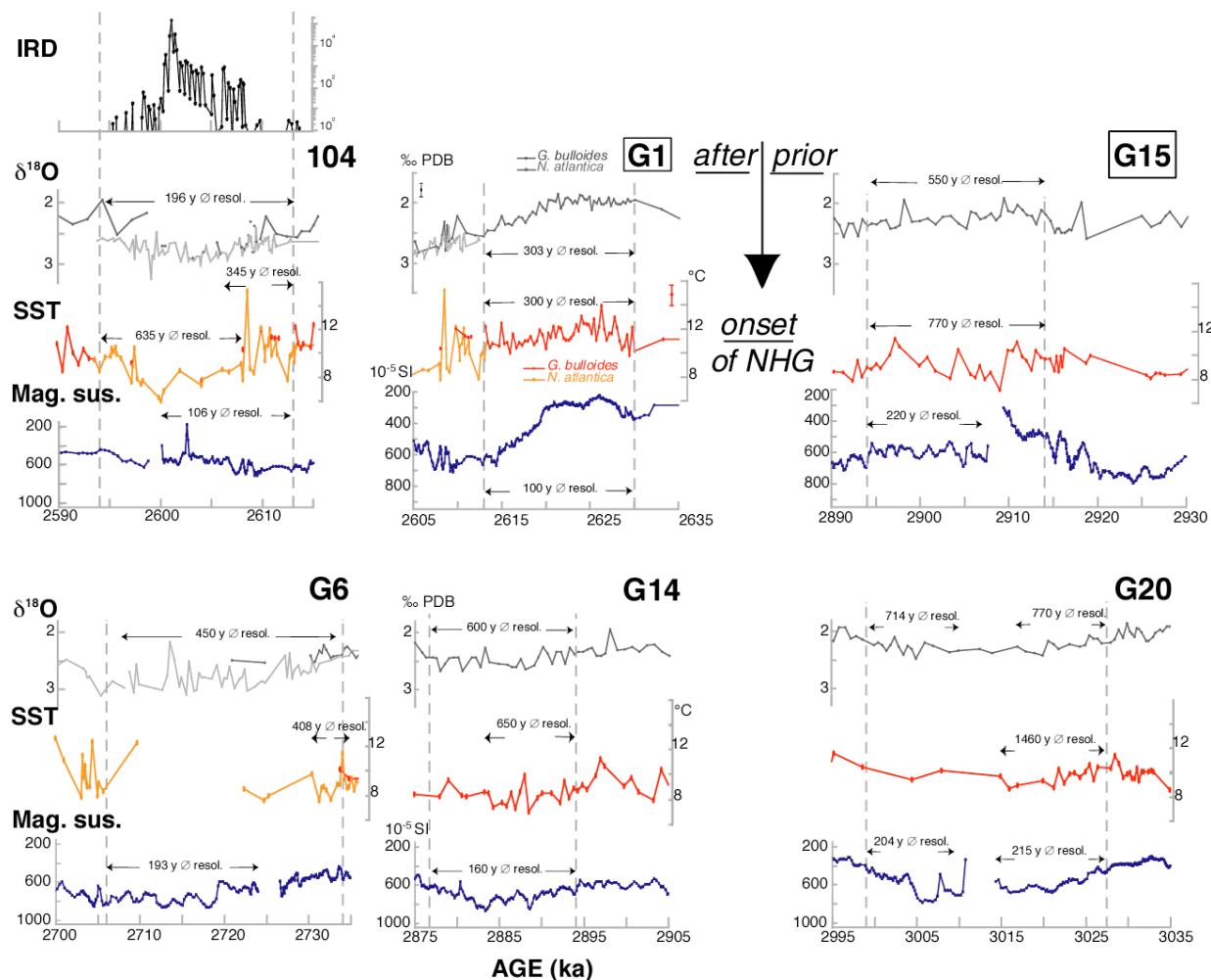


**Fig. 7:** Planktic  $\delta^{18}\text{O}$ , SST, and magnetic susceptibility records for selected interglacial (framed numbers) and glacial stages prior and after the onset of NHG (vertical arrow). Onset and end of each stage are marked by vertical broken lines. Horizontal arrows delineate the intervals where spectral analyses have been performed (see Fig. 8), numbers indicate average time resolution. SST measured on *N. atlantica* (orange dots) and on *G. bulloides* (red dots). Planktic  $\delta^{18}\text{O}$  measured on *N. atlantica* (grey) and *G. bulloides* (black). IRD values for MIS 104 plotted on log-scale in numbers of IRD / g dry sediment.

#### 4.3 Millennial-scale variability during glacial stages

After MIS G6, IRD discharge became a persistent feature at Site 984 during glacial stages, indicating permanent ice cover on Greenland (Fig. 2). Large amounts of IRD were deposited for the first time during MIS 104 (~5000 grains/g 2.608-2.598 Ma; Fig. 7). Based on visual inspection, distinct IRD maxima within MIS 104 are spaced by 500-560 yr.

To study climate variability over the onset of NHG, we focused our high-resolution study on glacial stages 104, G6, G14, and G20, the time resolution of which is ranging from 200 yr to 900 yr (Figs. 2, 7). Details of planktic  $\delta^{18}\text{O}$ , SST, and magnetic susceptibility records are shown in Fig. 7 and Table 2.

In the time domain, planktic  $\delta^{18}\text{O}$  displays variations of 0.1-0.4‰ PDB over intervals of ~350 yr prior to the onset of NHG (MIS G20). Late Pliocene glacial SST are poorly recorded because of low or zero abundance of planktic foraminifer specimens during glacial stages MIS

G6 and MIS G20. Where properly documented, SST varies by up to 3°C over ~600-yr intervals during G20. Short-term variations in magnetic susceptibility reach 40-160  $10^{-5}$  SI. After the onset of NHG (MIS G14, G6, and 104), planktic  $\delta^{18}\text{O}$  variations slightly increased to ~0.3-0.4‰ over intervals of 500-yr. Moreover, planktic  $\delta^{18}\text{O}$  variations occasionally obtained an asymmetric pattern with an abrupt “warming” of ~0.3-0.4‰ over 1.3 kyr, followed by a more gradual “cooling” over 2-3 kyr, such as found during MIS G6, perhaps also during MIS 104. Short-term amplitudes in SST variations have increased to 3°C, in magnetic susceptibility up to 60-300  $10^{-5}$  SI, possibly a signal of increased changes in bottom current activity after MIS G14.

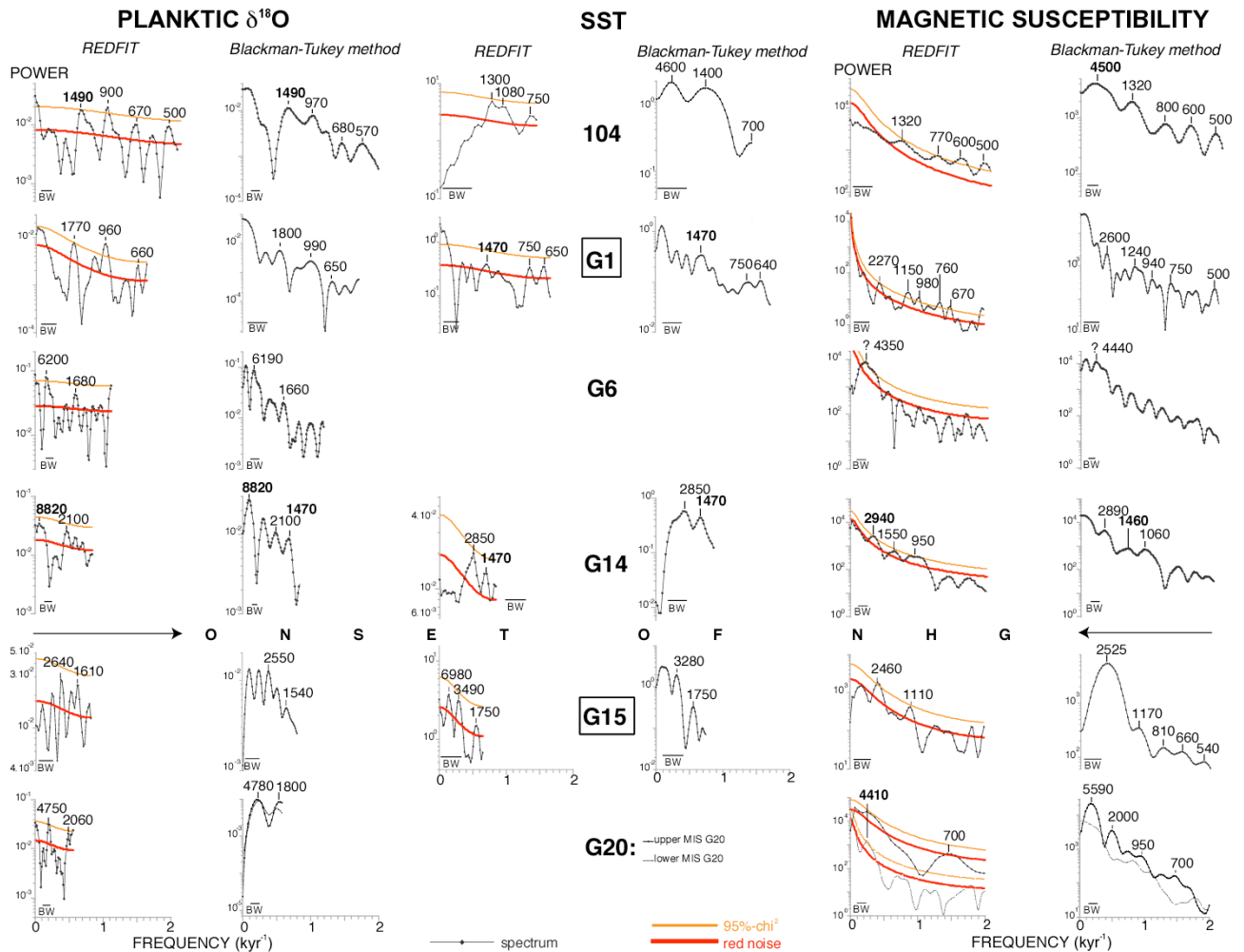


**Fig. 8:** Frequency spectra of selected interglacial (framed numbers) and glacial paleoclimatic records from Site 984 (bold numbers are marine isotope stages), obtained with the REDFIT (left-hand panels) and Blackman-Tukey (AnalySeries package; right-hand panels) methods. Periods statistically most significant are labelled in yr. BW = bandwidth. Red-noise and 95-% confidence levels are marked as bold red and orange thin lines, respectively. Spectral analyses were performed on the various proxy records depicted in Fig. 7 and on the intervals delineated by arrows, with the following exceptions: The SST record for MIS 104 was analyzed from 2606 to 2613 ka, the planktic  $\delta^{18}\text{O}$  record for MIS G20 was analyzed from 3000-3010 ka and from 3017-3027 ka, the magnetic susceptibility record for MIS G20 was analyzed from 2999-3007 ka and from 3015-3027 ka. Onset of NHG is marked by horizontal arrows.

In the frequency domain, planktic  $\delta^{18}\text{O}$  and magnetic susceptibility display strong periodicities near 5.6, 4.4-4.7, and 1.8/2.0 kyr (Fig. 8 and Table 3B) prior to the onset of NHG (MIS G20). Magnetic susceptibility also shows 950 and 700-yr cyclicities.

After the onset of NHG, the periodicities displayed by planktic  $\delta^{18}\text{O}$ , SST, and magnetic susceptibility are listed in Table 3B for stages G14, G6, and 104. Planktic  $\delta^{18}\text{O}$  shows some power near 9 kyr during stage G14, and near 6 kyr during MIS G6. Most important, all oceanographic variables (planktic  $\delta^{18}\text{O}$ , SST, and magnetic susceptibility) started to display significant periodicities at 1460-1490 yr and its multiples, at 2800/2900 yr, and at 4500 yr. Moreover, planktic  $\delta^{18}\text{O}$  and magnetic susceptibility also vary on shorter periodicities near 950 yr, 600-700 yr, and 450-550 yr, displayed during both MIS G14 and 104.

**Table 3:** Climate periodicities in selected Late Pliocene isotopic stages (Fig. 8). x refers to stages after the onset of NHG (MIS G1, 104, G6, and G14), o to stages prior to the onset of NHG (MIS G15 and G20), and xo to stages both prior and after the onset of NHG. DO-style periods are marked bold. A. Interglacial stages. B. Glacial stages.

**A.**

Periodicities (yr)	Planktic $\delta^{18}\text{O}$	SST	Magnetic Susceptibility
7000		x	
<b>4410</b>			x
3500		x	
2300-2600	x		xo
1750	o	x	
1600	x		
<b>1470</b>		o	
1150-1170			o
950	o		o
750		o	xo
650	o	o	
500			xo

**B.**

Periodicities (yr)	Planktic $\delta^{18}\text{O}$	SST	Magnetic Susceptibility
<b>8820</b>	x		
ca. 6000	x		
<b>ca. 4500</b>	o		o
2800-2900		x	x
2100-2200	x		
1800	o		
<b>1470-1490</b>	x	x	x
1200-1300		x	
950	x		xo
750		x	x
650	x		xo
500	x		x

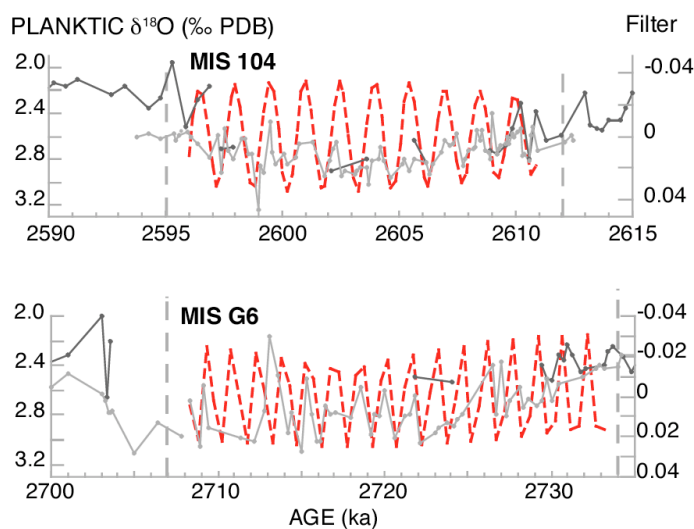
## 5 Discussion

### 5.1 Changes in climate variability over the onset of NHG

It is the major objective of this study to search for significant changes in millennial-scale climate variability over the times prior and after the onset of NHG. Such changes may be considered as evidence for the conceptual model that DO cycles have mainly been triggered by continental ice breakouts and meltwater pulses, since DO periodicities have been largely constrained to semiglacial and glacial periods in the middle and late Pleistocene, intervals when the sea level was lowered by  $> 45$  m (Schulz et al., 1999). In case this concept is right, no DO-style periodicities must be expected for the times prior to the onset of NHG. On the other hand, if solar or lunar cyclicities, which have been dominant during the Holocene interglacial (Bond et al., 2001; Sarinthein et al., 2003; Keeling & Whorf, 2000), have primarily forced the DO-style cycles, these cycles also should have perpetuated prior to the onset of NHG.

Indeed, DO-like cycles and their multiples only started with glacial stage G14 during the onset of NHG (Fig. 8), when the IRD numbers at ODP Site 907 (Fig. 2A) came close to the local IRD concentrations found during any Pleistocene stadial event (Helmke et al., 2005) and thus support the model of ice-breakouts. This holds true also for Site 984 from MIS G6 to 104 onwards (Fig. 2A). Further support comes from the increased climate variability during the stages after MIS G14 as depicted in the amplitudes of planktic  $\delta^{18}\text{O}$ , SST, and magnetic susceptibility (Fig. 7, Table 2).

**Fig. 9:** Filtered 1.47 kyr (DO) signal (red broken line) in glacial planktic  $\delta^{18}\text{O}$  records of MIS 104 and G6 for *N. atlantica* (grey line) and *G. bulloides* (black line). Bandwidth of 0.02 corresponds to periods between 1.428 and 1.514 kyr.



During glacial stages 104 and G6, the 1470-yr period forms an important fraction of climate variability, as seen in the planktic  $\delta^{18}\text{O}$  records filtered for a frequency of  $1/1470$  yr (Fig. 9). Improved age control may certainly lead to an improved extraction of the “classic” 1470-yr DO period. In conclusion, DO cycles did not perpetuate prior to the onset of NHG and may indeed be closely tied to the build-up (2.9-2.74 Ma) and subsequent instability of Northern Hemisphere-ice sheets, in particular that on Greenland.

However, solar forcing and/or other forcings may also be involved with millennial-scale climatic change. The potential lunar 1.7-1.8-kyr periodicity (Keeling & Whorf, 2000) only occurs in glacial and interglacial stages prior to NHG, when no DO cycles are registered. In addition, solar cycles that only dominate Quaternary interglacial (Holocene) climatic variability with  $900 \pm 100$  and  $500 \pm 100$  yr periodicities are resolved in both glacial and interglacial stages prior *and*



after the NHG (Fig. 8). Hence it is likely that they present an ongoing but weak forcing mechanism that is largely hidden behind DO cycles during glacial stages after NHG.

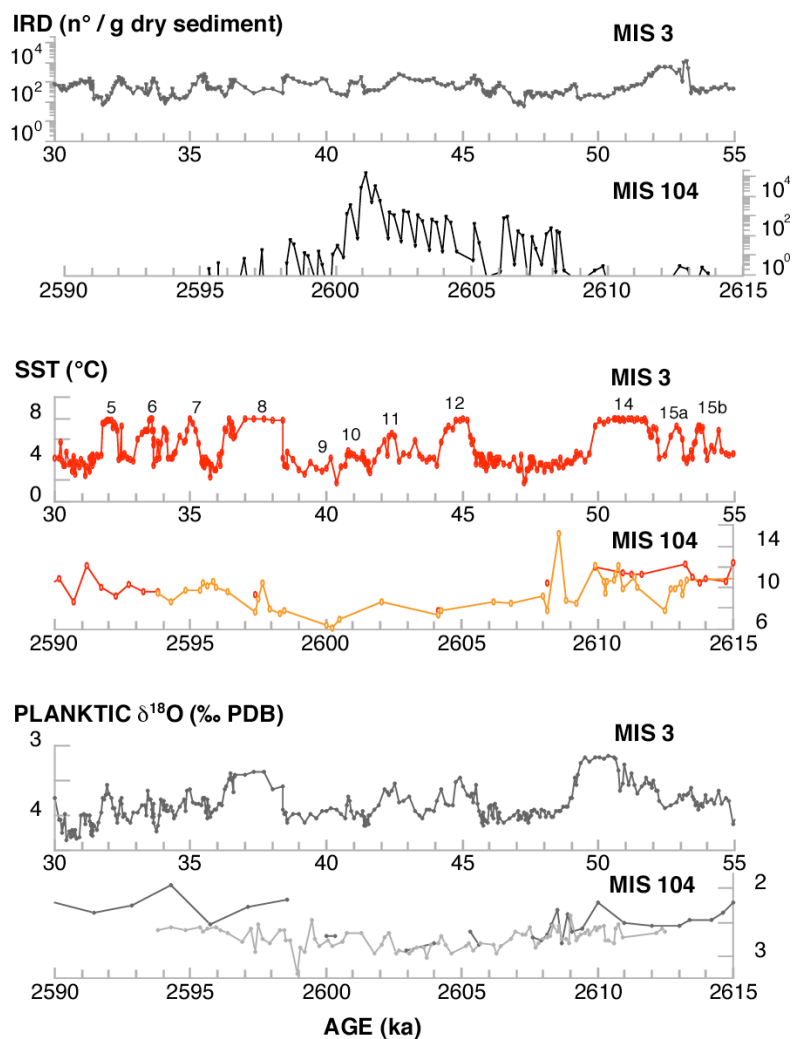
Interglacial stages do not show any significant evolution in the variability of planktic  $\delta^{18}\text{O}$ , SST, and magnetic susceptibility, neither in the time nor in the frequency domain (Fig. 8, Table 3A) during and subsequent to NHG, at least until MIS G1. In conclusion, Late Pliocene interglacial climate prior and after the onset of NHG already largely resembles that of the Holocene.

Interglacial and glacial frequency spectra also consist of a broad array of longer millennial-scale periods (Fig. 8, Table 1, 3A, and 3B) near 15, 9, 4, and 2.0-2.6 kyr, which in part come close to periods found elsewhere (Niemitz & Billups, 2005: Early Pliocene planktic  $\delta^{18}\text{O}$  records of the tropical Atlantic Ocean; ODP Site 925). Similar periodicities near  $\sim 11$ ,  $\sim 5.5$ , and  $\sim 2$  kyr were also reported in the color reflectance of Early Pliocene lacustrine sediments in the Ptolemais Basin (Greece; Steenbrink et al., 2003) and for the mid-Pliocene warm period (Draut et al., 2003).

## **5.2 Millennial-scale variability in Late Pliocene glacial stage 104 compared to Pleistocene semiglacial stage 3**

The Pliocene climatic records of Site 984 can be directly compared to the late Pleistocene climate variability recorded in neighbor core SO82-5 (59°N, 31°W; Fig. 1) for MIS 3 (30-55 ka; DO cycles 5 to 15; van Kreveld et al., 2000). There are only few similarities (Fig. 10). During MIS 104 IRD discharge was higher and more highly variable than during MIS 3. In contrast, SST variations during MIS 3 show far stronger positive and negative excursions ( $\Delta 4^\circ\text{-}6^\circ\text{C}$ ) prior and after DO interstadials 8 to 15b than during MIS 104, where hardly any SST variations are recognized ( $\Delta 1^\circ\text{-}2^\circ$ ). Possibly, this is a result of too low sampling resolution, in part however, a genuine difference from MIS 3. This low SST variability matches a low planktic  $\delta^{18}\text{O}$  variation by 0.3-0.4‰ during MIS 104 in contrast to values reaching 0.9‰ during MIS 3. The low  $\delta^{18}\text{O}$  amplitudes of MIS 104 are unexpected also in view of the high variations in IRD, that would require pertinent  $\delta^{18}\text{O}$  freshwater pulses. In summary, we hardly find during MIS 104 the features characteristic of late Pleistocene DO cycles (abrupt climatic jumps and large amplitudes of variability).

**Fig. 10:** Comparison between IRD, SST, and planktic  $\delta^{18}\text{O}$  records of MIS 3 (van Kreveld et al., 2000) and MIS 104 (this study) from the Rekjanes Ridge. IRD records plotted on a log-scale. SST for MIS 3 were obtained by means of the SIMMAX transfer function method (Pflaumann et al., 2003). SST for MIS 104 are based on Mg/Ca measured on *N. atlantica* (orange dots) on *G. bulloides* (red dots). Planktic  $\delta^{18}\text{O}$  for MIS 104 was measured on *N. atlantica* (grey) and *G. bulloides* (black).



## 6 Conclusions

Late Pliocene sub-Milankovitch climate variability was studied at ODP Site 984 for the period between 2.5 and 3.1 Ma in the time and frequency domains with a time resolution ranging from 100 to 900 yr, with the following results:

- Climate variability in the high-latitude North Atlantic shows a dominant 41-kyr obliquity cycle for planktic  $\delta^{18}\text{O}$ , SST, and magnetic susceptibility records.
- Separate spectral analyses performed on selected glacial and interglacial stages resulted in a broad array of millennial-scale periodicities which are regarded as coming close to significance, since the relative duration of any single orbital cycle is well constrained in contrast to the accuracy of absolute Pliocene age control, the uncertainty of which may still reach up to 10,000 yr.
- During glacial stages after the onset of NHG (G14, G6, and 104), a DO-style periodicity (1470 yr and its multiples of 2900 and 4400 yr) started to occur, in contrast to the variability spectrum during MIS G20 prior to the onset where no such frequencies occur. This suggests that synglacial DO cycles were indeed linked to Northern Hemisphere-ice sheet instabilities.
- During cold stages prior to 2.9 Ma, climate variability was dominated by cyclicities characteristic of solar cycles near 500 ( $\pm 100$ ) and 900 ( $\pm 100$ ) yr.

- Since periodicities that come close to solar cycles (near 500 yr and 900 yr) characterize glacial and interglacial stages both prior and after the onset of NHG, solar forcing may have persisted in controlling climate variability through all times, possibly also triggering the DO cycles subsequent to the onset of NHG.
- Late Pliocene interglacial stages showed fairly stable climate conditions with dominant solar cyclicities and did not display any significant evolution in climatic amplitude and periodicities subsequent to the onset of NHG. In total, they already resembled the Holocene climate regime, as first suggested by Draut et al. (2003) for the mid-Pliocene warm period (3-3.33 Ma).
- The Late Pliocene DO-style events of isotope stage 104 have not yet attained most features characteristic of DO cycles during Pleistocene stage 3. In particular, the amplitudes of planktic  $\delta^{18}\text{O}$  and SST are much weaker during MIS 104 than during MIS 3.

Future studies of millennial-scale climate variability in particular will need to improve on the precision of the Pliocene age model on millennial scales. Possibly, the initially orbitally tuned records may be tuned in a second step to 950-yr or other solar cyclicities in an iterative approach. After the onset of NHG (2.9-2.8 Ma) the records of glacial stages may also be tuned to the potential 1470-yr DO cycle.

## 7 Acknowledgments.

M. Schulz was helpful in kindly commenting on time series analysis techniques and on an early manuscript version. We appreciate C. Sieler's great help with handling computer software. Two anonymous reviewers comments greatly helped to improve our manuscript. This study was supported by the Deutsche Forschungsgemeinschaft (DFG) FOR 451 within the Kiel Research Unit "Ocean Gateways".

## 8 References

- Arbic, B.K., D.R. Mac Ayeal, J.X. Mitrovica, and G.A. Milnes (2004), Ocean tides and Heinrich events, *Nature*, *432*, 460.
- Austin, W.E.N., and J.R. Evans (2000), Benthic foraminifera and sediment grain size variability at intermediate water depths in the Northeast Atlantic during the late Pliocene-early Pleistocene, *Marine Geology*, *170*, 423-441.
- Bartoli, G., M. Sarnthein, and M. Weinelt (2005), Final closure of Panama and the onset of northern hemisphere glaciation, *Earth Planet. Sci. Lett.*, *237*, 33-44, doi:10.1016/j.epsl.2005.06.020.
- Becker J., L. J. Lourens, F. J. Hilgen, E. vanderLaan, T. J. Kouwenhoven, and G.-J. Reichert (2005), Late Pliocene climate variability on Milankovitch to millennial time scales: A high-resolution study of MIS 100 from the Mediterranean, *Palaeogeog. Palaeoclim. Palaeoecol.*, *228*, 338-360, doi:10.1016/j.palaeo.2005.06.020.
- Bond, G., B. Kromer, J. Beer, R. Muscheler, M.N. Evans, W. Showers, S. Hoffmann, R. Lotti-Bond, I. Hajdas, and G. Bonani (2001), Persistent solar influence on North Atlantic climate during the Holocene, *Science*, *294*, 2130-2136.
- Bond, G.C. and R. Lotti (1995), Iceberg discharges into the North Atlantic on millennial time scales during the last glaciation, *Science*, *267*, 1005-1010.
- Braun H., M. Christl, S. Rahmstorf, A. Mangini, C. Kubatzki, K. Roth, and B. Kromer (2005), Possible solar origin of the 1,470-year glacial climate cycle demonstrated in a coupled model. *Nature*, *438*, 208-211, doi:10.1038/nature04121.

- Clemens, S.C. (2005), Millennial-band climate spectrum resolved and linked to centennial-scale solar cycles, *Quat. Sci. Rev.*, *24*, 521-531.
- Draut, A.E., M.E. Raymo, J.F. McManus, and D.W. Oppo (2003), Climate stability during the Pliocene warm period, *Paleoceanography*, *18* (4), 1078, doi:10.1029/2003PA00889.
- Elderfield, H. and G. Ganssen (2000), Past temperature and  $d^{18}O$  of surface ocean waters inferred from Mg/Ca ratios, *Nature*, *405*, 442-445.
- Ganopolski, A. and S. Rahmstorf (2001), Rapid changes of glacial climate simulated in a coupled climate model, *Nature*, *409*, 153-158.
- van Geel, B., O.M. Raspopüov, H. Renssen, J. van der Plicht, V.A. Dergachev, and H.A.J. Meijer (1999), The role of solar forcing upon climate change., *Quat. Sci. Rev.*, *18*, 331-338.
- Groote P. M., M. Stuiver, J. W. C. White, S. Johnsen, and J. Jouzel (1993), Comparison of oxygen isotope records from the GISP2 and GRIP Greenland ice cores, *Nature*, *366*, 552-534.
- Helmke J. P., H. A. Bauch, H. Röhl, and A. Mazaud (2005), Changes in sedimentation patterns of the Nordic seas region across the mid-Pleistocene. *Mar. Geol.*, *215*, 107-122, doi:10.1016/j.margeo.2004.12.006.
- Hoyt, D.V. and K.H. Schatten (1993), A discussion of plausible solar irradiance variations, 1700-1992, *J. Geophys. Res.*, *98* (A11), 18895-18906.
- Hu, F.S., D. kauffman, S. Oneji, D. Nelson, A. Shemesh, Y. Huang, J. Tian, G. Bond, B. Clegg, and T. Brown (2003), Cyclic variation and solar forcing of Holocene climate in the Alaskan Subarctic, *Science*, *301*, 1890-1893.
- Hyde, W.T. and T.J. Crowley (2002), Stochastic forcing of Pleistocene ice sheets: Implications for the origin of millennial-scale climate oscillations, *Paleoceanography*, *17* (4), 1067, doi:10.1029/2001PA000669.
- Jansen, E., M.E. Raymo, P. Blum, and T.D. Herbert (Eds.), (1996), *Proc. ODP, Init. Results, 162*: College Station, TX (Ocean Drilling Program).
- Jansen, E., T. Fronval, F. Ranck, and J.E.T. Channell (2002), Pliocene-Pleistocene ice rafting history and cyclicity in the Nordic Seas during the last 3.5 Myr, *Paleoceanography*, *15* (6), 709-721.
- Keeling, C.D. and T.P. Whorf (2000), The 1,800-year oceanic tidal cycle: A possible cause of rapid climate change, *Proc. Natl. Acad. Sci. USA*, *97* (8), 3814-3819.
- Kissel, C., C. Laj, L. Labeyrie, T. Dokken, A. Voelker, D. Blamart (1999), Rapid climatic variations during marine isotope stage 3: Magnetic analysis of sediments from Nordic Seas and North Atlantic, *Earth Plant. Sci. Lett.*, *171*, 489-502.
- van Kreveld, S., M. Sarnthein, H. Erlenkeuser, P. Groote, S. Jung, M.J. Nadeau, U. Pflaumann, and A. Voelker (2000), Potential links between surging ice sheets, circulation changes, and the Dansgaard-Oeschger cycles in the Irminger sea, 60-18 kyr., *Paleoceanography*, *15* (4), 425-442.
- Lacasse, C. and P. van den Bogaard (2002), Enhanced airborne dispersal of silicic tephras during the onset of Northern Hemisphere glaciations, from 6 to 0 Ma records of explosive volcanism and climate change in the subpolar North Atlantic, *Geology*, *30* (7), 623-626.
- Lisiecki, L.E. and M.E. Raymo (2005), A Pliocene-Pleistocene stack of 57 globally distributed benthic  $d^{18}O$  records, *Paleoceanography*, *20*, PA1003, doi:10.1029/2004PA001071 .
- Martin, P.A. and D.W. Lea (2002), A simple evaluation of cleaning procedures on fossil benthic foraminiferal Mg/Ca, *Geochem. Geosys. Geophys.*, *3*, 8401, doi:10.1029/2001GC000280 .
- Mashiotta, T.A., D.W. Lea, and H.J. Spero (1999), Glacial-interglacial changes in Subantarctic sea surface temperature and  $d^{18}O$ -water using foraminiferal Mg, *Earth Planet. Sci. Lett.*, *170*, 417-432.
- MIntyre, K., M.L. Delaney, and C. Ravelo (2001), Millennial-scale climate change and oceanic processes in the late Pliocene and early Pleistocene, *Paleoceanography*, *16* (5), 535-543.
- Muscheler, R. and J. Beer (2004), Solar forced Dansgaard/Oeschger events?, *American Geophysical Union*, Fall meeting 2004, abstract #U41B-07.
- Niemitz, M.D. and K. Billups (2005), Millennial-scale variability in western tropical Atlantic surface ocean hydrography during the early Pliocene, *Mar. Micropal.*, *54*, 155-166.

- Paillard, D. and L. Labeyrie (1994), Role of the thermohaline circulation in the abrupt warming after Heinrich events, *Nature*, 372, 162-164.
- Paillard, D., L. Labeyrie, and P. Yiou (1996), Macintosh program performs time-series analysis, *EOS Trans, AGU*, 77, 379.
- Pflaumann U., M. Sarnthein, M. Chapman, L. d'Abreu, B. Funnell, M. Huels, T. Kiefer, M. Maslin, H. Schulz, J. Swallow, S. van Kreveld, M. Vautravers, E. Vogelsang, and M. Weinelt (2003), Glacial North Atlantic: Sea-surface conditions reconstructed by GLAMAP 2000, *Paleoceanography*, 18 (3), 10-1, doi:10.1029/2002PA000774.
- Ruddiman W. F., M. Raymo, and A. McIntyre (1986), Matuyama 41,000-year cycles: North Atlantic Ocean and northern hemisphere ice sheets, *Earth and Planetary Science Letters*, 80, 117-129.
- Sakai, K. and W.R. Peltier (1997), Dansgaard-Oeschger oscillations in a coupled atmosphere-ocean climate model, *Journal of Climate*, 10 (5), 949-970.
- Sarnthein, M., S. van Kreveld, H. Erlenkeuser, P. M. Grootes, M. Kucera, U. Pflaumann, and M. Schulz (2003), Centennial-to-millennial-scale periodicities of Holocene climate and sediment injections off the western Barents shelf, 75°N, *Boreas*, 32, 447-461.
- Schulz M., W. H. Berger, M. Sarnthein, and P. M. Grootes (1999), Amplitude variations of 1470-year climate oscillations during the last 100,000 years linked to fluctuations of continental ice mass, *GRL*, 26 (22), 3385-3388.
- Schulz, M., A. Paul, and A. Timmermann (2002) Relaxation oscillators in concert: A framework for climate change at millennial timescales during the late Pleistocene, *Geophys. Res. Lett.*, 29 (24), 2193.
- Schulz, M. and M. Mudelsee (2002), REDFIT: Estimating red-noise spectra directly from unevenly spaced paleoclimatic time series, *Computers and Geosciences*, 25 (3), 421-426.
- Shackleton, N.J., M.A. Hall, and D. Pate (1995), Pliocene Stable Isotope stratigraphy of Site 846. *Proc. ODP, Scientific Results*, 138, 337-353.
- Shindell, D., D. Rind, N., Balachandran, J. Lean, and P. Lonergan (1999), Solar cycle variability, ozone, and climate, *Science*, 284, 305-308.
- Steenbrink, J., M. L., Kloosterboer - van Hoeve, and F. J. Hilgen (2003), Millennial-scale climate variations recorded in Early Pliocene color reflectance time series from the lacustrine Ptolemais Basin (NW Greece), *Global and Planetary Change*, 36, 47-75.
- Tiedemann, R., M. Sarnthein, and N.J. Shackleton (1994), Astronomic timescale for the Pliocene Atlantic  $\delta^{18}O$  and dust flux records of Ocean drilling Program site 659, *Paleoceanography*, 9 (4), 619-638.
- Trauth, M.H., M. Sarnthein, and M. Arnold (1997), Bioturbational mixing depth and carbon flux at the seafloor, *Paleoceanography*, 12 (3), 517, 97PA00722.
- de Villiers, S., M. Greaves, and H. Elderfield (2002), An intensity ratio calibration method for the accurate determination of Mg/Ca and Sr/Ca of marine carbonates by ICP-AES, *Geochem. Geophys. Geophys.*, 3, doi: 10.1029/2001GC000169.
- Voelker, A.H.L. and workshop participants (2002), Global distribution of centennial-scale records for Marine Isotope Stage (MIS) 3: a database, *Quat. Sci. Rev.*, 21, 1185-1212.
- Wang Y. J., H. Cheng, R. L. Edwards, Z. S. An, J. Y. Wu, C.-C. Shen, and J. A. Dorale (2001), A high-resolution absolute-dated Late Pleistocene record from Hulu Cave, China, *Science*, 294, 2345-2348.
- Willis, K.J., A. Kleczkowski, K.M. Briggs, and C.A. Gilligan (1999), The role of sub-Milankovitch climatic forcing in the Initiation of the northern hemisphere glaciation, *Science*, 285, 568-571.



## Chapter 6

# Gateway-controlled decline of primary production in the northern North Atlantic at 2.74 Ma ?

M. Weinelt<sup>a\*</sup>, G. Bartoli<sup>a</sup>, H. Erlenkeuser<sup>b</sup>, and M. Sarnthein<sup>a</sup>

<sup>a</sup>Kiel University, Institute for Geosciences, Olshausenstr. 40, D-24118 Kiel, Germany

<sup>b</sup>Leibniz-Laboratory for Radiometric Dating and Stable Isotope Research, Kiel University, Max-Eyth-Str. 11, D-24118 Kiel, Germany

\*corresponding author. Tel.: +494318802939; fax: +494318804376.

E-mail address: [mw@gpi.uni-kiel.de](mailto:mw@gpi.uni-kiel.de) (M. Weinelt)

*To be submitted to Mar. Micropal.*

## Abstract

Late Pliocene benthic foraminifera assemblages and benthic stable-isotope records at ODP Site 984 (North Atlantic) were studied to compare changes in northern Atlantic surface productivity prior and after the final closure of the Central American Seaways (CAS) linked to the onset of Northern Hemisphere Glaciation (NHG; 2.82-2.95 Ma). An abrupt and fundamental change in the benthic fauna at 2.74 Ma (marine isotope stage -MIS- G6) from assemblages marked by high-carbon flux indicative species such as *Bolivina pacifica* to feeding opportunists like *Cassidulina teretis* assemblages. This faunal switch suggests a profound reorganization of the North Atlantic productivity regime. Accordingly, primary production was high when the CAS were open. A decline in productivity precisely coincides with a major reorganization of Upper North Atlantic Deep Water (UNADW), as recorded by benthic  $\delta^{18}\text{O}$  and  $\delta^{13}\text{C}$  suggesting an abrupt cooling and further increase in ventilation at intermediate depth of UNADW. This coincidence suggests that the change in marine productivity resulted from the onset of a glacial thermohaline circulation mode marked by higher surface water stratification and higher seasonality. Indeed, detailed faunal records of MIS 104 (~2.6 Ma) display remarkable similarities with Late Pleistocene MIS 2 and 3. Short-term fluctuations in benthic faunas suggest a response to rapid environmental changes.

**Keywords:** Late Pliocene, faunal turnover, marine productivity, oxygen isotopes.

## Introduction

Intensification of Northern Hemisphere Glaciation (NHG) in the Late Pliocene is generally linked to the final closure of the Central American Seaway (CAS), leading to a profound reorganization of Atlantic circulation patterns promoting heat and moisture transport to the high northern latitudes and finally leading into a fast ice-build up. Recently Bartoli et al. (2005) could show that the evolution of the North Atlantic heat transport to the high latitudes via the thermohaline circulation (THC) occurred in several marked steps, disrupted by repeated setbacks, and was indeed intimately linked to the evolution of the Caribbean vs. tropical Pacific salinity divergence. The Late Pliocene onset of harsher environmental conditions at high northern latitudes also lead to a profound reorganization of North Atlantic faunal provinces, giving rise to the establishment of modern assemblages and pronounced glacial to interglacial fluctuations.

A major faunal turnover of benthic foraminifera faunas in the deep Atlantic centered at 3.2-2.4 Ma as evidenced by high numbers of last occurrences, few new appearances, and pronounced changes in relative species abundances (Thomas, 1987). These changes were generally attributed to changes in North Atlantic deepwater masses. During that time for example *Nutallides umbonifera*, a species associated with southern source deepwater (SOW), made its appearance in the deep North Atlantic was thus considered to record the onset of Antarctic Bottom Water (AABW) and a weakening of THC (Thomas, 1987). Schnittker (1984) based on a comparison of benthic foraminifera assemblages and benthic  $\delta^{18}\text{O}$  values at Site 552 from Rockall Plateau have postulated a dependency of faunas from THC strength, though he concedes a secondary imprint by coeval environmental changes at sea surface. Likewise Ishman (1996) attributed faunal shifts in the deep northern Atlantic at 2.9 Ma to a major shift of Northern compound water. Austin and Evans (2000), from presence of high-current speed adapted benthic foraminifera species and coeval changes in mean sortable silt, another proxy for current speed, have inferred increased current strength at intermediate depths during glacials and concluded a shoaling of North Atlantic THC during the Late Pliocene/Early Pleistocene.

Today it is widely agreed that primary control on population density and composition of benthic foraminiferal faunas in the deep sea is by food supply, in turn linked to primary production in overlying surface water (e.g. Lutze and Colbourn, 1984). Therefore an array of productivity proxies has been found on benthic foraminifera, including total abundance or accumulation rates (Herguera, 1992), occurrence of indicator species following specific strategies for food acquisition (Jorissen et al., 1995), shell morphology of dominant species (Corliss, 1991), or relative species abundances (Altenbach et al., 1999). The latter in an extensive comparison of benthic assemblages in 382 core tops from the North Atlantic and Arctic Ocean to carbon flux rates identified upper and lower tolerance levels of 60 single species.

The northern North Atlantic is a region highly sensitive to productivity change. Apart from nutrient advection here at the interface of Atlantic and polar water masses primary production is strongly influenced by environmental factors like surface stratification, ice coverage, and pronounced seasonality exerting strong control on vertical nutrient cycling. Late Pleistocene shifts in benthic faunal patterns in the northern northeast Atlantic suggest a strong productivity decrease during glacial intervals which has been considered a result of southward expansion of sea-ice coverage (Thomas et al., 1995). Short-term changes in productivity in marine isotope stages (MIS) 3 and 2 also followed the D-O cyclicity where the occurrence of massive production maxima at stadial-interstadial transitions have been related to migrations of the subpolar front (Weinelt et al., 2003), or to rapid changes in vertical nutrient cycling (Schmittner, 2005).

So far little is known on changes of Late Pliocene productivity patterns in the Atlantic over the time of the final closure of the CAS and onset of NHG. Based on patterns of organic carbon accumulation in the low-latitude Atlantic over the time of Late Pliocene climate deterioration Sarnthein and Fenner (1988) found an intensified productivity in the equatorial and eastern margin upwelling zones in the Atlantic. They considered this intensification a response to strengthened wind stress in turn enhancing upwelling intensity. Likely, Ettwein et al. (2002) based on nitrogen isotopes and diatom accumulation rates found a productivity increase in the South Atlantic Benguela Current and the onset of marked glacial-interglacial cyclicity which they however attributed to changes in of nutrient supply by Antarctic Intermediate Water.

Model experiments simulating the final closure of the CAS have predicted a global net increase in oceanic production resulting from global nutrient redistribution and a general increase in oceanic overturning rates (Schneider and Schmittner, in prep). Based on these patterns it has been postulated that the general productivity increase may have provided a positive feedback for cooling and NHG via lowering in the Late Pliocene  $\text{CO}_2$  levels. However, for the mid-to-high latitude North Atlantic the model predicted a contrasting strong decline in primary production by



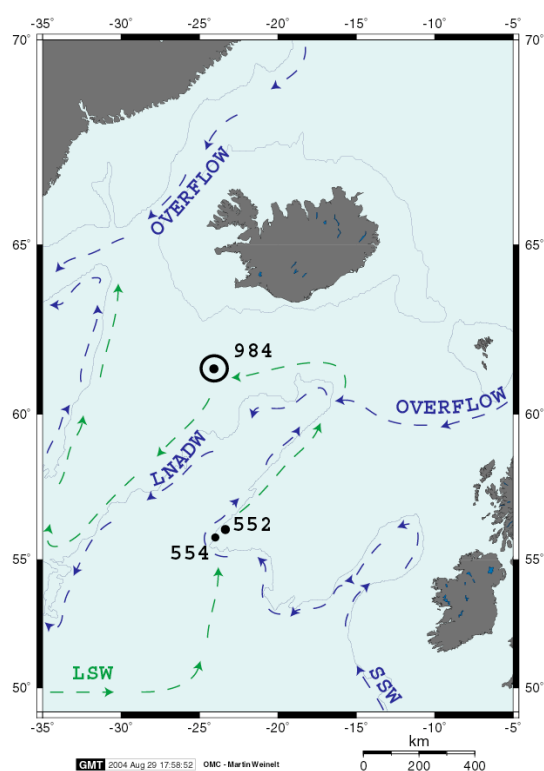
approximately 30% caused by the lack of advection of nutrient rich Pacific subsurface water to the high latitudes.

Here we use benthic stable isotope and faunal records of total abundance of benthic foraminifera and of selected single species over the onset of major NHG to test this hypothesis. Moreover, a detailed record of MIS 104 (i.e. one of the first severe glacials subsequent to the onset of NHG) is used to explore the impact of environmental variables on productivity on millennial-to-centennial scale time resolution.

## Methods and strategy

Site 984 is located on the Reykjanes ridge (61°25.517'N, 24°04.949'W, 1647 m water depth) monitoring environmental changes in Upper North Atlantic Deep Water (UNADW) and in surface water changes in the Irminger Current (Fig. 1).

**Figure 1.** Northeast Atlantic with site locations and modern deep-water currents. LSW stands for Labrador Sea Water, SSW for Southern Source Water, and NADW for North Atlantic Deep Water.



### *Benthic stable isotope records*

Low carbonate contents and discontinuity of benthic foraminifera occurrences have so far prevented any continuous  $\delta^{18}\text{O}$  record from high northern latitudes spanning the critical time interval of onset of NHG. Large samples (20 cc), high sampling density (at 10 cm spacing), and high sensitivity of the Kiel coupled carboprep. / mass spectrometer (measurements of 2 specimens from small size fractions possible) enabled us to overcome these shortcomings and to address questions of Late Pliocene paleoceanographic and environmental change in the subpolar Atlantic. Sample processing has been described in detail by Bartoli et al. (2005). Monospecific samples of 1 to 10 specimens were measured at the coupled carboprep. / Finnigan MAT 251 at the Leibniz Laboratory in Kiel. Accuracy is 0.08‰ for  $\delta^{18}\text{O}$  and 0.05‰ for  $\delta^{13}\text{C}$  measurements.

A composite  $\delta^{18}\text{O}$  record has established based on a suite of 6 different species/taxa, corrected for published offsets from isotopic equilibrium (Fig. 2). To further constrain these offsets and to test their validity for Pliocene forms, multiple species on the same sample were performed wherever possible (Fig. 2). In addition we employed *Elphidium excavatum*, a species strongly dominating the peak glacial faunas of Site 984. *E. excavatum* is generally known as a shallow-marine form, but with common occurrence in glaciomarine sediments of the deeper northern North Atlantic and Arctic Ocean. There is an ongoing debate on whether the widespread occurrence at intermediate depth in the northern Atlantic and Nordic Seas can be explained by downslope sediment transport solely or if these species may also invade deeper habitats, a hypothesis to be tested on its  $\delta^{18}\text{O}$  signature (Knudsen and Austin, 1996). Following this suggestion we measured  $\delta^{18}\text{O}$  values in 86 *E. excavatum* samples (1-3 specimens per sample).

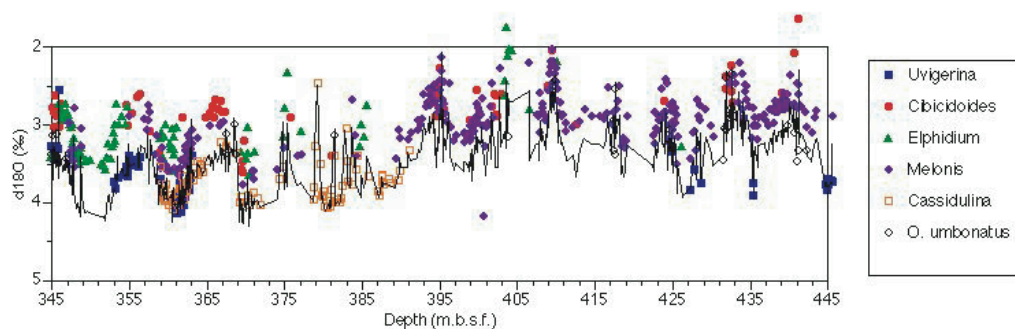


**Figure 2.** Composite of benthic foraminifera and single species  $\delta^{18}\text{O}$  records at Site 984. For the composite record *Melonis barleeanum* values were corrected for +0.34‰, *Cibicides/Cibicidoides* values for 0.64‰, *Cassidulina teretis* and *Oridorsalis umbonatus* values by -0.1‰ according to Shackleton (1984) and Jansen (1988). *Elphidium excavatum* values were corrected for 0.64‰, according to observed offsets relative to other species.

Results yielded a fairly regular offset as compared to  $\delta^{18}\text{O}$  equilibrium values by 0.64‰, particularly well matching few parallel *Cibicides wuellerstorfi* values (Fig. 2). This offset is however smaller than the one found by McCorkle et al. (1990) based on *Elphidium*  $\delta^{18}\text{O}$  values from few deep North Atlantic core tops (1.0‰). In our records *Elphidium* values display full glacial-to-interglacial  $\delta^{18}\text{O}$  amplitudes in harmony with other species, particularly well constrained for inception and termination of MIS 100 (Fig. 2). Since it is unlikely that such a pattern would emerge from exclusively transported specimens we consider the *Elphidium* values as *in situ* and retained them in the composite record. Because of the rare occurrence of suitable species reliably recording  $\delta^{13}\text{C}$  of DIC and thus serving as a proxy for deepwater ventilation, no continuous  $\delta^{13}\text{C}$  record could be established. Rare *C. wuellerstorfi* measurements were spliced with some additional values of *C. mundulus* and *Oridorsalis tener*. The latter were corrected for an offset of +1.0‰ according to A. Mackensen (personal communication, 2004).

#### *Benthic foraminifera assemblages and selection of indicator species*

More than 1000 samples were inspected for their foraminiferal contents and total numbers of benthic foraminifera were counted in the >150 $\mu\text{m}$  size fraction. Because of often small

individuum numbers only un-split samples were used (containing a total of 0 to >300 specimens) and only absolute abundances are reported here (excepting for MIS 104), referred to 10 g dry sediment.

Inspection of assemblages revealed large shifts in both, individuum numbers and faunal composition. Most common benthic foraminifera taxa in the late Pliocene section of Site 984 include *Melonis barleeanum*, pullenids, stilostomellids, unilocular forms, *Quinqueloculina seminula*, *Eggerella bradyi*, *Sigmoilopsis schlumbergeri*, *Cassidulina teretis*, *E. excavatum*. Namely the latter three species are confined to the younger part of the record, i.e. after 2.74 Ma (390 m core depth), though present with very small numbers during previous glacials. *Uvigerina peregrina* is common only in the glacial-interglacial transitions and in the oldest glacials. *Bolivina pacifica*, *M. pompiloides* are common only in the older part of the record. Accessorial occurrences include *O. tener*, *Gyrodina*, *Asterononion* which may reach high portions in some single levels. Notably, *C. wuellerstorfi* and also other *Cibicides/Cibicidoides* are very rare at Site 984, and in particular, widely absent from the older section of our records. Though not quantitatively registered, the gross distribution pattern of most common calcareous taxa is reflected in the  $\delta^{18}\text{O}$  records of Fig. 2. A detailed discussion on faunal patterns of Site 984 is given by Austin and Evans (2000), covering the interval subsequent to the onset of major NHG.

While no attempt was made to quantitatively analyze the entire assemblages, we chose two of the most common species displaying marked changes over the course of the Pliocene section of Site 984 and counted them at high resolution. Namely those were *B. pacifica* and *C. teretis* (TERQUEM) were selected because they were considered as indicative for certain productivity regimes:

Bolivinids are infaunal forms which generally occur with high numbers at ocean margins marked by high carbon flux at shallow to intermediate depths. They have been attributed to high productivity and/or low oxygen environments (Jorissen et al., 1995). *B. pacifica* has been described from the Iberian margin where it occurs in the upwelling areas, as well in the Santa Barbara basin. Altenbach et al. (1999) give high average organic carbon flux ranges of 10 to 40 g C m<sup>-2</sup> y<sup>-1</sup> for the occurrence of this species, though it may also tolerate carbon fluxes down to 1 and as high as 100 g C m<sup>-2</sup> y<sup>-1</sup>.

*C. teretis* is generally known as an Arctic feeding opportunist adapted to low and irregular food supply where it may change from infaunal to epifaunal habitats (Gooday and Lamdshead, 1989; Weinelt et al., 2001). Accordingly, Thomas et al. (1995) classified *C. teretis* into a group of phytodetritus feeders responding to a pronounced spring bloom, in principle thus indicating high seasonality of surface production. Based on inversed patterns of *Cassidulina* abundance and accumulation rates of total benthic specimens they have ruled out high glacial productivity levels for in the northeast Atlantic. Stratification of surface water or presence of sea ice, variables marking high-latitude subpolar environments with large seasonal and/or inter-annual differences and leading to low and irregular food supply would thus favor the occurrence of *C. teretis* over species adapted to sustained food supply. Today *C. teretis* has a widespread occurrence at intermediate depths of the Arctic, Nordic, and Labrador Seas and extending into the Iceland Shetland Channel. In contrast, it is absent from in the warmer UNADW south of the Iceland Faroe Ridge (IFR). Therefore its distribution has also been attributed to very cold Norwegian Sea Deep Water (NSDW) (<2°C; Mackensen, 1987). During Late Pleistocene glacials this species occurred south of the IFR and here distinctly responded to millennial scale Dansgaard-Oeschger (D-O) variability marking MIS 3 and 2 (Rasmussen et al., 1996; Rasmussen and Thomsen, 2004).

Also the total abundances of benthic foraminifera may serve as a proxy for productivity (Herguera, 1992). However, because of the differential behavior of feeding opportunists, Thomas et al. (1995) have suggested to correct total faunal abundances for those species for interpretations in terms of productivity. Following this approach we corrected the total benthic

foraminifera numbers for *C. teretis*. However still remaining other opportunists not quantitatively registered may bias the residual record.

### ***Nutrient concentrations, sea surface stratification, and IRD***

To explore the response of benthic faunas to environmental change at the surface faunal records are compared to (qualitative) nutrient and  $\delta^{18}\text{O}$  water records. Lacking other evidence we employed the planktonic  $\delta^{13}\text{C}$  record of *Globigerina bulloides* as a proxy for nutrient concentrations in surface water.

$\delta^{18}\text{O}_{\text{water}}$  was deduced from  $\delta^{18}\text{O}$  of *G. bulloides* and *Neogloboquadrina atlantica* corrected for Mg/Ca temperatures (Bartoli et al., 2005) according to the paleo-equation by Shackleton (1974).  $\delta^{18}\text{O}_{\text{water}}$  is a proxy for sea surface salinity (SSS). Since the evolution of Late Pliocene ice volume is not well constrained, and in particular, the glacial-interglacial ice volume fluctuations are unknown, no proper correction can be made, preventing in turn to isolate the  $\delta^{18}\text{O}$  signal actually due to local salinity change. Yet a rough correction by larger Late Pliocene steps as inferred from comparison with  $\delta^{18}\text{O}$  records from the deep Atlantic and Pacific is possible (Bartoli et al., 2005).

To study the history of iceberg discharge, up to 300 lithic grains of ice-rafted debris (IRD) were counted in the size fraction  $>150\ \mu\text{m}$ . Values are given as number of grains / g dry sediment, except for MIS 104 where % of IRD versus foraminifera and volcanic glass were calculated.

### ***Age control***

The age model of Site 984 was adopted from Bartoli et al. (submitted) who defined 76 age tie points by tuning the planktonic  $\delta^{18}\text{O}$  record to the benthic  $\delta^{18}\text{O}$  stack LR04 (Lisiecki & Raymo, 2005), integrating 25 worldwide benthic  $\delta^{18}\text{O}$  records over the time span 1-3 Ma. Tuning was performed by graphical correlation of peaks and stage boundaries using the AnalySeries 1.2 software (Paillard et al., 1996). MIS 104 was defined by a biostratigraphic datum, LO of *Ebriopsis cornuta*, that was identified between 359.74 and 369.06 mbsf and provided an age of 2.61 Ma (Jansen et al., 1996). Moreover MIS 104 boundaries were defined in the planktonic  $\delta^{18}\text{O}$  record by 2 stratigraphic tie points placed on the edge. However, an uncertainty of 1-4 kyr remains (in terms of absolute age) because of (1) the low time resolution of the LR04 stack for the interval 2.5-3.1 Ma, (2) differences between the last occurrence of IRD near the top of MIS 104 and the position of the major planktonic  $\delta^{18}\text{O}$  decrease.

Accordingly, the sedimentation rates range from 4 to 58 cm/kyr (26 cm/kyr on the average). In between the 76 stratigraphic tie points, ages were deduced by linear interpolation assuming constant sedimentation rates.

### ***Sediment accumulation rate***

As a measure for fluctuations in sediment and benthic foraminifera accumulation we calculated the sediment accumulation rates. Dry bulk density (DBD) was determined at approximately one-meter distances for the cores at Site 984 (Jansen et al., 1996). We interpolated the DBD and the sedimentation rates data with the AnalySeries 1.2 software (Paillard et al., 1996) to reach a time resolution of 200 yr for each record.

## **Results**

### ***Long term and glacial-to-interglacial trends***

The records of stable isotopes and benthic foraminifera reported in Fig. 3 reveal pronounced long-term trends as well as glacial-to-interglacial fluctuations in the North Atlantic hydrography and benthic foraminifera populations at intermediate depth, spanning the time over intensified

NHG from 3.05 to 2.5 Ma. Perhaps the most striking feature is an abrupt and fundamental change in the benthic faunas, as represented by *C. teretis* and *B. pacifica* (Fig. 3E). Whereas *C. teretis* firstly appeared at 2.74 Ma at Site 984 (and probably coevally the northern North Atlantic in general; Schnittker, 1983), *B. pacifica*, common up to interglacial G7, abruptly disappeared from the site. This change precisely coincided with a pronounced drop in benthic  $\delta^{18}\text{O}$  by 0.6‰ at 2.74 Ma (MIS G6), and with the onset of regular glacial IRD deposition at the site (Fig. 3A and B).

The outlined faunal change suggests a response to a profound change in subpolar productivity which was apparently irreversible. Prior to that turning point, the common occurrence of *B. pacifica* suggests a high productivity environment, resulting in high carbon flux at Site 984. Generally, at Site 984 *B. pacifica* was a common form reaching 2 to 10 % in the assemblages. Highest absolute abundances were reached during interglacials, where it commonly occurred in a highly diverse assemblage, whereas highest proportions in the assemblages were reached during glacials G20-G14, and glacial-interglacial transitions. Here, it eventually became dominant. Probably, also the absence of *C. wuellerstorfi*, a species adapted to well ventilated deepwater and high-current regimes and absent from high flux areas (Altenbach et al., 1999) supports this finding. After 2.74 Ma *C. teretis* immediately started to dominate the faunas, in particular during glacial and transitional periods. *B. pacifica* only during peak interglacial intervals of MIS 103 and 99 with small numbers transiently returned to the site.

No major change is however reflected in the levels of total benthic foraminifera abundances, displaying a rather constant pattern over the course of the entire record with pronounced glacial-interglacial cyclicity both, prior and subsequent to 2.74 Ma. During interglacials total abundances ranged between 40 and 120 individuals per 10 g dry sediment, and during glacials between zero and <40.

Taking the total abundances as a measure for productivity, they would imply an ongoing alternation of high interglacial and low glacial productivity. Even when corrected for numbers of *C. teretis*, following the approach by Thomas et al. (1995) this pattern does not significantly change, but the glacial and transitional numbers further decrease (Fig. 3D). Accordingly, high productivity would have also marked peak interglacials subsequent to 2.74 Ma. Maximum abundances exceeding 100 specimens were reached in MIS 99 and 103, and here a high productivity further supported by the transient return of *B. pacifica*. Taking into account sediment accumulation rates generally ranging between 5 and 40 g C cm<sup>-2</sup> kyr<sup>-1</sup>, maximum foraminiferal numbers of 3000 to 5300 were reached per cm<sup>-2</sup> kyr<sup>-1</sup> during interglacials.

The low glacial foraminiferal numbers, also reflected in the (low resolution) record of carbonate content, have been previously interpreted as a result of severe carbonate dissolution during glacials (Austin and Evans, 2000). However, the few benthic foraminifera present during those intervals are generally well preserved and display “normal“ isotopic signatures well in the expected range. Thus they question the dissolution hypothesis and rather suggest indeed low production of carbonate shells and/or strong dilution of sediments with IRD during severe glacial periods. Major gaps lacking any benthic foraminifera however mark glacial stages 100, 102, G12, here spanning also the subsequent interglacial G11, and G16.

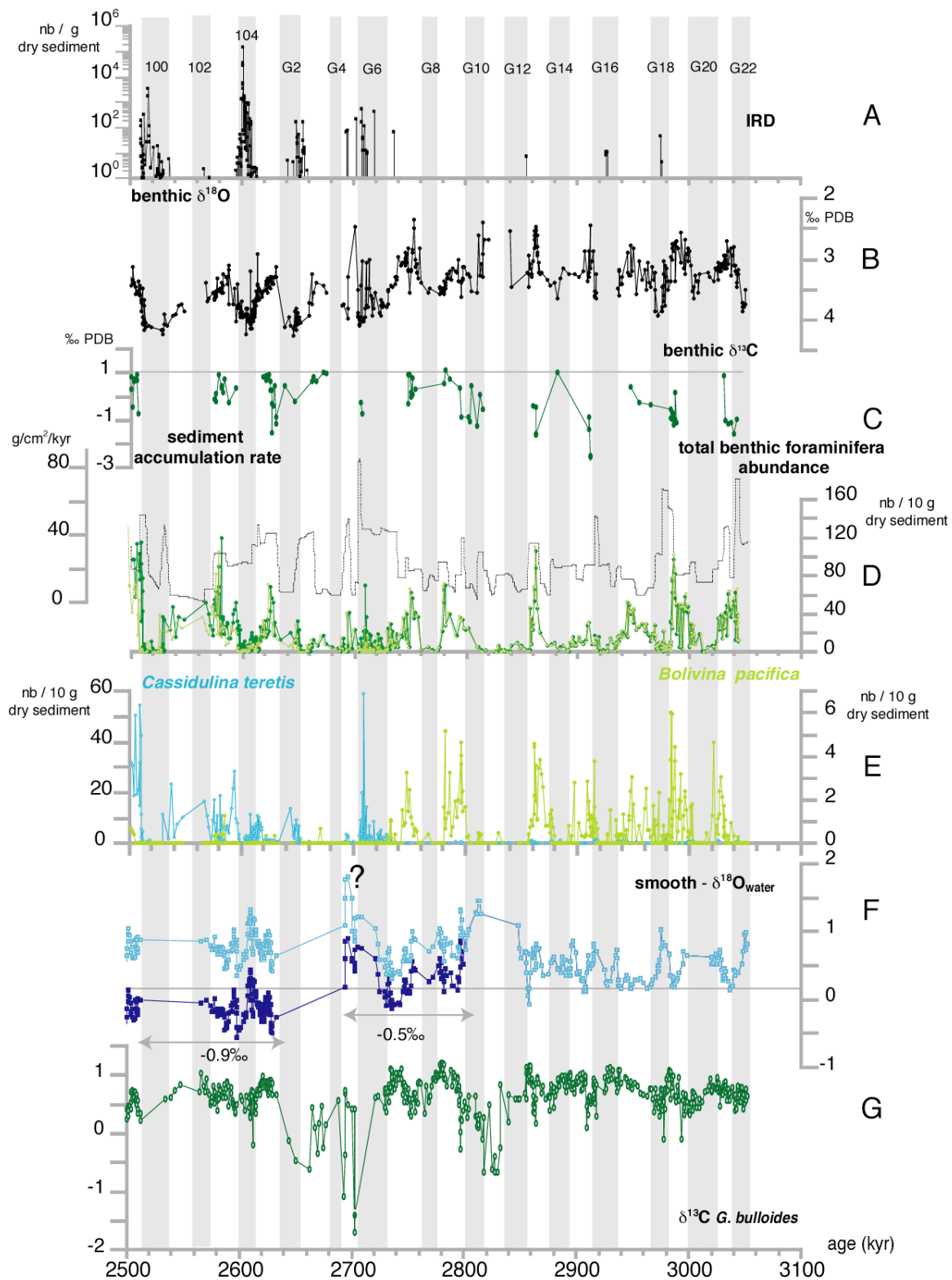


**Figure 3.** Pliocene paleoclimatic records at S. 984. (A) IRD record in number / g dry sediment, on log-scale. Glacial Marine Isotope Stages are numbered and highlighted. (B) Composite benthic  $\delta^{18}\text{O}$  record. (C) Benthic  $\delta^{13}\text{C}$  record (*Cibicides wuellerstorfi*). (D) Sediment accumulation rate in  $\text{g}/\text{cm}^2/\text{kyr}$ , total foraminifera abundance, and total foraminifera abundance corrected for *C. teretis* in number of specimens / 10 g dry sediment. (E) Abundance of benthic foraminifera *Cassidulina teretis* and *Bolivina pacifica* in / 10 g dry sediment. (F) Smoothed  $\delta^{18}\text{O}_{\text{water}}$  in ‰ SMOW, open symbol: uncorrected, closed symbol: corrected for  $0.5\text{‰}$  between 2.8–2.7 Ma and for  $0.9\text{‰}$  after 2.7 Ma. (G) Planktonic  $\delta^{13}\text{C}$  record (*Globigerina bulloides*).

A marked change in deep water masses as suggested by the abrupt drop in benthic  $\delta^{18}\text{O}$  values, is also documented in the benthic  $\delta^{13}\text{C}$  record (Fig. 3C), suggesting a change towards better ventilation of UNADW. Though hard to concisely identify in the discontinuous  $\delta^{13}\text{C}$  record, this change appears to have occurred around 2.8 Ma (i.e. in G9), and clearly preceded the other changes reported here. It marked a regular interglacial onset of *C. wuellerstorfi* occurrence with high  $\delta^{13}\text{C}$  signatures (1‰), recording fairly well ventilated UNADW. Values were well in the range of Early Pleistocene UNADW (McIntyre et al., 2001) at the same site, but still below the modern Labrador Sea Water (LSW) recorded from the same region (1.3‰; Jung, 1996). Glacial or transitional values were in contrast more depleted (-1.2 and 0.5‰). Prior to 2.8 Ma, interglacial values were strongly depleted (most values < -1‰). Interestingly, because opposite to the “post-closure“ patterns, few high values here fall into glacial or transitional intervals. The strongly depleted  $\delta^{13}\text{C}$  values coinciding with high benthic foraminiferal abundances and high numbers of *B. pacifica* during early interglacials, may indicate a strong overprint of the water DIC values by a fluff signal (Mackensen et al., 1994).

Coeval changes at the sea surface conditions potentially controlling productivity change via nutrient cycling should depict in the  $\delta^{13}\text{C}$  record of *G. bulloides* and in the  $\delta^{18}\text{O}_{\text{water}}$  record, serving as proxies for nutrient concentrations and sea surface stratification, respectively (Fig. 3G and H). Accordingly, regular  $\delta^{13}\text{C}$  fluctuations ranging between 0.0-0.3‰ and 1.0-1.3‰ may suggest alternations between low and high nutrient conditions over the course of the record. This general pattern was disrupted by two major events displaying strongly depleted  $\delta^{13}\text{C}$  values of -0.8 and -1.2 to -1.8‰ at 2.84-2.82 Ma and at 2.71-2.69 Ma, respectively. For these events with values perhaps beyond the range of “normal surface ocean values“ and coinciding with intervals of extremely low foraminifera abundances (both planktonic and benthic) indeed an overprint by a dissolution signal cannot be excluded. Therefore also unreliably low  $\delta^{18}\text{O}$  values of these intervals were rejected.

From 2.8 Ma on (i.e. MIS G9) high  $\delta^{13}\text{C}$  values reaching 1‰–1.3‰ were clearly confined to interglacials. In contrast, during glacials, low values ranged between 0.0 and 0.5‰ suggesting poor to moderate ventilation (and likely relatively high nutrient concentrations) of surface water. Maximum ventilation (and lowest nutrient concentrations) as suggested by maximum  $\delta^{13}\text{C}$  values exceeding 1.2‰ were reached during interglacials G7 and G9. Here they coincide with a time of a particularly strong THC, as reflected in high surface temperature at the site (Bartoli et al., 2005).

Because of this coincidence and an antiphasing of (low)  $\delta^{13}\text{C}$  values and high productivity as suggested by benthic foraminifera, we surmise that the  $\delta^{13}\text{C}$  pattern was not a pure nutrient signal but probably superimposed by large fluctuations in atmospheric oceanic  $\text{CO}_2$  exchange in turn depending on THC strength. Interestingly, prior to 2.8 Ma a partially inversed pattern is observable where early glacial stages G12-G18 were well ventilated, whereas early interglacials show moderate to poor ventilation and here indeed high nutrient concentrations coinciding with high productivity. Moreover, in this older portion of the record  $\delta^{13}\text{C}$  patterns appear to follow a higher frequency periodicity, perhaps reflecting precessional cycles.

The  $\delta^{18}\text{O}_{\text{water}}$  record with values generally ranging between zero and 1.4‰ reflects both, changes in Late Pliocene ice volume and in local salinity (Fig. 3F). A step towards higher values by 0.3‰ occurred at 2.8 Ma. This step was however smaller than the one expected due the rapidly growing ice sheets during that time, suggesting therefore an imprint of counteracting local salinity effects. When corrected for an assumed ice volume effect of 0.5‰ for the interval 2.8-2.69 Ma, and by 0.9‰ for the interval of 2.64-2.5 Ma (according to Bartoli et al., 2005), a pattern emerges where the  $\delta^{18}\text{O}$  values stepwise descended from 0.2‰ by 0.7‰ and finally reached values of -0.5‰. This rough estimate, which does not take into account glacial-to-interglacial ice volume fluctuations, may reflect a significant drop in surface salinity and thus an increase in surface stratification in the subpolar North Atlantic following a time of strong THC.

*MIS 104*

MIS 104 was one of the first severe glacials following the onset of major NHG at 2.74 Ma. Nearly continuous occurrence of planktonic and benthic foraminifera make it an ideal test case to explore Late Pliocene millennial scale variability (Bartoli et al., submitted). The high-resolution records in Fig. 4 reveal a marked asymmetric pattern where a gradual decrease in benthic foraminifera abundance was paralleled by an increase in IRD (Fig. 4A) and in planktonic and benthic  $\delta^{18}\text{O}$  (Fig. 4B) reflecting increasingly glacial conditions, while SST, SSS and planktic  $\delta^{13}\text{C}$  variations remained constant (Fig. 4). Whereas in the first half of MIS 104 IRD layers alternated with layers rich in planktonic foraminifera and with relatively high numbers of benthics up to 20 (Fig. 4F), in the second half abundance of foraminifera, both planktonic and benthic, declined towards zero, and IRD inversely increased to almost 100%. This “glacial maximum” phase is followed by a highly unstable termination where the general trend of slowly decreasing  $\delta^{18}\text{O}$  values, and increasing SST (Fig. 4G) and foraminiferal abundances was marked by several setbacks of IRD deposition and large fluctuations in benthic foraminiferal abundances.

Benthic faunas of MIS 104 were strongly dominated by *C. teretis* (mostly 40-80%). *M. barleeaanum*, *U. peregrina* and *E. excavatum* occurred as accessory species. Whereas *Uvigerina* and *Melonis* were confined to transitional intervals, marked also by higher total abundances of benthics and by relatively high SST (>9°C) but also by high variability, *Elphidium* seemingly had an affinity for the colder intervals (Fig. 4C and E). In general the faunal record of MIS 104 displays marked similarities as compared to Late Pleistocene glacial MIS 3 and 2 (Thomas et al., 1995; Rasmussen et al., 1996). Per analogy with the latter, presence of *Uvigerina* and *Melonis* would support relatively high productivity during warmer (interstadial) phases, whereas *Cassidulina* and *Elphidium* would support stadial phases with extremely low productivity.



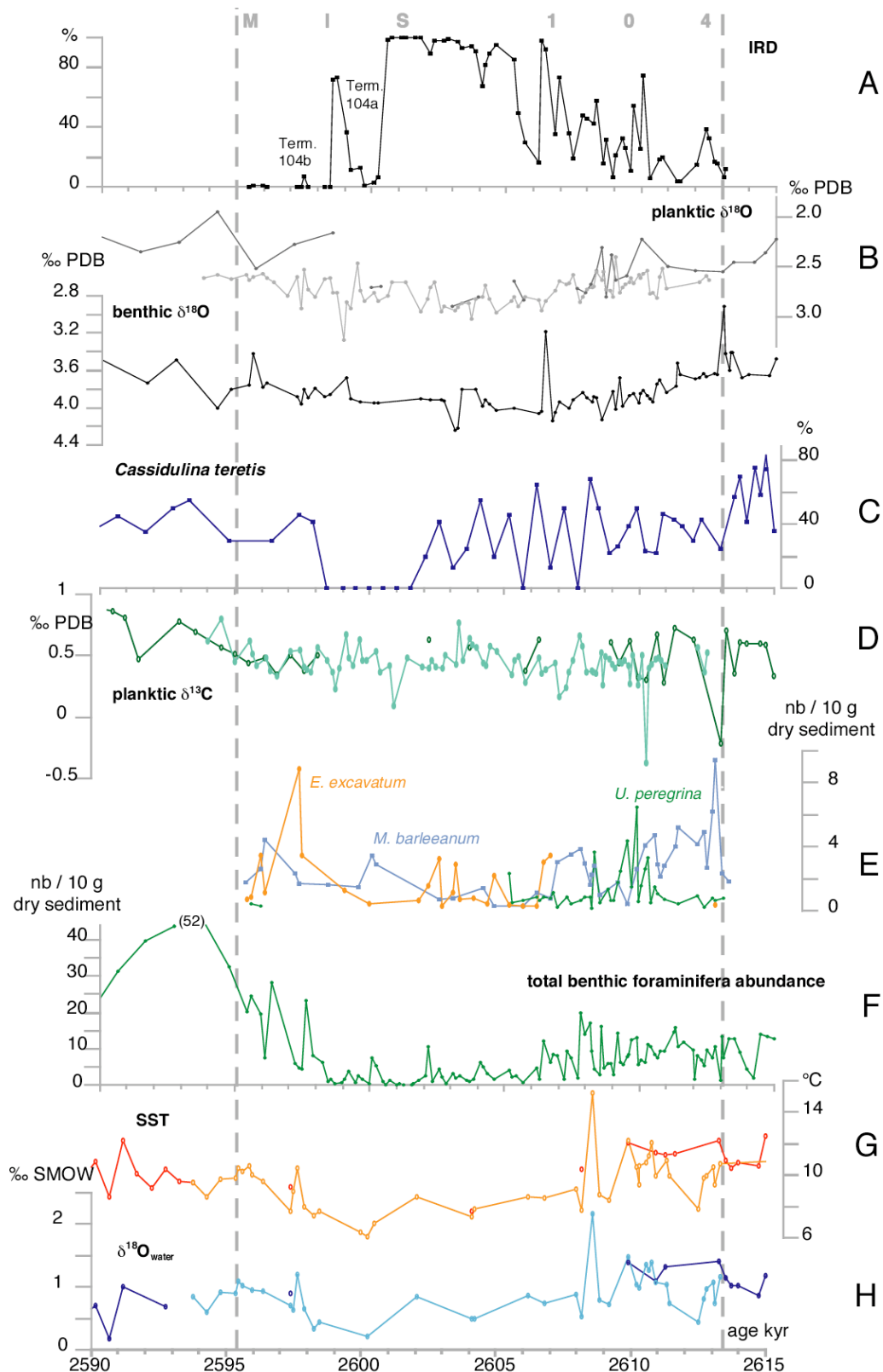


**Figure 4.** Paleoclimatic records at S. 984 during MIS 104. (A) IRD record in %. (B) Planktonic and composite benthic  $\delta^{18}\text{O}$  record. (C) Abundance of *Cassidulina teretis* in %. (D) Planktonic  $\delta^{13}\text{C}$  record (*Globigerina bulloides* and *Neogloboquadrina atlantica*). (E) Abundance of benthic foraminifera *Elphidium excavatum*, *Uvigerina peregrina*, and *Melonis barleeaanum* in / 10 g dry sediment. (F) Total benthic foraminifera abundance in number of specimen / 10 g dry sediment. (E) SST in °C (based on Mg/Ca concentrations in shells of *G. bulloides* and *N. atlantica*). (G)  $\delta^{18}\text{O}_{\text{water}}$  in ‰ SMOW (*G. bulloides* and *N. atlantica*).

## General discussion and conclusions

Benthic foraminifera of Site 984 support a Late Pliocene scenario in the northern North Atlantic which was profoundly different from today's and from (Late) Pleistocene scenarios, prior to the final closure of the CAS. Accordingly, productivity and carbon flux in the northern northeast Atlantic were elevated, as suggested by high proportions of high-flux indicating *B. pacifica* in the faunas at intermediate depths. High nutrient conditions, high production at the sea surface, and high carbon flux are moreover supported by depleted  $\delta^{13}\text{C}$  values of *G. bulloides*, a strong "fluff" overprint of the (sporadic) benthic  $\delta^{13}\text{C}$  values, and probably by the wide absence of *C. wuellerstorfi* suggest. According to Altenbach et al. (1999), presence of *B. pacifica* and absence of *C. wuellerstorfi* may be linked to carbon flux well above  $10 \text{ g C m}^{-2} \text{ yr}^{-1}$ . This scenario is consistent with model results by Schneider and Schmittner (in prep.) predicting increased nutrient levels (i.e. 10 to 20  $\mu\text{mol kg}^{-1}$  higher  $\text{NO}_3$  concentration) and consequently increased primary production (by 30%) in the high latitude North Atlantic with an open CAS. In the model, this increase resulted from the advection of nutrient-rich Pacific water to the northern Atlantic. Different from the model predictions however, according to our data, productivity remained high during MIS G9 to G7, marking a major step in the closure of the CAS, resulting in particularly strong THC and warm climates at high latitudes (Bartoli et al., 2005).

Only by 2.74 Ma (MIS G6) this high-production phase apparently abruptly ended as suggested by the takeover of opportunistic species, here represented by *C. teretis*. They suggest a response to the onset of a very different production regime, perhaps marked by strong seasonality and/or related to higher surface stratification, favoring species able to exploit low and irregular and food supply (Gooday and Lambshead, 1989; Thomas et al., 1995). Coeval first appearance of *C. teretis* at various sites in the northern North Atlantic (e.g. reported by Schnitker (1984) at Rockall Plateau Site 552) suggests a widespread decline in northern North Atlantic productivity with the onset of intensification of NHG. Possibly, *C. teretis* invaded the North Atlantic from the Nordic Seas, a hypothesis still lacking evidence, because of the poor carbonate preservation in the Nordic Seas (Jansen et al., 2000). However, the reasons for this supposed decline in productivity are unclear.

Abruptness of the onset of this new productivity regime and precise coincidence with profound changes in UNADW hydrography as reported in benthic  $\delta^{18}\text{O}$  suggest a close linkage between those variables. Bartoli et al. (2005) considered the increase in benthic  $\delta^{18}\text{O}$  at 2.74 Ma as a result of UNADW cooling which they related to the onset of LSW. This was inferred from a comparison with benthic  $\delta^{18}\text{O}$  records from the deep Atlantic. Similarly, Loubere (1987) observed a divergence of deep and intermediate water  $\delta^{18}\text{O}$ , and a shift in grain sizes at Site 554, and concluded on the establishment of a new water mass at intermediate depths at 2.9 Ma (supposedly corresponding to 2.74 Ma when corrected to the new timescale by Lisiecki and Raymo, 2005). Different from Bartoli et al. (2005) he considered this new water mass as Mediterranean Outflow Water (MOW). However, MOW should also have a fairly depleted  $\delta^{13}\text{C}$  signature (not reported by Loubere), not the case at Site 984. At the contrary, the  $\delta^{13}\text{C}$  values and the more regular occurrence of *C. wuellerstorfi* do point to an improved ventilation in UNADW. Moreover, first Mg/Ca data of benthic foraminifera at Site 984 suggest cold temperatures of 1.2–1.8°C in MIS 104 (Bartoli, unpublished data).

Yet it is unlikely that a cooling of UNADW alone would exert such a profound control on the benthic assemblages as might be argued (e.g. Lutze and Colbourn, 1984; Thomas et al., 1995). A change in surface water hydrography suppressing nutrient supply to the photic zone and linked to changes in UNADW is thus required to explain the postulated decline in primary production. The cease of advection of nutrient-rich Pacific subsurface water as predicted by Schneider and Schmittner (in prep.) would not fully explain the observed changes, since at 2.74 Ma the CAS was already closed (Bartoli et al., 2005). The advection of Pacific subsurface water should however have ceased prior to the final closure. No conclusive pattern of nutrient levels could be

deduced from the planktonic  $\delta^{13}\text{C}$  record to test this hypothesis, because the nutrient signal at Site 984 appears strongly modulated by glacial-interglacial changes in atmospheric-oceanic exchange. A decrease of SSS and thus an increase in stratification is however indeed suggested by a decrease of  $\delta^{18}\text{O}_{\text{water}}$  values. A decrease of SSS may be expected because of the deposition of IRD at the site, indicating that by that time the ice-sheets on Greenland and perhaps also the Laurentide ice-sheet had grown to the shelf-edges, eventually releasing icebergs and thus meltwater.

We therefore consider it as likely that an increase in stratification may have blocked the vertical transport of nutrients to the photic zone and thus lowered productivity. Such a scenario linked to a weaker THC would have also lead to a stronger seasonality, perhaps favoring sea-ice formation during winter. A general increase in stratification at high latitudes has been postulated as an important positive feedback for NHG via affecting the subpolar density structure (Sigman et al., 2004). In summary, our data lend support to a scenario, where the decline in North Atlantic primary productivity was not directly induced by the cessation of nutrient-rich Pacific advection, but a response to the subsequent climate deterioration.

The benthic foraminiferal records display a pronounced glacial-interglacial cyclicality with low abundances marking glacial intervals. Rich faunas and high diversity (Austin and Evans, 2000) during peak interglacials suggest the return of more favorable conditions to the site. Arguably this may have been caused by higher interglacial sea-level which would have newly flooded the CAS and reactivated the advection of Pacific water to the high latitude North Atlantic, or a simple response to more favorable climatic conditions.

Though we cannot totally rule out the possibility that the low foraminiferal numbers marking peak glacials were partially a result of severe carbonate dissolution (Austin and Evans, 2000), we rather consider them as a result of extremely low production and/or dilution with IRD. The detailed faunal records of MIS 104 further constrain this hypothesis. It shows remarkable similarities with records of MIS 3 and 2 from the subpolar Atlantic, as marked by highly unstable environmental conditions (van Kreveld et al., 2000) and a pronounced response of benthic foraminifera (Rasmussen et al., 1996). Poor faunas of MIS 104 at Site 984 were generally strongly dominated by *C. teretis* with alternating contributions of *E. excavatum* during coldest periods and of *M. barleeianum* and *Uvigerina* during warmer transitional phases (Fig. 4). Rasmussen et al. (1996) and Rasmussen and Thomsen (2004) associated *C. teretis* with “Atlantic intermediate water species” and concluded on flow reversals of Glacial North Atlantic Intermediate Water during stadials and *Melonis* to interstadials with recovered THC. Thomas et al. (1995), in contrast, attributed glacial faunas dominated by *C. teretis* to a low-nutrient regime in the glacial North Atlantic, and *Melonis* and *Uvigerina* to relatively higher level. Following the line of Thomas et al. (1995), short-term fluctuations in benthic faunas may thus reflect millennial-scale fluctuations in productivity. An increased climate instability was also found by Bartoli et al. (submitted), marking the onset of increasingly subpolar conditions, after the final closure of the CAS.

## Acknowledgements

This study was supported by the German Science Foundation (DFG) in the frame of the Research Unit “Ocean Gateways” at Kiel University. We thank M. Gustavsson and H. Gebhardt for assistance with taxonomy of *Bolivina* and *Elphidium*. Bill Austin provided additional samples of Site 984.

Data will be available on <http://www.pangea.de>

## References

Altenbach, A.V., Pflaumann, U., Schiebel, R., Thies, A., Timm, S., Trauth M., 1999. Scaling percentages of benthic foraminifera with flux rates of organic carbon. *J. Foraminifera Res.* 29, 173-185.

- Austin, W. E. N., Evans J. R., 2000. Benthic foraminifera and sediment grain size variability at intermediate water depth in the Northeast Atlantic during the late Pliocene-early Pleistocene, *Marine Geology* 170, 423-441.
- Bartoli G., M. Sarnthein, M. Weinelt, H. Erlenkeusr, D. Garbe-Schönberg, D.W. Lea, 2005. Late Pliocene onset of NHG and the final closure of Panama, *Earth Planet. Sci. Lett.* (in press).
- Bartoli, G., Sarnthein, M., Weinelt, M., submitted. Late Pliocene millennial-scale climate variability in the northern North Atlantic prior and after the onset of northern hemisphere glaciation. Submitted to *Paleoceanography*.
- Corliss, B.H., 1991. Morphology and microhabitat preferences of benthic foraminifera from the northwest Atlantic Ocean. *Mar. Micropaleontology* 17, 195-236.
- E. Jansen, Bleil, U., Henrich, R., Kringstad, L., Slettemark, B., 1988. Paleoenvironmental changes in the Norwegian Sea and the Northwest Atlantic during the last 2.8 m.y.: Deep Sea Drilling Project/Ocean Drilling Program sites 610, 642, 643 and 644. *Paleoceanography* 3, 563-581.
- Ettwein, V.J., Stickley, C.E. Maslin, M.A., Laurie, E.R., Rosell-Melé, A., Vidal, L., Brownless, M., 2002. Fluctuations in productivity and Upwelling intensity at site 1083 during the intensification of the Northern hemisphere glaciation (2.40-2.65 MA). *In: Wefer, G., Berger, W.H., and Richter, C. (Eds.) Proc. ODP, Sci. Res.* 175.
- Gooday, A.J., Lamshead, P.J.D., 1989. Influence of seasonally deposited phytodetritus on benthic foraminiferal populations in the bathyal northeast Atlantic: The species response. *Mar. Ecol. Prog. Ser.* 58, 53-67.
- Herguera, J.C., 1992. Deep-sea benthic foraminifera and biogenic opal: Glacial to postglacial productivity changes in the western equatorial Pacific. *Mar. Micropal.* 19, 79-98.
- Ishman, S.E., 1996. A benthic foraminiferal record of middle to late Pliocene (3.15-2.85) deep water change in the North Atlantic. *Mar. Micropal.* 27, 165-180.
- Jansen, E., Fronval, T., Ranck, F., Channell, J.E.T., 2000. Pliocene-Pleistocene ice rafting history and cyclicity in the Nordic Seas during the last 3.5 Myr. *Paleoceanography* 15 (6), 709-721.
- Jansen, E., Raymo, M.E., Blum, P. Herbert, T. D. (Eds.) 1996. *Proc. ODP, Init. Results*, 162: College Station, TX (Ocean Drilling Program).
- Jorissen, F.J., de Stitger, H.C., and J.G.V. Widmark, 1995. A conceptual model explaining benthic foraminiferal microhabitats. *Mar. Micropaleontology* 26, 3-15.
- Jung, S. J. A., 1996. Wassermassenaustausch zwischen NE-Atlantik und Nordmeer während der letzten 300 000/80 000 Jahre im Abbild stabiler O- und C-Isotope. *Ber.Sonderforschungsbereich 313, Univ. Kiel, Nr 61, S.1-104.* PhD thesis.
- Knudsen, K.L., W.E.N. Austin, 1996. Late glacial foraminifera. *In: Andrews, J.T., Austin, W.E.N., Bergsten, H., and A.E. Jennings (eds.) Late Quaternary Paleocyanography of the North Atlantic Margins, Geological Society Special Publication No 111, 7-10.*
- van Kreveld, S. et al., 2000. Potential links between surging ice sheets, circulation changes, and the Dansgaard-Oeschger cycles in the Irminger sea, 60-18 kyr. *Paleoceanography* 15 (4), 425-442.
- Lisiecki, L.E., Raymo, M.E., 2005. A Pliocene-Pleistocene stack of 57 globally distributed benthic  $\delta^{18}\text{O}$  records. *Paleoceanography*, 20: PA1003.
- Loubere, P., 1987. Changes in mid-depth North Atlantic and Mediterranean circulation during the Late Pliocene – isotopic and sedimentological evidence. *Mar. Geol.* 77, 15-38.
- Lute, G.H., W.T. Colbourn, 1984. Recent benthic foraminifera from the continental margin off northwest Africa: Community structure and distribution. *Mar. Micropal.* 8, 361-401.
- Mackensen, A., 1987. Benthische Foraminiferen auf dem Island Schottland Rücken: Umwelt-Anzeiger an der Grenze zweier ozeanischer Räume. *Paläont. Z.*, 61, 149-179.
- Mackensen, A., Grobe, H., Hubberten, H.-W., Kuhn, G., 1994. Benthic foraminiferal assemblages and the  $\delta^{13}\text{C}$ -signal in the Atlantic sector of the Southern Ocean: glacial-to-interglacial contrasts. *In: Zahn, R., Pedersen, T., Kaminski, M., Labeyrie, L. Eds. , Carbon Cycling in the Glacial Ocean: Constraints on the Ocean's Role in Global Change. NATO ASI Series I: Global Environmental Change. Springer-Verlag, Heidelberg, pp. 105-144.*
- Mc Intyre, K., Delaney, A., Ravelo, C., 2001. Millennial-scale climate change and oceanic processes in the late Pliocene and early Pleistocene. *Paleoceanography* 16, 553-543.
- McCorkle, D. C., Keigwin, L. D., Corliss, B. H., Emerson S. R., 1990. The influence of microhabitats on the carbon isotopic composition of deep-sea benthic foraminifera. *Paleoceanography* 5, 161- 185.
- Paillard, D., Labeyrie, L., Yiou, P., 1996. Macintosh program performs time-series analysis. *EOS Trans, AGU*, 77, 379.
- Rasmussen, T.L., Thomsen, E., 2004. The role of the North Atlantic Drift in the millennial timescale glacial climate fluctuations. *Paleogeogr. Paleoclimatol. Paleoecol.* 210, 101-116.

Rasmussen, T.L., Thomsen, E., Labeyrie, L., van Weering, T.C.E., 1996. Circulation changes in the Faeroe – Shetland Channel correlating with cold events during the last glacial period (58 –10 ka). *Geology* 24, 937–940.

Sarnthein, M., Fenner, J., 1988. Global wind-induced change of deep-sea sediment budgets, new ocean production and CO<sub>2</sub> reservoirs ca. 3.3-2.35 Ma BP. *Phil. Trans. R. Soc. Lond.* 318, 487-504.

Schmittner, A. 2005. Decline of the marine ecosystem caused by a reduction in the Atlantic overturning circulation. *Nature* 434, 628-633.

Schneider, B., Schmittner, A. Simulating the impact of the Panamanian seaway closure on ocean circulation, marine productivity and nutrient cycling, in prep.

Schnitker, D., 1984. High resolution records of benthic foraminifers in the Late Neogene of the northeastern Atlantic – In: D.G. Roberts, D. Schnitker, et al. (eds.). *Init. Rep. of the DSDP*, 81, 611-622.

Shackleton, N.J., 1974. Attainment of isotopic equilibrium between ocean water and the benthonic foraminifera genus *Uvigerina*: isotopic changes in the ocean during the last glacial. *Cent. Nat. Rech. Sci. Colloq. Int.* 219, 203-209.

Shackleton, N.J. et al., 1984. Oxygen isotope calibration of the onset of ice-rafting and history of glaciation in the North Atlantic region. *Nature* 307: 620-623.

Sigman, D.M., Jaccard, S.L., Haug, G.H., 2004. Polar ocean stratification in a cold climate. *Nature* 428: 59-63.

Thomas, E., Booth, L., Maslin, M., Shackleton, N.J., 1995. Northeastern Atlantic benthic foraminifera during the last 45,000 years: Changes in productivity seen from bottom. *Paleoceanography* 10, 545-562.

Thomas, E., 1987. Late Oligocene to Recent benthic foraminifers from Deep Sea Drilling Project Sites 608 and 610, Northeastern Atlantic. In: Ruddiman, W. F., Kidd, R. B., Thomas, E. et al. (eds) *Proc. of the DSDP, Init. Repts.* 94, 813-814.

Weinelt, M., Kuhnt, W., Sarnthein, M., Altenbach, A., Costello, O., Erlenkeuser, H., Pflaumann, U., Simstich, J., Struck, U., Thies, A., Trauth, M. H., Vogelsang, E., 2001. Paleoceanographic Proxies in the Northern North Atlantic, In: *The Northern North Atlantic: A changing environment*, M. Schlüter, P. Schäfer, W. Ritzrau, J. Thiede (eds.), Springer, Berlin, 319-352.



**Integrated Ocean Drilling Program  
Expedition 303 Preliminary Report**

**North Atlantic Climate**

**Ice sheet–ocean atmosphere interactions on millennial  
timescales during the late Neogene-Quaternary using a  
paleointensity-assisted chronology for the North Atlantic**

25 September–16 November 2004

Shipboard Scientific Party

January 2005

## **PUBLISHER'S NOTES**

Material in this publication may be copied without restraint for library, abstract service, educational, or personal research purposes; however, this source should be appropriately acknowledged.

### **Citation:**

Shipboard Scientific Party, 2005. North Atlantic climate: ice sheet–ocean atmosphere interactions on millennial timescales during the late Neogene–Quaternary using a paleointensity-assisted chronology for the North Atlantic. *IODP Prel. Rept.*, 303. <http://iodp.tamu.edu/publications/PR/303PR/303PR.PDF>.

### **Distribution:**

Electronic copies of this series may be obtained from the Integrated Ocean Drilling Program (IODP) Publication Services homepage on the World Wide Web at [iodp.tamu.edu/publications](http://iodp.tamu.edu/publications).

This publication was prepared by the Integrated Ocean Drilling Program U.S. Implementing Organization (IODP-USIO): Joint Oceanographic Institutions, Inc., Lamont-Doherty Earth Observatory of Columbia University, and Texas A&M University, as an account of work performed under the international Integrated Ocean Drilling Program, which is managed by IODP Management International (IODP-MI), Inc. Funding for the program is provided by the following agencies:

European Consortium for Ocean Research Drilling (ECORD)

Ministry of Education, Culture, Sports, Science and Technology (MEXT) of Japan

Ministry of Science and Technology (MOST), People's Republic of China

U.S. National Science Foundation (NSF)

## **DISCLAIMER**

Any opinions, findings, and conclusions or recommendations expressed in this publication are those of the author(s) and do not necessarily reflect the views of the participating agencies, IODP Management International, Inc., Joint Oceanographic Institutions, Inc., Lamont-Doherty Earth Observatory of Columbia University, Texas A&M University, or Texas A&M Research Foundation.



The following scientists and personnel were aboard the *JOIDES Resolution* for Expedition 303 of the Integrated Ocean Drilling Program.

## Shipboard Scientific Party

**James E.T. Channell**  
**Co-Chief Scientist**  
Department of Geological Sciences  
University of Florida  
241 Williamson Hall  
Gainesville FL 32611-7340  
USA  
[jetc@nersp.nerdc.ufl.edu](mailto:jetc@nersp.nerdc.ufl.edu)  
Work: (352) 392-3658  
Fax: (352) 392-9294

**Tokiyuki Sato**  
**Co-Chief Scientist**  
Institute of Applied Sciences, Mining College  
Akita University  
Tegata-Gakuencho 1-1  
Akita 010-8502  
Japan  
[toki@quartet.ipc.akita-u.ac.jp](mailto:toki@quartet.ipc.akita-u.ac.jp)  
Work: (81) 18-833-5261  
Fax: (81) 18-837-0401

**Mitchell J. Malone**  
**Expedition Project Manager/Staff Scientist**  
Integrated Ocean Drilling Program  
Texas A&M University  
1000 Discovery Drive  
College Station TX 77845-9547  
USA  
[malone@iodp.tamu.edu](mailto:malone@iodp.tamu.edu)  
Work: (979) 845-5218  
Fax: (979) 845-0876

**Stuart Robinson**  
**Logging Staff Scientist**  
Borehole Research Group  
Lamont-Doherty Earth Observatory  
of Columbia University  
PO Box 1000, 61 Route 9W  
Palisades NY 10964  
USA  
[stuartr@ldeo.columbia.edu](mailto:stuartr@ldeo.columbia.edu)  
Work (845) 365 8695  
Fax: (845) 365 3182

**Gretta Linda Bartoli**  
**Sedimentologist**  
Institute for Geosciences  
Christian-Albrechts-Universität zu Kiel  
Olshausenstrasse 40  
24118 Kiel  
Germany  
[gb@gpi.uni-kiel.de](mailto:gb@gpi.uni-kiel.de)  
Work: (49) 431-880-2884  
Fax: (49) 431-880-4376

**Shun Chiyonobu**  
**Paleontologist (nannofossils)**  
Institute of Geology and Paleontology  
Tohoku University  
Graduate School of Science  
Aramaki-aza-Aoba  
Aoba-ku, Sendai 980-8587  
Japan  
[chiyonobu@dges.tohoku.ac.jp](mailto:chiyonobu@dges.tohoku.ac.jp)  
Work: (81) 18-889-2371

**John (Jed) E. Damuth**  
**Sedimentologist**  
Department of Geology  
University of Texas at Arlington  
PO Box 19049  
500 Yates Street, Room 107  
Arlington TX 76019-0049  
USA  
[damuth@uta.edu](mailto:damuth@uta.edu)  
Work: (303) 471-2090  
Fax: (817) 272-2628

**Lucia de Abreu**  
**Physical Properties Specialist**  
Department of Earth Sciences  
University of Cambridge  
The Godwin Laboratory  
Pembroke Street - New Museums Site  
Cambridge CB2 3SA  
United Kingdom  
[ld206@cus.cam.ac.uk](mailto:ld206@cus.cam.ac.uk)  
Work: (44) 1223-334870  
Fax: (44) 1223-334871

**Anne De Vernal**

**Palynologist**

GEOTOP

Université du Québec à Montréal

CP 8888, Succursale Centre Ville

Montréal Québec H3C 3P8

Canada

[devernal.anne@uqam.ca](mailto:devernal.anne@uqam.ca)

Work: (514) 987-3000, ext 8599

Fax: (514) 987-3635

**Atsuhito Ennyu**

**Inorganic/Organic Geochemist**

Department of Earth and Planetary Sciences

Hokkaido University

N 10 W 8

Sapporo 060-0810

Japan

[aennyu@nature.sci.hokudai.ac.jp](mailto:aennyu@nature.sci.hokudai.ac.jp)

Work: (81) 11 706 4498

Fax: (81) 11 706 2986

**Estela Vazquez Esmerode**

**Sedimentologist**

University of Copenhagen

Geologisk Institut

Oster Voldgade 10

1350 Copenhagen

Denmark

[estelav@geol.ku.dk](mailto:estelav@geol.ku.dk)

Work: (45) 264-34987

**Satoshi Funakawa**

**Paleontologist (radiolarians)**

Department of Geology, Faculty of Agriculture

Utsunomiya University

Utsunomiya, Tochigi 321-8505

Japan

[funakawa@msg.biglobe.ne.jp](mailto:funakawa@msg.biglobe.ne.jp)

Work: (81) 28-649-5426

Fax: (81) 28-655-4802

**Samuel S. Henderson**

**Physical Properties Specialist**

Department of Geological Sciences

Rutgers, The State University of New Jersey

610 Taylor Road

Piscataway NJ 08854-8066

USA

[samhend@rci.rutgers.edu](mailto:samhend@rci.rutgers.edu)

Work: (732) 445-3507

Fax: (732) 445-3374

**David A. Hodell**

**Stratigraphic Correlator**

Department of Geological Sciences

University of Florida

214 Williamson Hall

PO Box 112120

Gainesville FL 32611

USA

[dhodell@geology.ufl.edu](mailto:dhodell@geology.ufl.edu)

Work: (352) 392-6137

Fax: (352) 392-9294

**Masashi Ito**

**Inorganic Geochemist**

Institute for Frontier Research

on Earth Evolution (IFREE)

Japan Marine Science and Technology Center

2-15 Natsushimacho

Yokosuka 237-0061

Japan

[masasitou@jamstec.go.jp](mailto:masasitou@jamstec.go.jp)

Work: (81) 468-67-9793

Fax: (81) 468-67-9775

**Kiichiro Kawamura**

**Sedimentologist**

Research Group 3

Fukada Geological Institute

2-13-12 Honkomagome

Bunkyo-ku 113-0021

Japan

[kichiro@fgi.or.jp](mailto:kichiro@fgi.or.jp)

Work: (81) 3-3944-8010

Fax: (81) 3-3944-5404

**Noriko Kawamura**

**Sedimentologist**

Graduate School of Human and

Environmental Studies

Kyoto University

Yoshida-Nihonmatsu-cho

Sakyo-ku, Kyoto 606-8501

Japan

[kwmr@gaia.h.kyoto-u.ac.jp](mailto:kwmr@gaia.h.kyoto-u.ac.jp)

Work: (81) 75-753-6891

Fax: (81) 75-753-2972

**Lawrence A. Krissek**  
**Sedimentologist**  
Department of Geological Sciences  
Ohio State University  
130 Orton Hall  
155 South Oval Mall  
Columbus OH 43210-1308  
USA  
[krissek@mps.ohio-state.edu](mailto:krissek@mps.ohio-state.edu)  
Work: (614) 292-1924  
Fax: (614) 292-1496

**Sasha N.B. Leigh**  
**Sedimentologist**  
School of Geography and Geosciences  
St. Andrews University  
Irvine Building, North Street  
St. Andrews, Fife  
Scotland KY16 9AL  
United Kingdom  
[snbl@st-andrews.ac.uk](mailto:snbl@st-andrews.ac.uk)  
Work: (44) 07929 714 848

**Chuanlian Liu**  
**Paleontologist (nannofossils)**  
School of Ocean and Earth Science  
Tongji University  
1239 Siping Road  
Shanghai 200092  
People's Republic of China  
[clliu@online.sh.cn](mailto:clliu@online.sh.cn)  
Work: (86) 21-65984876  
Fax: (86) 21-65988808

**Alain Mazaud**  
**Paleomagnetist**  
Laboratoire des Sciences du Climat  
et de l'Environnement (LSCE)  
CNRS  
Domaine du CNRS, Avenue de la Terrasse  
Gif-sur-Yvette  
91198 France  
[mazaud@lsce.cnrs-gif.fr](mailto:mazaud@lsce.cnrs-gif.fr)  
Work: (33) 1 69 82 3527  
Fax: (33) 1 69 82 3568

**Stephen Obrochta**  
**Sedimentologist**  
Division of Earth and Ocean Sciences  
Duke University  
Durham NC 27708  
USA  
[spo@duke.edu](mailto:spo@duke.edu)  
Fax: (919) 684-5833

**Oscar E. Romero**  
**Paleontologist (diatoms)**  
Department of Geosciences  
Universität Bremen  
PO Box 33 04 40  
28334 Bremen  
Germany  
[oromero@uni-bremen.de](mailto:oromero@uni-bremen.de)  
Work: (49) 421 218 7759  
Fax: (49) 421 218 8916

**Ralf Schiebel**  
**Paleontologist (foraminifers)**  
Earth Science  
Eidgenössische Technische Hochschule—Zentrum  
Sonneggstrasse 5  
8092 Zürich  
Switzerland  
[schiebel@erdw.ethz.ch](mailto:schiebel@erdw.ethz.ch)  
Work: (41) 1 6323676  
Fax: (41) 1 6321080

**Chieko Shimada**  
**Paleontologist (diatoms)**  
Graduate School of Life and Environmental  
Sciences  
University of Tsukuba  
1-1-1 Tennodai  
Tsukuba 305-8572  
Japan  
[cshim@arsia.geo.tsukua.ac.jp](mailto:cshim@arsia.geo.tsukua.ac.jp)  
Work: (81) 29-853-4465  
Fax: (81) 29-851-9764

**Joseph S. Stoner**  
**Paleomagnetist**  
Institute of Arctic and Alpine Research  
University of Colorado at Boulder  
1560 30th Street  
Campus Box 450  
Boulder CO 80309-0450  
USA  
[joseph.stoner@colorado.edu](mailto:joseph.stoner@colorado.edu)  
Work: (303) 492-7641  
Fax: (303) 492-6388

**Roy H. Wilkens**  
**Stratigraphic Correlator**  
Hawaii Institute of Geophysics and Planetology  
University of Hawaii at Manoa  
1680 East West Road  
Honolulu HI 96822  
USA  
[rwilkens@hawaii.edu](mailto:rwilkens@hawaii.edu)  
Work: (808) 956-5228  
Fax: (808) 956-3188

**James D. Wright**  
**Sedimentologist**  
Department of Geological Sciences  
Rutgers, The State University of New Jersey  
Room 238 Wright Geological Laboratory  
610 Taylor Road  
Piscataway NJ 08854-8066  
USA  
[jdwright@rci.rutgers.edu](mailto:jdwright@rci.rutgers.edu)  
Work: (732) 445-5722  
Fax: (732) 445 3374

**Makoto Yamasaki**  
**Paleontologist (foraminifers)**  
Institute of Applied Earth Sciences  
Faculty of Engineering and Resource Science  
Akita University  
1-1 Tegata-Gakuencho  
Akita 010-8502  
Japan  
[yamasaki@keigo.mine.akita-u.ac.jp](mailto:yamasaki@keigo.mine.akita-u.ac.jp)  
Work: (81) 18-889-2383  
Fax: (81) 18-837-0401

## **Transocean Officials**

**Alexander Simpson**  
**Master of the Drilling Vessel**  
Overseas Drilling Ltd.  
707 Texas Avenue South, Suite 213D  
College Station TX 77840-1917  
USA

**Wayne Malone**  
**Drilling Superintendent**  
Overseas Drilling Ltd.  
707 Texas Avenue South, Suite 213D  
College Station TX 77840-1917  
USA

## **IODP Shipboard Personnel and Technical Representatives**

**Ronald M. Grout**  
Operations Superintendent

**Roy Davis**  
Laboratory Officer

**Paula Clark**  
Marine Computer Specialist

**Trevor J. Cobine**  
Marine Laboratory Specialist: Paleomagnetism

**Lisa K. Crowder**  
Marine Laboratory Specialist: Underway  
Geophysics

**John Michael Davis**  
Marine Computer Specialist

**John Eastlund**  
Programmer Specialist

**Dennis Graham**  
Marine Laboratory Specialist: Chemistry

**Michiko Hitchcox**  
Yeoperson

**Ted Gustafson**  
Marine Laboratory Specialist: Downhole Tools/  
Thin Sections

**Leah Shannon Housley**  
Imaging Specialist

**Eric Jackson**  
Marine Laboratory Specialist: X-Ray

**Jan Jurie Kotze**  
Marine Instrumentation Specialist

**Chieh Peng**  
Assistant Laboratory Officer

**Steve Prinz**  
Marine Laboratory Specialist: Physical Properties

**Pieter Pretorius**  
Marine Instrumentation Specialist

**Paula Weiss**  
Marine Laboratory Specialist: Curator

**Robert M. Wheatley**  
Marine Laboratory Specialist: Chemistry

**Javier Espinosa**  
Schlumberger Engineer

## **ABSTRACT**

Integrated Ocean Drilling Program (IODP) Expedition 303 was designed to sample and study climate records, including the composition and structure of surface or bottom waters and detrital layer stratigraphy indicative of ice sheet instability, at strategic sites that record North Atlantic Pliocene–Quaternary climate. The sites are distributed from the mouth of the Labrador Sea (Eirik Drift and Orphan Knoll) to the central Atlantic in the region of the Charlie Gibbs Fracture Zone. The sites were chosen on the basis of the importance of the climate or paleoceanographic record, adequate sedimentation rates in the 5–20 cm/k.y. range, and the attributes for a stratigraphic template based on relative geomagnetic paleointensity and oxygen isotope data.

## **INTRODUCTION**

The focus of Integrated Ocean Drilling Program (IODP) Expedition 303 was to place late Neogene–Quaternary North Atlantic climate history into a paleointensity-assisted chronology (PAC) based on oxygen isotopes and geomagnetic paleointensity. The nine primary drilling locations (Fig. F1) are known, either from previous Ocean Drilling Program (ODP)/Deep Sea Drilling Project (DSDP) drilling or from conventional piston cores, to have the following attributes:

- They contain distinct records of millennial-scale environmental variability (in terms of ice sheet–ocean interactions, deep circulation changes, or sea-surface conditions);
- They provide the requirements for developing a millennial-scale stratigraphy (through geomagnetic paleointensity, oxygen isotopes, microfossils, and regional environmental patterns); and
- They document the details of geomagnetic field behavior.

The ultimate objective is to generate a chronostratigraphic template for North Atlantic climate proxies to allow their correlation at a sub-Milankovitch scale and their export to other parts of the globe.

## **BACKGROUND**

### **Geological Setting**

The North Atlantic Ocean is undoubtedly one of the most climatically sensitive regions on Earth because the ocean-atmosphere-cryosphere system is prone to mode jumps that are triggered by changes in freshwater delivery to source areas of deepwater formation. During the last glaciation, these abrupt jumps in climate state are manifest by Dansgaard/Oeschger (D/O) cycles and Heinrich events in ice and marine sediment cores. Given the paramount importance of the North Atlantic as a driver of global climate change, we drilled at nine key locations to extend the study of millennial-scale climate variability over the last few million years. What is the rationale for studying millennial-scale variability in the North Atlantic over the last few million years rather than just the last glacial cycle (recoverable by conventional piston cores)? Determining the long-term evolution of millennial-scale variability in surface temperature, ice sheet dynamics, and thermohaline circulation can provide clues to the mechanisms responsible for abrupt climate change. For example, the

average climate state evolved toward generally colder conditions with larger ice sheets during the Pliocene–Pleistocene. This shift was accompanied by a change in the spectral character of climate proxies from dominantly 41 k.y. to 100 k.y. periods between ~920 and 640 ka (Schmieder et al., 2000). Among the numerous questions to be answered are the following:

- When did “Heinrich events” first appear in the sedimentary record of the North Atlantic?
- Are they restricted to the “100 k.y. world” when ice volume increased substantially?
- Is the quasi-periodic 1500 y cycle documented for the last climate cycle a stable feature of the North Atlantic throughout the Pleistocene?
- How has millennial-scale variability evolved during the Pleistocene as orbital and glacial boundary conditions changed?

## **SCIENTIFIC AND OPERATIONAL OBJECTIVES OF EXPEDITION 303**

### **Climate-Related Objectives**

Stratigraphy is the fundamental backbone of our understanding of Earth’s history, and stratigraphic resolution is the main factor that limits the timescale of processes that can be studied in the past. Sub-Milankovitch-scale climate studies face the challenge of finding a stratigraphic method suitable for correlation at this scale (see Crowley, 1999). Even under optimal conditions, chronologies based on  $\delta^{18}\text{O}$  are unable to provide sufficient stratigraphic resolution. Within the North Atlantic region, recent improvements in stratigraphic resolution have resulted in a new understanding of the dynamics of millennial-scale climate variability over the last ~100 k.y. (e.g., Bond et al., 1993; McManus et al., 1994; van Kreveld et al., 2000; Sarnthein et al., 2001). These stratigraphies have utilized chronologies from the Greenland Summit ice cores (GRIP/GISP2) and the recognition of regional lithostratigraphic linkages such as Heinrich events and higher-frequency ice-rafted debris (IRD) layers, ash layers, and susceptibility cycles combined with planktonic/benthic  $\delta^{18}\text{O}$ , acceleration mass spectrometry (AMS) $^{14}\text{C}$  dates, and geomagnetic paleointensity data (e.g., Bond et al., 1992, 1993, 1999; McManus et al., 1994; Stoner et al., 1998, 2002; Voelker et al., 1998; Kissel et al., 1999; Laj et al., 2000).

The objective of the expedition is to integrate stable isotope and relative geomagnetic paleointensity data with paleoceanographic proxies and, in so doing, generate integrated North Atlantic millennial-scale stratigraphies for the last few million years.

Understanding the mechanisms and causes of abrupt climate change is one of the major challenges in global climate change research today (see Clark et al., 1999, p. vii) and constitutes a vital initiative of the Initial Science Plan of IODP. Ideally, the best approach to this problem would be to collect records of climate variability from a dense geographic network of sites, but this is impractical in paleoceanographic research. In the absence of dense coverage, the most viable approach is to obtain long, continuous time series from key regions and compare the response and timing of climate change among sensitive regions. We intend to develop PACs to establish the phase relationships among globally distributed millennial-scale records. Building global correlations on millennial timescales is an essential step to understanding the underlying mechanisms of abrupt climate change.

A persistent quasi-periodic ~1500 y cycle that is apparently independent of glacial or interglacial climate state has been observed for the past 80 k.y. (Bond et al., 1997, 1999). The millennial-scale cyclicity in the Holocene appears to be mirrored in the last interglacial (marine isotope Stage [MIS] 5e) and is defined by the same petrologic proxies in both interglacials. The presence of this cyclicity in interglacials and the IRD petrology that defines it indicate that the cyclicity does not reflect ice sheet instability or changes in calving of coastal glaciers, but rather changes in sources or survivability of drifting ice, driven by changes in the size and intensity of the subpolar cyclonic gyre (Bond et al., 1999). The Holocene cycles reflect a mechanism operating on at least hemispheric scale (Sirocko et al., 1996; Campbell et al., 1998; De Menocal et al., 2000), indicating that the MIS 5e and Holocene cyclicities have a common origin possibly related to solar forcing (Bond et al., 2001). The implication is that the 1500 y cycle may have been a dominant feature of the Earth's ocean-atmosphere climate over a very long time, which leads to the following questions:

- How far back in time does the ~1500 y cycle extend?
- Do D/O cycles simply represent an amplification of this?
- Do distinct modes of variability persist through other glacial and interglacial intervals?
- If so, is the pacing always the same or does millennial-scale variability evolve during the late Pleistocene?



Recently published evidence from earlier interglacials (MIS 11 and 13) in both the subpolar and subtropical North Atlantic suggests that interglacial cyclicity at those times may have had a significantly longer pacing, on the order of 5000 y or more. The interglacial records from MIS 11 and 13 in Oppo et al. (1998) and McManus et al. (1999), for example, show rather sporadic events that, regardless of age model, cannot occur every 1500 y. Similarly, an MIS 11 record from ODP Site U1063 off Bermuda indicates large shifts in benthic  $\delta^{13}\text{C}$  on the order of 5–6 k.y. (Poli et al., 2000). In contrast, data from MIS 11 at ODP Site 980 implies the presence of 1–2 k.y. pacing (McManus et al., 1999), suggesting that the 1500 y cycle may be operating in MIS 11 and in other pre-MIS 5e interglacials. If this is true, then the interglacial climate variability may reflect a persistent, perhaps periodic, process operating continuously within the Earth's climate (rather than red noise resulting from a highly nonlinear climate system).

The best evidence for the 1500 y cycle during interglacials seems to be coming from IRD proxies that monitor changes in the subpolar gyre in the North Atlantic. Our drilling sites are positioned to monitor such changes. In contrast to ODP Site 980 (Feni Drift), our sites are located well within the main present-day routes of iceberg transport into the North Atlantic and are therefore well suited to capture faint interglacial signals that respond to shifting ocean surface circulation. If we can connect the 1500 y cycle to paleointensity records, we will have a means of directly comparing both signals with climate records from well outside the North Atlantic region.

## **Geomagnetic-Related Objectives**

Understanding the changes in the ice sheet-ocean-atmosphere system that gave rise to millennial-scale climate changes requires the precise long-distance correlation of ice cores and marine sediment cores. Geomagnetic paleointensity records from marine sediment cores have been shown to contain a global signal suitable for fine-scale correlation (see Meynadier et al., 1992; Guyodo and Valet, 1996; Channell et al., 2000; Stoner et al., 1995, 2000, 2002; Laj et al., 2000), at least for the last glacial cycle.

Beyond the range of AMS  $^{14}\text{C}$  dating, geomagnetic paleointensity data may provide the only viable means of sub-Milankovitch-scale long-distance correlation. Paleointensity records have been applied to stratigraphic correlation in the Labrador Sea for the last 200 k.y. (Stoner et al., 1998), throughout the North Atlantic for the last 75 k.y. (Laj et al., 2000), and for the Atlantic realm for the last 110 k.y. (Stoner et al., 2000). As variations in geomagnetic paleointensity control atmospheric production of  $^{10}\text{Be}$

and  $^{36}\text{Cl}$  isotopes and the flux of these isotopes is readily measurable in ice cores, paleointensity records in marine cores provide an independent link between marine sediment and ice core records (e.g., Mazaud et al., 1994). The lows in paleointensity at ~40 and ~65 ka are readily identifiable as highs in  $^{10}\text{Be}$  and  $^{36}\text{Cl}$  fluxes (Baumgartner et al., 1998; Raisbeck et al., 1987) in the Vostok and GRIP ice cores, respectively. Frank et al. (1997) showed that  $10^4$ – $10^5$  y variability in  $^{10}\text{Be}$  production rate, as determined from globally distributed deep-sea cores over the last 200 k.y., can be matched to sediment paleointensity data. This observation and the similarity of globally distributed paleointensity records indicate that much of the variability in paleointensity records is globally correlative. The few high-resolution paleointensity records available beyond 200 ka also indicate that fine-scale features are correlative. For example, the paleointensity record for the MIS 9–11 interval (300–400 ka) from the Iceland Basin (ODP Sites 983 and 984) can be correlated to the sub-Antarctic South Atlantic (ODP Site U1089) at suborbital (millennial) scale (Stoner et al., 2003).

In addition to the practical use of magnetic field records for correlation of climate records, further drilling of high-sedimentation-rate drift sites will impact the “solid Earth” theme of IODP by documenting the spatial and temporal behavior of the geomagnetic field at unprecedented resolution. Such data are required to elucidate processes in the geodynamo-controlling secular variation and polarity reversal of the geomagnetic field. Recently derived records of directional secular variation and paleointensity from drift sites (e.g., ODP Legs 162 and 172) have substantially advanced our knowledge of magnetic secular variation, magnetic excursions, and directional/intensity changes at polarity reversal boundaries (see Channell and Lehman, 1997; Channell et al., 1998, 2002; Lund et al., 1998, 2001a, 2001b). Numerous directional magnetic excursions have been observed within the Brunhes Chron at ODP Leg 172 drift sites (Lund et al., 1998, 2001a, 2001b) and in the Matuyama Chron at ODP Leg 162 sites (Channell et al., 2002). These excursions (or brief subchronozones) correspond to paleointensity minima and have estimated durations of a few thousand years. From ODP Leg 162 records and records from the Pacific Ocean, it has been suggested that spectral power at orbital frequencies in paleointensity records may reflect a fundamental property of the geodynamo (Channell et al., 1998; Yamazaki, 1999; Yamazaki and Oda, 2002) rather than climate-related influences on paleointensity records (Guyodo et al., 2000).

There is no doubt that North Atlantic drift sites have revolutionized our understanding of the behavior of the geomagnetic field by providing Brunhes Chron paleomagnetic records at unprecedented resolution. The records can now provide useful

constraints for numerical simulations of the geodynamo (e.g., Glatzmaier and Roberts, 1995; Gubbins, 1999; Coe et al., 2000). As a result of these parallel advances, our understanding of the geomagnetic field is on the threshold of substantial progress.

The Expedition 303 sites will provide high-resolution paleomagnetic records extending through the Matuyama Chron (to ~3 Ma). They will allow us to assess the temporal and spatial variability of the geomagnetic field in the Brunhes Chron and compare these records with reversed polarity records from the Matuyama Chron, and to address the following questions:

- Are the characteristics of secular variation different for the two polarity states?
- Are polarity transition fields comparable for sequential polarity reversals?
- Does the geomagnetic field exhibit a complete spectrum of behavior from high-amplitude secular variation to polarity reversals that has not hitherto been documented for lack of high-resolution records?

The nonaxial-dipole (NAD) components in the historical field vary on a centennial scale, and this has been interpreted to indicate similar repeat times in the past (Hulot and Le Mouél, 1994; Hongre et al., 1998). If this is correct, paleointensity records from cores with sedimentation rates less than ~10 cm/k.y. are unlikely to record anything but the axial dipole field. On the other hand, standing NAD components have been detected in the 5 m.y. time-averaged field, although the distribution of these NAD features remains controversial (Kelley and Gubbins, 1997; Johnson and Constable, 1997; Carlot and Courtillot, 1998). Refinement of time-averaged field models as the paleomagnetic database is augmented will lead to a better grasp of how the nonzonal terms in the time-averaged field may influence paleointensity records.

## **RELATIONSHIP TO PREVIOUS NORTH ATLANTIC DRILLING**

Two previous ODP legs to the North Atlantic recovered sequences that are continuous and have sedimentation rates high enough to study oceanic variability on sub-Milankovitch timescales. During Leg 162, four sites were drilled on sediment drifts south of Iceland. These sequences are yielding invaluable insight into the nature of millennial-scale climate variability in the North Atlantic (Raymo et al., 1998, 2004; McManus et al., 1999; Raymo, 1999; Flower et al., 2000; Kleiven et al., 2003). Similarly, during Leg 172 in the northwest Atlantic between ~30° and 35°N, sequences were recovered with high deposition rates that are suitable for millennial- and perhaps centennial-scale studies (Keigwin, Rio, Acton, et al., 1998). Given the successes

of Legs 162 and 172, why are additional sites needed in the North Atlantic? The sites drilled during Expedition 303 will augment those of Legs 162 and 172 in two fundamental ways. First, most of our sites are located in the North Atlantic “IRD belt” where massive iceberg discharges are recorded by coarse layers of ice-rafted detritus that are depleted in planktonic foraminifers and have oxygen isotopic values indicative of reduced sea-surface salinities. Site 980 (from ODP Leg 162) does lie within the IRD belt, but it is located on its distal northeastern edge and, consequently, lacks the strong sea-surface response to millennial-scale IRD events that is so well displayed to the south and west. Second, the depth distribution of the Expedition 303 sites (2273–3884 meters below sea level [mbsl]) is ideal for monitoring millennial-scale changes in the production of North Atlantic Deep Water (NADW). Leg 162 sites span 1650–2170 mbsl and provide the intermediate-depth end-member for studies of the formation of Glacial North Atlantic Intermediate Water (GNAIW). Leg 172 drift sites provide a relatively complete depth transect spanning 1291–4595 mbsl. The Expedition 303 sites unify the record of millennial-scale variability in the North Atlantic by bridging the “gap” between Legs 162 and 172. The sites will also expand the geographic range of sites needed to distinguish between latitudinal changes in the mixing zone between southern and northern source waters and changes due to vertical migration of water mass boundaries (Flower et al., 2000).

Data and modeling studies point to changes in the modes of NADW formation as one of the principal factors driving millennial-scale climate change in the high-latitude North Atlantic and Europe (for review, see Alley et al., 1999). Expedition 303 sites (Fig. F1) are distributed so that they monitor the major deepwater end-members of NADW: Norwegian-Greenland Seawater (Site U1304) and Labrador Seawater (Sites U1305–U1307) as well as the final NADW mixture (Sites U1302 and U1303). Alley et al. (1999) discussed three distinct modes of thermohaline circulation in the North Atlantic: modern (M), glacial (G), and Heinrich (H). The modern mode is marked by deep-water formation in the Nordic Seas and North Atlantic where the three end-members mix to form NADW. In the glacial mode, deepwater formation is suppressed in the Nordic Seas and GNAIW forms farther south in the North Atlantic. In the Heinrich mode, both deep- and intermediate-water formation is greatly reduced. The modern mode may be a relatively rare feature of the Pleistocene (Raymo et al., 2004). Together with the depth transects drilled during Legs 162 and 172, the Expedition 303 sites will permit monitoring deep- and intermediate-water formation during all three modes of formation.

## OPERATIONAL STRATEGY

The (high-resolution) stratigraphic goals require high sedimentation rates (>5 cm/k.y.) at the chosen sites, as well as complete and undisturbed recovery of the stratigraphic sequence. The drilling strategy consisted of advanced piston coring (APC) in three or more holes at each site to ensure complete and undisturbed recovery of the stratigraphic section. The “fast track” magnetic susceptibility core logger (MSCL) allowed near real-time drilling decisions to aid complete recovery of the stratigraphic section. We used the “drillover” strategy employed during ODP Leg 202 to maximize APC recovery and penetration. The depth limit of APC coring is traditionally controlled by the overpull required to retrieve the core barrel. In cases where the full APC stroke was achieved but excessive force was required to retrieve the core barrel (often the limit of APC penetration), the drillover strategy entailed advance of the rotary bit to free the APC barrel. APC coring was generally terminated when the full APC stroke could no longer be achieved. Because of the pivotal role of magnetic studies in the objectives of the proposal, nonmagnetic core barrels were generally used. However, due to the relative fragility and high cost of nonmagnetic core barrels, the normal steel magnetic barrels were used after the initiation of drillover. This proved to be a prudent policy, as four steel core barrels were bent during drillover at Site U1308.

Two factors influenced the decision to terminate holes at the limit of the APC and therefore *not* to utilize extended core barrel (XCB) technique:

- The increase in drilling disturbance associated with the XCB, particularly in the upper part of the XCB section, has not been conducive to the generation of high-resolution PAC chronologies. Poor recovery and “biscuiting” are common in poorly consolidated lithologies recovered by XCB.
- At all locations other than Site U1304 the deeper stratigraphic section has been sampled in the region (although not at any individual site other than Site U1308) during previous DSDP or ODP drilling legs.

## SITE RESULTS

### Sites U1302 and U1303

The overall objective at Sites U1302 and U1303 was to explore the record of Laurentide Ice Sheet (LIS) instability at this location close to Orphan Knoll (Fig. F1). Piston cores collected at Site U1303 (HU91-045-094P, MD99-2237, and MD95-2024) show

the presence of numerous detrital layers within the last glacial cycle, some of which are rich in detrital carbonate (Hillaire-Marcel et al., 1994; Stoner et al., 1995, 1996). The digital image of Core 303-1303B-1H is shown in Figure F2, illustrating that these detrital layers are recognizable visually and in magnetic susceptibility (MS) and gamma ray attenuation (GRA) density measured on the shipboard multisensor track (MST). Isotopic data from planktonic foraminifers indicate that these detrital layers are associated with low-productivity meltwater pulses (Hillaire-Marcel et al., 1994). The objective at Sites U1302 and U1303 is to document this manifestation of LIS instability both during and prior to the last glacial cycle. The two sites are separated by 5.68 km. Drilling revealed a very similar stratigraphic sequence at the two sites. The MST data could be correlated from site to site at fine scale. The rationale for drilling Site U1302 was that the single-channel air gun seismic data (Toews and Piper, 2002) indicated a thicker section above mud waves at Site U1302 than at Site U1303 (the site of the piston cores mentioned above). We moved to Site U1303 after encountering a coarse-grained debris flow at ~105 meters composite depth (mcd) at Site U1302 that caused the cessation of APC penetration. The same debris flow, however, was encountered at Site U1303. The top of the debris flow coincides with a strong reflector in the air-gun seismic data, at ~100 ms two-way traveltime, which can be traced between the two sites.

Five holes, offset from each other by 30 m, were cored with the APC system at Site U1302 with an average recovery of 90.3%. Three holes (Holes 1302A–1302C) were cored to total depth (maximum of 107.1 meters below seafloor [mbsf]) (Table T1), which was limited by the presence of a debris flow. Holes U1302D and U1302E consisted only of two cores each to capture the intervals at the top of the succession and provide overlap with coring gaps from the previous holes. Water depth was estimated to be 3555 mbsl based on recovery of the mudline core in Hole U1302D. We cored two APC holes 30 m apart at Site U1303. Penetration depth was limited by the debris interval to 93.9 mbsf in Hole U1303A (73.6% recovery) and 85.7 mbsf in Hole U1303B (83.5% recovery). Water depth at Site U1303 was estimated to be 3518 mbsl based on recovery of the mudline core in Hole U1303B.

An almost complete composite section was constructed at Site U1302 spanning the interval 0–107 mcd. It was not possible to construct a complete composite record at Site U1303. However, the density and MS records from Sites U1302 and U1303 are remarkably similar and can be easily correlated. Using a short segment of one core from Site U1303 and the composite record from Site U1302 provides a continuous stratigraphic sequence to ~107 mcd (Fig. F3).

The sediments at Sites U1302 and U1303 are dominated by varying mixtures of terrigenous components and biogenic debris (primarily quartz, detrital carbonate, and nannofossils), so that the most common lithologies are clay, silty clay, silty clay with nannofossils, nannofossil silty clay, silty clay nannofossil ooze, and nannofossil ooze with silty clay. Dropstones are present throughout the cores. Calcium carbonate content ranges from 1 to 47 wt%. The sediments at Sites U1302 and U1303 have been designated as a single unit due to the gradational interbedding of these lithologies at scales of a few meters or less. This unit has been subdivided into two subunits, however, based on evidence for downslope mass flows at the base of the section. Subunit IA (0–106 mcd) is composed of undisturbed sediments, whereas Subunit IB (106–132 mcd) contains abundant intraclasts in a matrix of sand-silt-clay and is interpreted to be debris flow deposits.

Samples from Site U1302 reveal rich assemblages of calcareous, siliceous, and organic-walled microfossils. Coccoliths are abundant and well preserved in most samples and permit establishment of biostratigraphic schemes that are complemented by a few datums from diatoms and palynological data. According to these schemes, the composite sequence of Site U1302 covers an interval spanning <1.16 m.y. and approximately the last 0.95 m.y., whereas the composite sequence of Site U1303 probably corresponds to an interval spanning approximately the last 0.85 m.y. (Fig. F4). The mean sedimentation rate at these sites is 13.4 cm/k.y. (Fig. F5). Beyond the biostratigraphic schemes, the micropaleontologic assemblages provide insight into paleoclimatologic and paleoceanographic conditions. In particular, the relative abundance of the planktonic foraminifer *Neogloboquadrina pachyderma* (sinistral) and some dinocyst assemblages allow identification of glacial and interglacial conditions from some core catcher samples.

The pore water chemistry from Sites U1302 and U1303 is dominated by reactions associated with organic matter degradation, despite the relatively low organic matter content of the sediments (~0.5 wt%). Sulfate concentrations decrease from seawater values to 5.9 mM close to the base of the recovered section indicating that sulfate reduction is almost complete by 109 mcd. Corresponding increases in alkalinity and ammonium downcore are byproducts of organic matter reactions. Alkalinity does not reach concentrations expected for the degree of sulfate reduction indicating alkalinity is being consumed within the cored interval. The decrease in calcium (to a minimum of 5.5 mM, a 52% decrease from seawater values) suggests precipitation of carbonate minerals as one possible explanation for the alkalinity profiles. Strontium concentra-

tions remain at seawater values or lower throughout the cored interval indicating that carbonate dissolution and recrystallization are not important processes at these sites.

Overall, sediments of lithologic Subunit IA from Sites U1302 and U1303 are excellent geomagnetic field recorders as indicated by the fidelity of the shipboard paleomagnetic record. Inclinations vary coherently around those expected for the site latitudes. Declinations show consistent behavior within cores and, when Tensor corrected, between cores. Directional geomagnetic excursions are observed in three replicate sections from Holes 1302C, 1303A, and 1303B at ~31.40 mcd and are interpreted to represent the Iceland Basin Event at ~187 ka. Magnetization intensities are strong and magnetic properties look favorable for shore-based paleointensity studies. Within the debris flow (lithologic Subunit IB), the paleomagnetic record is not of the same quality. There is some evidence for reversed magnetizations within apparently undisturbed sediment within or below the debris flow, possibly denoting the uppermost Matuyama Chron, but the scattered magnetization directions in Subunit IB do not allow further interpretation (Fig. F4). In addition, it appears that the removal of the drill string magnetic overprint is greatly facilitated by the utilization of nonmagnetic core barrels.

The MS records obtained at these sites are strongly influenced by the detrital layer stratigraphy (Fig. F2) superimposed on a pattern of glacial–interglacial variability (Fig. F3). At both sites, natural gamma ray (NGR) variation is consistent with both MS and density measurements (i.e., low MS and density values correspond to low NGR counts: 20–22 cps), which suggests these intervals were characterized by carbonate-dominated sedimentation. The downcore MST records not only provide a guide to the glacial–interglacial cycles, possibly back to MIS 17 but also provide a millennial-scale record of LIS instability through recognition of Heinrich-like detrital events. Detrital events in the Heinrich layer 1–6 (H1–H6) interval are easily recognized in the MST data at Sites U1302 and U1303 and can be unambiguously correlated to similar records in neighboring piston cores such as MD95-2024 and MD99-2237 that record the last glacial cycle. The sedimentary succession at Sites U1302 and U1303 provides a record of LIS instability back to at least MIS 17. This record is a proximal analog to the classic Heinrich-layer stratigraphy of the central Atlantic.

## Site U1304

The objective at Site U1304 was to obtain a deepwater record from the southern edge of the Gardar Drift to compare with the intermediate depth site on the northern part



of the Gardar Drift sampled during ODP Leg 162 (Site 983). Site U1304 lies in a partially enclosed basin north of the Charlie Gibbs Fracture Zone (GFZ), 217 km west-northwest of DSDP Site 611. The mean sedimentation rate at Site U1304 (14.9 cm/k.y.) (Fig. F5) is about six times that in the same interval at DSDP Site 611. Excellent preservation of benthic and planktonic microfossils enhances the potential for a high-resolution environmental record. The site will provide a monitor of NADW and sea-surface temperatures (SSTs) and a record of central Atlantic detrital layer stratigraphy.

Four holes were cored with the APC coring system to a maximum depth of 243.8 mbsf at Site U1304 (Fig. F6; Table T1). Overall recovery was 102.6%. Hole U1304C was limited to 69.6 m penetration when operations had to be terminated because of deteriorating weather conditions (heave in excess of 4 m at the rig floor). After waiting more than 3 h for the weather to abate, Hole U1304D was spudded and the interval 0–52 mbsf drilled before APC coring continued to total depth. The interval from 180.3–181.3 mbsf was also drilled in Hole U1304D (i.e., not cored) due to an apparent hard interval impeding APC penetration. Water depth was estimated to be 3065 mbsl based on recovery of the mudline cores in Holes 1304C and 1304D. The drillover technique was utilized in Holes 1304A, 1304B, and 1304D to extend APC coring past initial refusal depth.

Correlation of cores among holes at Site U1304, utilizing mainly MS and NGR (Fig. F6), provides a continuous stratigraphic sequence to ~258.1 mcd with a single potential break within an 8 m thick diatom mat at ~199.3 mcd. The spliced composite section relies on sections from Holes 1304A and 1304B because good weather conditions during the early occupation of Site U1304 led to excellent recovery and good core quality.

The sediments at Site U1304 are predominantly interbedded diatom oozes and nanofossil oozes with less common intervals of clay and silty clay, which also contain abundant nanofossils and/or diatoms. Calcium carbonate content ranges from 5 to 70 wt% and organic carbon content is low (generally <0.5 wt%). This sedimentary succession has been designated as a single unit because the various lithologies are generally interbedded on a scale of only centimeters to decimeters. Most contacts between nanofossil ooze and clay intervals are gradational, although sharp contacts are also observed. The contacts between diatom ooze beds and the other lithologies are generally sharp. Redeposited beds of silt and sand-sized particles are rare, as are disturbed units related to mass-transport processes (e.g., slumps and debris flows).

Thus, the section cored at Site U1304 apparently represents a relatively continuous pelagic section where the sediments record changes in productivity in response to oceanographic and climatic fluctuations.

Recurring laminated diatom sequences are the most prominent feature at Site U1304. The thicker diatom mats are clearly distinguished by very low MS values (Fig. F6). Diatom assemblages are dominated by needle-shaped species of the *Thalassiothrix/Lioloma* complex. All other groups investigated (coccoliths, planktonic and benthic foraminifers, radiolarians, and palynomorphs) are present in high-to-moderate abundance and are well preserved. Biostratigraphic datums mainly derive from coccoliths and are consistent with datums provided by diatoms, planktonic foraminifers, dinoflagellate cysts, and magnetostratigraphy (Fig. F4). The composite sequence covers the uppermost Pliocene and the entire Quaternary. The microfossil assemblage indicates only minor redeposition.

Preliminary paleoceanographic and paleoclimatologic interpretation of the microflora and microfauna reveals large-amplitude changes in surface water temperature and trophic conditions. Diatom layers were formed during both cold and warm phases, according to the diatom and planktonic foraminiferal assemblages. The presence of the benthic foraminifer *Epistominella exigua* documents recurring flux pulses of fresh organic matter to the seafloor. A shift from dominance of autotrophic to dominance of heterotrophic dinocyst assemblages is recorded after 1.2 Ma, which may suggest a general change in trophic conditions of the surface ocean.

Site U1304 sediments document an almost continuous sequence including the Brunhes Chron and part of the Matuyama Chron including the Jaramillo Subchron, the Cobb Mountain Subchron, and the top of the Olduvai Subchron (Fig. F4). Short intervals of apparent normal polarity were recognized in the Matuyama Chron below the Cobb Mountain Subchron. Mean sedimentation rates of 17.8 cm/k.y. are estimated for the last 0.78 m.y. and 12.2 cm/k.y. for the interval from 0.78 to 1.77 Ma, with an overall mean sedimentation rate of 14.9 cm/k.y. (Fig. F5).

Site U1304 pore water profiles indicate active sulfate reduction (minimum value of 2.8 mM at 214 mbsf) with corresponding increases in alkalinity and ammonium. Alkalinity values do not reach concentrations expected for the degree of sulfate reduction. Calcium concentrations decrease downcore to 2.7 mM, a ~75% reduction from standard seawater values. The decrease in calcium and consumption of alkalinity suggests active carbonate mineral precipitation. However, Sr concentrations remain at

seawater values or lower, indicating that carbonate dissolution and recrystallization reactions are not important processes in the cored interval.

The Quaternary sequence recovered at Site U1304 provides a high-resolution, high-sedimentation-rate (average ~15 cm/k.y.) record of environmental change at a sensitive location close to the subarctic convergence between the surface Labrador Current and the North Atlantic Current. Good preservation of both calcareous and siliceous microfossils, abundant benthic foraminifers, and a high-fidelity magnetostratigraphic record indicate that the environmental record, including the monitoring of NADW, can be placed in a tight chronological framework.

## Site U1305

Site U1305 is located close to the southwest extremity of the Eirik Drift, 82.2 km south of ODP Site 646. The thickness of the sediments above the mid–Upper Pliocene seismic reflector R1 (~540 m) is almost twice that at ODP Site 646. The water depth (3459 mbsl) means that the seafloor at Site U1305 lies below the main axis of the Western Boundary Undercurrent (WBUC) and hence preserves expanded interglacial intervals and relatively condensed glacial intervals. The high mean sedimentation rate (>17 cm/k.y. for the Quaternary) promises a high-resolution record of ice sheet instability and changes in surface and deepwater masses.

Three holes were cored at Site U1305 with the APC system to a maximum depth of 287.1 mbsf (Fig. F7; Table T1) with an average recovery of 104%. Six cores had to be obtained by drillover in Hole U1305A, two in Hole U1305B, and none in Hole U1305C. After completing coring operations, Hole U1305C was prepared for logging and the triple combination (triple combo) tool string was deployed to ~258 mbsf (~29 m from the bottom of the hole). The hole was logged successfully on the first pass, but the tool became stuck when attempting to retrieve it into the drill pipe after a short second pass. The tool was eventually freed, and upon retrieval we discovered that one of the caliper arms had broken off and the logging line had been damaged. Because of heave state (up to 4 m), the hole condition, tool safety, and operational constraints, we decided to forego the deployment of the Formation MicroScanner (FMS)-sonic tool string, concluding operations at Site U1305.

The sediments at Site U1305 are designated as a single unit dominated by varying mixtures of terrigenous components and biogenic material, primarily clay minerals, quartz, detrital carbonate, and nannofossils. Calcium carbonate content ranges from

1 to 49 wt%. The most common lithologies are dark gray to very dark gray silty clay, silty clay with nannofossils, nannofossil silty clay, silty clay nannofossil ooze, and nannofossil ooze with silty clay. In addition, olive-gray sandy silt laminae and centimeter- to decimeter-scale intervals of silty clay with detrital carbonate are present at Site U1305. The sediments are gradationally interbedded at scales of a few meters or less.

Calcareous, siliceous, and organic-walled microfossils show generally good preservation and abundance in the upper ~200 mcd (Fig. F4). However, the abundance of microfossil assemblages is variable below this depth with generally poorer preservation. All microfossil groups investigated are dominated by subpolar to polar assemblages. Planktonic foraminifers show a bimodal test-size distribution. The small test-sized planktonic foraminifers, which are cold-water species, coexist with increased abundance of benthic foraminifers, possibly indicating transport by bottom currents.

The sediments at Site U1305 carry well-defined magnetization components and appear to provide useful records of geomagnetic transitions. Natural remanent magnetization (NRM) intensities are strong both before and after demagnetization and show variability at both the meter scale and throughout the sequence. NRM intensities decrease by ~50% below 166 mcd. Directional magnetization data allow identification of the Brunhes and part of the Matuyama Chron, including the Jaramillo, Cobb, and Olduvai Subchrons (Fig. F4). The Cobb Mountain Subchron and the top of the Olduvai Subchron are less clearly identified because of the incomplete removal of the normal polarity drill string magnetic overprint.

A continuous stratigraphic composite section was constructed to ~295 mcd with a single problematic interval between 197.2 and 206 mcd (Fig. F7). The mean sedimentation rate calculated using biostratigraphic and magnetostatigraphic datums is 17.5 cm/k.y. for the entire section cored at Site U1305 (Fig. F5). Using only paleomagnetic datums results in sedimentation rates that are still relatively uniform with the exception of a greater mean sedimentation rate between 1.07 and 1.19 Ma (from the base of the Jaramillo to the top of the Cobb Mountain Subchrons) that averages 29.3 cm/k.y.

Despite the low organic carbon content (mean = <0.4 wt%), organic matter diagenesis dominates the pore water chemistry. Sulfate decreases linearly downcore and is completely reduced by 58 mbsf. Methane increases immediately below the sulfate reduction zone, reaching a maximum of 46,000 ppmv at 228 mbsf. Ethane fluctuates

between 2 and 14 ppmv within the methanogenic zone, but no higher hydrocarbons were detected. Alkalinity increases downcore reaching a maximum of 18.9 mM at the sulfate/methane interface (SMI). Calcium reaches a minimum of 2.58 mM at the same depth, suggesting carbonate precipitation associated with anaerobic methane oxidation at the SMI. Similar to previous Expedition 303 locations, dissolved strontium at Site U1305 is at or below seawater values indicating little or no carbonate dissolution or recrystallization.

Physical property records at Site U1305, in particular MS and density, are highly variable, recording lithologic and mineralogic changes (Fig. F7). Low MS and density values usually coincide with the presence of silt-sized detrital carbonate. Natural gamma radiation increases toward the transition between detrital carbonate and terrigenous-dominated layers, suggesting a relative increase in the clay component. Site U1305 sediments are also characterized by an overall downcore increase in density (from 1.3 to ~1.9 g/cm<sup>3</sup>), decreasing porosity (from 80% to 62%) and low velocities (1500–1600 m/s).

Data from wireline logging in Hole U1305C span the 95.3–265.9 mbsf interval. The triple combo tool string was successfully deployed, yielding downhole records of density, porosity, NGR, electrical resistivity, and photoelectric factor. Density and porosity are generally inversely related to each other, with density increasing downhole and porosity decreasing. Density and porosity data are in some places affected by the large diameter of the hole (up to ~18 in), although these intervals most likely correspond to softer sediments that are more easily washed away. Density and gamma ray logging data show similar downhole trends to those observed in core data, suggesting that it will be possible to correlate core and logging data. The logging data also exhibit stratigraphic trends that appear to be cyclic, possibly caused by temporal changes in lithology. Successful core-log integration will permit an assessment of the origin and significance of the trends in the logging data.

The initial analysis of MST, archive multisensor track (AMST), biostratigraphic, and paleomagnetic data indicates that a complete and continuous high-resolution record (mean sedimentation rate of 17.3 cm/k.y.) covering the uppermost Pliocene and Quaternary has been recovered at Site U1305. The record represents a rich archive of environmental change that will document episodes of instability in the surrounding (Laurentide, Greenland, and Inuitian) ice sheets, the history of surface currents and deepwater currents, and, hence, the strength of the WBUC that contributes to NADW. Good preservation of both planktonic and benthic foraminifers for isotopic analysis

and a high-fidelity paleomagnetic record indicate that the environmental record has the necessary attributes for construction of a paleointensity-assisted chronostratigraphy.

## Site U1306

Site U1306 was placed at the crossing of two seismic lines (Lines 19 and 24) in the multichannel seismic (MCS) network obtained over the Eirik Drift during Cruise KN-166 (*Knorr*, Principal Investigator [PI]: Greg Mountain) in summer 2002. At this location, mean Upper Pliocene and Quaternary sedimentation rates were estimated to be ~18 cm/k.y. based on identification of seismic reflector R1, which can be correlated to the mid–Upper Pliocene at ODP Site 646. The placement of the site was designed to yield a high-resolution, high-sedimentation-rate Quaternary environmental record from a water depth (2273 mbsl) within the main axis of the WBUC. Based on a nearby conventional piston core from a similar water depth (Core HU90-013-012) (*Hillaire-Marcel et al.*, 1994), we expect glacial intervals to be expanded relative to interglacial intervals.

Four holes were cored with the APC system at Site U1306 reaching a maximum depth of 309.3 mbsf (Fig. F8; Table T1). Hole U1306D was cored to 180.0 mbsf to provide necessary stratigraphic overlap for the upper portion of the succession. Five intervals totaling 13 m were drilled without coring to adjust the stratigraphic offset between holes or to get through difficult-to-core intervals. Five cores were obtained by drill-over. Average recovery was 102.5% for the cored interval.

The sediments at Site U1306 are designated as a single lithostratigraphic unit, composed of Holocene to uppermost Pliocene terrigenous and biogenic sediments, which are gradationally interbedded at scales of a few meters or less. Calcium carbonate content is low ranging from 0.3 to 12.3 wt% (mean = 3.2 wt%). The most common lithologies are silty clay, silty clay with diatoms, nannofossil silty clay, and silty clay nannofossil ooze. Dropstones are present throughout the cored interval, and large dropstones (~4 cm) are common to abundant. Centimeter- to decimeter-scale beds of olive-gray or greenish gray silty clay or clay with high detrital carbonate content are present in all holes at Site U1306, but are thinner and less common than at Site U1305.

Rich assemblages of calcareous, siliceous, and organic-walled microfossils are present at Site U1306 (Fig. F4), although benthic foraminifers are barren in many samples

below 175 mcd. Large variations in abundance of microfossils occur downcore. Although preservation is moderate to good in the upper part of the succession, preservation generally decreases below ~170 mcd for calcareous and siliceous microfossils. All samples contain moderately well to well-preserved palynomorphs, but variable numbers of dinocysts, which are abundant only in a few samples. Some redeposition is indicated by the presence of reworked nannofossils and palynomorphs of Cretaceous to Miocene age through the cored interval. The dominant components of each microfossil group reflect cold SSTs for most of the time represented by the sedimentary sequence.

The sediments at Site U1306 carry well-defined magnetization components and document an apparently continuous sequence including the Brunhes Chron and much of the Matuyama Chron. The Jaramillo, Cobb Mountain, and Olduvai Subchrons are clearly identified (Fig. F4). Within the Brunhes Chron, the Iceland Basin Event (~187 ka) was observed in three of the holes.

A continuous stratigraphic composite section was constructed to ~337 mcd (Fig. F8). Below 287 mcd, cores were recovered in two holes only, but the section is complete with only a single tenuous tie near the base of the record. The mean sedimentation rate calculated using biostratigraphic and magnetostatigraphic datums is 15.6 cm/k.y. for the entire section cored at Site U1306 (Fig. F5). Using only paleomagnetic datums, interval sedimentation rates vary between 12.4 and 19.3 cm/k.y.

Pore water chemical profiles at Site U1306 document very similar reactions to nearby Site U1305. Complete sulfate reduction is achieved at shallow depths at Site U1306 (85 mbsf) despite the low organic carbon content (mean = 0.3 wt%). Methane increases below 85 mbsf, reaching a maximum of 46,000 ppmv. Alkalinity reaches a maximum of 18.7 mM at the SMI, whereas calcium concentration attains a minimum value (3.7 mM), indicating carbonate mineral precipitation associated with methane oxidation. From 114 to 258 mbsf, sulfate increases again slightly (1.5 mM). This interval corresponds to pH and iron fluctuations, which are antithetic to each other, and may indicate zones of anaerobic pyrite oxidation. Dissolved strontium remains at or below seawater values, suggesting little or no carbonate dissolution or recrystallization.

Physical property records at Site U1306 are highly variable, recording lithologic and mineralogic changes (Fig. F8). The higher carbonate content in the upper ~100 mcd results in average lower NGR and MS values than in the sediments below. Site U1306

sediments are characterized by an overall downcore increase in density (1.5–~1.8 g/cm<sup>3</sup>) and decreasing porosity (~70%–50%).

Based on current knowledge from nearby piston cores, Site U1306 has expanded glacial intervals. This sedimentary pattern is complementary to that at Site U1305 where interglacials are likely to be relatively expanded. The apparently complete Quaternary record recovered at Site U1306 provides a high-resolution, high-sedimentation-rate record of detrital events derived from instability of surrounding ice sheets, and provides a monitor of the activity of the WBUC that supplies a component of NADW to the Labrador Sea. The site appears to have the attributes required for the generation of a well-constrained age model based on oxygen isotopes, micropaleontology, and geomagnetic paleointensity.

## Site U1307

Site U1307 is positioned in 2575 m of water at common depth point (CDP) 14375 on seismic Line 25a in the MCS network obtained over the Eirik Drift during Cruise KN-166 (*Knorr*, PI: Greg Mountain) in summer 2002. The location was chosen because of potential access to Pliocene sediments below the Quaternary sequence drilled at Site U1306. A thinner Quaternary sedimentary sequence at Site U1307 allowed the Pliocene sequence to be sampled using the APC.

Two holes were cored with the APC system at Site U1307, reaching a maximum depth of 162.6 mbsf (Fig. F9; Table T1). Two partial strokes of the APC required drilling two intervals in Hole U1307A that were difficult to APC core (50.5–52.5 mbsf and 73.7–77.7 mbsf). Five cores were advanced by recovery. Only one core was a partial stroke in Hole U1307B, and no intervals required drillover. Average recovery was 102% for the cored intervals at Site U1307. Coring was terminated due to excessive heave when a passing storm system began to affect drilling operations.

The Lower Pliocene to Pleistocene sedimentary succession at Site U1307 (Fig. F4), which is subdivided into three units, records variations in the input of terrigenous and biogenic components (mostly quartz, detrital carbonate, nannofossils, and foraminifers). Unit I (0–49.55 mcd) is composed of Holocene and Pleistocene mixtures of foraminifers, silty clay, and nannofossils (silty clay with foraminifers, foraminifer silty clay, and nannofossil silty clay). Minor lithologies include eight discrete foraminifer silty sand and sandy foraminifer ooze beds. Unit II (49.55–133.86 mcd) is composed mainly of Pleistocene to Upper Pliocene silty clay with little biogenic component.



Unit III (133.86–173.6 mcd) is composed of Upper to Lower Pliocene silty clay, silty clay with nannofossils, and nannofossil silty clay. With the exception of the foraminifer sand beds, calcium carbonate content is low (mean = 3.8 wt%).

The abundances of calcareous, siliceous, and organic-walled microfossils at Site U1307 are common to rare with moderate to poor preservation. A possible hiatus (duration ~0.25 m.y.) or a condensed interval (~1.21–1.45 Ma) is indicated between ~56 and 61 mcd (Figs. F4, F9). The dominant components of each microfossil group reflect subpolar to polar conditions during the Pleistocene. In the lower Upper Pliocene (before 2.74 Ma), the nannofossil assemblage suggests warmer surface water conditions.

Paleomagnetic directional data yield an almost continuous sequence and permit unambiguous identification of the Brunhes, Matuyama, and Gauss Chrons (Fig. F4). Within the Matuyama Chron, the Jaramillo, Olduvai, and Reunion Subchrons are clearly recognized. Within the Gauss Chron, the Kaena and Mammoth Subchrons are also recognized, with the base of the section corresponding to the top of the Gilbert Chron.

With only two holes drilled, it was impossible to construct a complete spliced record for Site U1307. However, several long intervals of overlap between holes allowed segments to be correlated between holes (0–56.5 mcd, 76.4–104.7 mcd, and 104.7–146.2 mcd), which were then appended in the record (Fig. F9). The mean linear sedimentation rate calculated using biostratigraphic and magnetostatigraphic datums is 4.8 cm/k.y. (Fig. F5). Using only magnetostratigraphic datums, interval sedimentation rates vary between 2.7 and 7.6 cm/k.y.

As for the other Eirik Drift sites, pore water geochemical profiles reflect the influence of organic matter remineralization reactions. Sulfate decreases linearly from the uppermost sample to 79 mbsf, where it remains at or below ~1 mM. The methane profile is atypical, decreasing from 200 ppmv in the uppermost sample near the sediment/water interface to a low of ~30 ppmv at 54 mbsf and then increasing again below the sulfate reduction zone to a high of 26,000 ppmv. Calcium and strontium attain minimum values (5.5 mM and 76  $\mu$ M, respectively) at the base of the sulfate reduction zone where alkalinity reaches a maximum (10 mM), suggesting carbonate mineral precipitation.

Physical property records at Site U1307 document high-frequency changes in sediment composition (Fig. F9). The variability in sediment composition recorded in MS,

NGR, and density likely reflect changes in paleoceanographic conditions in the overlying and surrounding water masses and ice sheets at a range of timescales. Site U1307 sediments are also characterized by an overall downcore increase in density (from 1.55 to ~1.76 g/cm<sup>3</sup>) and variable but generally decreasing porosity (from ~70% to 40%).

Site U1307 demonstrates that the Pliocene sediments of the Eirik Drift are located at penetration depths achievable with the APC. Apart from one possible hiatus (in the 1.2–1.4 Ma interval), the sedimentary record at Site U1307 is apparently continuous (Fig. F4) with a mean sedimentation rate of ~5 cm/k.y. (Fig. F5). The base of the recovered section correlates to the uppermost Gilbert Chron, indicating that the record extends back to ~3.6 Ma (Fig. F4). The sediments from Site U1307 will provide information on the history of bottom and surface currents, the Laurentide and Greenland ice sheets, and age control for seismic reflectors that will provide constraints on the sedimentary architecture of the Eirik Drift. The Pliocene–Quaternary history at this site can be placed into a tight age model, as the sediments have the attributes required for high-resolution chronostratigraphy based on paleontologic, isotopic, and magnetic methods.

## Site U1308

Site U1308 constitutes a reoccupation of DSDP Site 609 (Fig. F1). During DSDP Leg 94 (June–August 1983), two principal holes (Holes 609 and 609B) were drilled with the variable-length hydraulic piston corer (VLHPC) and XCB. Two cores were collected from Hole 609A to recover the mudline, and seven XCB cores were collected from Hole 609C to recover the 123–190 mbsf interval. Samples from DSDP Site 609 have played a major role in driving some of the most exciting developments in paleoceanographic research during the last 10–15 years, such as the recognition and understanding of Heinrich layers, the recognition of the 1500 y pacing in hematite-stained grains and Icelandic glass, and the correlation of ice core  $\delta^{18}\text{O}$  to SST proxies. The majority of the analyses from Site 609 have dealt with the record younger than MIS 6, partly because of the lack of a continuous pristine composite record. A primary objective at Site U1308 was to recover a demonstrably complete composite record, hence, considerably enhance the potential for Pliocene–Quaternary climatic records from this site.

Six holes were cored with the APC system at Site U1308: (1) Hole U1308A to 341.mbsf, (2) Hole U1308B to 198.3 mbsf, (3) Hole U1308C to 279.9 mbsf, (4) Hole

U1308D to 6.7 mbsf, (5) Hole U1304E to 193.0 mbsf, and (6) Hole U1308F to 227.0 mbsf (Fig. F10; Table T1). Water depth was estimated to be 3871 mbsl. Average recovery was 95.4% for the cored intervals. Sea swell up to 6 m affected Hole U1308A core quality below ~170 mbsf. We therefore waited ~16 h for the swell to abate before coring Hole U1308B. Coring in Hole U1308B was terminated after three successive poor-recovery cores suggested accumulation of debris either in the hole or in the bottom hole assembly (BHA). However, we could not spud Hole U1308C because of incomplete firing of the APC indicating the problem was bit obstruction. Holes U1308C, U1308D, and U1308E were cored after clearing the bit, but core recovery was not optimal (<100%) due to loss of core from the base of core liners and (possibly related) crushed core liners. The bit was cleared again before coring Hole U1308F with an average recovery of 100.7%, although crushed liners were still commonplace.

The upper Miocene through Quaternary sedimentary succession at Site U1308 (Fig. F4), which is subdivided into two units, records variations in the input of terrigenous and biogenic sediments (primarily nannofossil ooze, nannofossil silty, and silty clay). Unit I (0–196.85 mcd) is composed of a Holocene–Upper Pliocene sequence of interbedded biogenic and terrigenous sediments with dropstones. Subunit IIA (196.85–262.14 mcd) is composed of Upper Pliocene nannofossil ooze interbedded with terrigenous sediment-rich layers but at a lower frequency than Unit I. Subunit IIB (262.14–355.89 mcd) is entirely composed of lowermost Upper Pliocene to uppermost Miocene nannofossil ooze.

Diverse assemblages of calcareous, siliceous, and organic-walled microfossils were recovered at Site U1308 (Fig. F4). Calcareous microfossils are abundant with good preservation in the upper ~200 mcd grading to moderate preservation below this depth. Siliceous microfossils are rare to common and moderately preserved above ~255 mcd (Upper Pliocene–Pleistocene) with radiolarians locally abundant only in the middle part of the cored sequence. Siliceous microfossils are barren below 255 mcd. The concentration of terrestrial palynomorphs is low. Dinocysts are common to abundant in the upper 200 mcd but less common below. Microfossil assemblage changes observed at Site U1308 document the onset of Northern Hemisphere glaciation, as well as seasonal changes in bioproductivity and hydrographic fronts.

Paleomagnetic directional data document an apparently continuous sequence of polarity transitions. Identification of the Brunhes, Matuyama, and Gauss Chrons are unambiguous (Fig. F4). The Gilbert Chron is tentatively recognized in the lower part

of Hole U1308A. The Jaramillo, Cobb Mountain, Olduvai, Reunion, Kaena, and Mammoth Subchrons are also clearly identified.

Six holes were cored at Site U1308 to ensure the complete recovery of the stratigraphic section to 247 mcd (Fig. F10). The unusually large number of holes was required because of poor recovery and core disturbance due to excessive heave and crushed core liners. There is one problematic interval between ~186 and ~196 mcd where inclined bedding and sharp lithologic contacts suggest a possible break in continuity of sedimentation. The mean linear sedimentation rate calculated using magnetostatic datums is ~8.3 cm/k.y. for the last ~3.5 m.y. (Fig. F5). Prior to that time, the mean sedimentation rate was ~3.3 cm/k.y. based on biostratigraphic markers (Fig. F5).

Interstitial water sulfate decreases downhole to 9 mM, but complete sulfate reduction is not achieved within the cored interval. Unlike all other Expedition 303 sites, strontium increases with depth to a maximum of 1592  $\mu\text{M}$  at Site U1308. The nearly linear strontium increase and the corresponding increase in Sr/Ca ratios indicate that recrystallization (not dissolution) of biogenic carbonate is occurring. The approximately linear downhole decreases in magnesium and potassium and increase in calcium below ~100 mbsf are consistent with the alteration of volcanic material and/or basement below the cored interval.

Physical property records at Site U1308 document long-term changes in sediment composition, which likely reflect fundamental changes in North Atlantic climate. The NGR and lightness ( $L^*$ ) records from lithologic Unit I (0–197 mcd) show a strong glacial–interglacial variability (Fig. F10). In Subunit IIA (197–262 mcd), MS and NGR values decrease both in absolute value and variability and  $L^*$  increases (Fig. F10). NGR shows a fairly abrupt change in absolute values and variability at the Unit II/I boundary at ~197 mcd (~2.74 Ma). In the white nannofossil ooze of lithologic Subunit IIB (262–356 mcd), MS and NGR values are significantly lower and less variable than in Subunit IIA. Data for Subunit IIB (262–356 mcd) are not shown in Figure F10, as the composite record does not extend below Subunit IIA.

The six holes at Site U1308 have been pieced together to produce a complete composite section to ~247 mcd. The base of the composite section correlates to the middle part of the Gauss Chron at ~3.2 Ma. A discontinuous record was recovered below this level to 356 mcd in upper Miocene white nannofossil ooze. The Upper Pliocene to Quaternary composite section will provide a means of studying the evolution of NADW, the extension of the central Atlantic detrital layer (Heinrich-type) stratigraphic

phy beyond the last glacial cycle, and the 1500 y cycle in the petrologic characteristics of IRD. The mean sedimentation rate for the composite section (7.6 cm/k.y.) indicates that these studies can be carried out at moderately high resolution. Good preservation of benthic and planktonic calcareous and siliceous microfossils indicates that the site will yield high-quality environmental and isotopic records. The pristine magnetostratigraphic record indicates that the site has good potential for the generation of a PAC that will place the environmental record into a global millennial-scale stratigraphic framework.

## **OVERVIEW OF EXPEDITION ACHIEVEMENTS**

The overall objectives of Expedition 303 were stated as follows: *“To establish late Neogene–Quaternary intercalibration of geomagnetic paleointensity, isotope stratigraphies and regional environmental stratigraphies and, in so doing, develop a millennial-scale stratigraphic template. Such a template is required for understanding the relative phasing of atmospheric, cryospheric, and oceanic changes that are central to our understanding of the mechanisms of global climate change on orbital to millennial timescales.”*

The site locations for Expedition 303 are known from previous ODP/DSDP drilling or from conventional piston cores to (1) contain distinct records of millennial-scale environmental variability (in terms of ice sheet–ocean interactions, deep circulation changes or sea-surface conditions), and (2) provide the requirements, including adequate sedimentation rates, for developing millennial-scale stratigraphies (through geomagnetic paleointensity, oxygen isotopes, and regional environmental patterns).

The drilling and core recovery phase of the expedition was a success because of the quality and nature of the cores recovered and the potential of the cores to meet the scientific objectives of the expedition. The common overall objective of Expeditions 303 and 306 (scheduled for March–April 2005) provided more flexibility to occupy sites as weather conditions allowed than is usual for an individual expedition. The October–November window in the North Atlantic ensured that this flexibility would be utilized.

It was decided in the early planning stages that the expedition would utilize the APC only. Cores acquired using the XCB, particularly in the interval immediately below the limit of APC drilling, are usually disturbed by the drilling process and do not meet the standards of core quality required for high-resolution stratigraphic studies.

Emphasis was placed on the recovery of complete, undisturbed composite sections utilizing multiple APC holes with drillover to increase the depth of APC recovery.

The overall objective at Sites U1302 and U1303 is to explore the record of LIS instability at this location close to Orphan Knoll (Fig. F1). Piston cores collected previously at or near Sites U1302 and U1303 (HU91-045-094P, MD99-2237, MD95-2024, and MD95-2025) show the presence of numerous detrital layers, some of which are rich in detrital carbonate (Hillaire-Marcel et al., 1994; Stoner et al., 1996, 2000; Hiscott et al., 2001). Isotopic data from planktonic foraminifers indicate that these detrital layers are associated with low-productivity meltwater pulses. The objective at Sites U1302 and U1303 is to document this manifestation of LIS instability further back in time to the base of the recovered section (~MIS 17). The mean sedimentation rates at Sites U1302 and U1303 are estimated to be ~13 cm/k.y. (Fig. F5), ensuring a high-resolution record.

At Site U1302, the first site to be drilled off Orphan Knoll (Fig. F1), we encountered a debris flow at ~105 mcd that was not recognized in seismic data (Toews and Piper, 2002). The top of the debris flow appears to be within the Brunhes Chron at ~700 ka, and the base of the section is estimated from nannofossil stratigraphy to be at ~950 ka (Fig. F4). To avoid the debris flow, we traversed in dynamic positioning (DP) mode (with the base of the drill string lifted a few hundred meters above the seafloor) to Site U1303, located 5.68 km northwest of Site U1302. The debris flow was again encountered at Site U1303 at approximately the same depth, and drilling was again discontinued. The presence of a debris flow at shallow depths (~105 mcd) also precluded downhole logging operations as planned in the prospectus, which was then deferred to the next planned site on Eirik Drift. Sites U1302 and U1303 can be easily correlated using a range of MST data, and it is clear that essentially the same section was recovered at the two sites. We generated a complete and continuous composite section by combining the five holes from Site U1302 and the two holes from Site U1303. Short segments of three cores from Site U1303 and the composite record from Site U1302 provide a continuous stratigraphic sequence to ~107 mcd.

- *Sites U1302 and U1303 near Orphan Knoll have a detrital layer stratigraphy that is a proximal analog to the detrital stratigraphy of the central Atlantic and provides a detailed record of the instability of the Laurentide Ice Sheet since 700 ka.*

While en route to prospective sites on the Eirik Drift (Sites U1305–U1307), the unfavorable weather forecast for this area forced the ship to be diverted to Site U1304 at the southern edge of the Gardar Drift (Fig. F1). The sediments at Site U1304 comprise

interbedded diatom and nannofossil oozes with clay and silty clay. The lithologies are generally interbedded on a centimeter or decimeter scale. Diatom assemblages are dominated by needle-shaped species of the *Thalassiothrix/Lioloma* complex. The site is located within the central Atlantic IRD belt and therefore provides a distal record (relative to that at Sites U1302 and U1303) of the ice sheet instability. Site U1304 provides a high-resolution, high-sedimentation-rate record at a water depth (3065 mbsl) sufficient to determine the millennial-scale changes in the influence of NADW at the site. The diatom-rich sedimentary section extends back into the uppermost Pliocene at 258 mcd. Mean sedimentation rates of 17.8 cm/k.y. are estimated for the last 0.78 m.y. and 12.2 cm/k.y. for the interval from 0.78 to 1.77 Ma. The diatom-rich stratigraphy implies that the site has been located at the subarctic convergence between the surface Labrador Current and the North Atlantic Current (see Bodén and Backman, 1996). The good preservation of benthic and planktonic foraminifers, the pristine magnetic properties, and the construction of a complete composite section from four holes indicate that the environmental record can be placed into a reliable and precise age model. With the clearing weather over Eirik Drift coinciding with completion of coring at Site 1304 and the scientific preference for obtaining logs at one of the Eirik Drift sites, logging was not conducted at Site 1304 in favor of Site 1305.

- *Site U1304 provides a high-sedimentation-rate, high-resolution pelagic record at the southern edge of the Gardar Drift suitable for monitoring NADW and recording the detrital layer stratigraphy of the central Atlantic IRD belt since latest Pliocene time.*

Three sites (Sites U1305, U1306, and U1307) were drilled on the Eirik Drift (Fig. F1). The first of these was the designated the “deepwater” site (Site U1305) in 3459 meters water depth at the western extremity of the Eirik Drift. The primary “shallow-water” site (Site U1306) in 2273 meters water depth is located 191 km northeast of Site U1305. The two sites were chosen by maximizing the thickness of the Quaternary sedimentary section in the MCS network obtained over the Eirik Drift during Cruise KN-166 (*Knorr*, PI: Greg Mountain) in summer 2002.

Conventional piston cores have shown that the sedimentation history on the Eirik Drift during the last glacial cycle is strongly affected by the WBUC, which sweeps along east Greenland and into the Labrador Sea (Hillaire-Marcel et al., 1994; Stoner et al., 1998). Based on two conventional piston cores (HU90-013-013P and HU90-013-012) from the Eirik Drift at similar water depths, the deepwater site (Site U1305) is expected to display relatively expanded interglacials and relatively condensed glacial intervals and the converse is true for the shallow-water site (Site U1306). The base of

the section at both sites lies within the Olduvai Subchron at ~300 mcd, and the mean sedimentation rates are 17–18 cm/k.y. Sites U1305 and U1306 will provide complementary high-resolution records of the history of the WBUC, detrital layer stratigraphy signifying instability of the surrounding ice sheets, and the attributes for well-constrained age models using stable isotopes, biostratigraphy, and geomagnetic paleointensity.

- *Sites U1305 and U1306 provide complementary records of Quaternary sedimentation on the Eirik Drift. The mean sedimentation rate (~17 cm/k.y.) is similar for both sites, but the patterns of sedimentation are expected to be different due to the contrasting water depths of the sites and the influence of the WBUC. The sites not only record the activity of the WBUC, and hence this component of NADW, but also monitor the detrital layer stratigraphy associated with instability of surrounding ice sheets, particularly the Greenland Ice Sheet.*

Site U1307 was not in the initial plan for Expedition 303, but was occupied when a storm moving northeastward across the North Atlantic blocked our passage to our intended next site (Site U1308). Site U1307 was placed at a location on the Eirik Drift (Fig. F1) where the Quaternary sedimentary section appears to be thinned relative to its thickness at Site U1306, providing APC access to the underlying Pliocene section. Two holes were drilled at Site U1307 reaching a maximum depth of 162 mcd in the uppermost Gilbert Chron (~3.6 Ma). The mean sedimentation rate for the recovered section was 4.9 cm/k.y. Interval sedimentation rates between polarity reversals ranged from 2.7 to 7.6 cm/k.y. Poor weather and excessive ship heave curtailed drilling at this site and the two holes were insufficient to generate a complete composite section. The site did, however, establish the feasibility of recovering the Pliocene sedimentary section on the Eirik Drift using the APC. The site extends the environmental record back to ~3.6 Ma and will provide invaluable age control throughout the MCS network established on the Eirik Drift by the KN-166 cruise in 2002.

- *Site U1307 provides a record of sedimentation on the Eirik Drift since ~3.6 Ma. The tight age control on the sedimentary record will be used to provide age control for seismic reflectors that can be traced through the KN-166 seismic network, thereby contributing to the understanding of the sedimentary architecture of the Eirik Drift.*

The final site of Expedition 303 was Site U1308, a reoccupation of DSDP Site 609. Shipboard and shore-based analytical techniques have changed considerably in the 21 y since this site was originally drilled (in 1983). For example, the shipboard facilities for the construction of composite section were introduced eight y later (1991).



DSDP Site 609 has been the focus of some of the most important developments in paleoclimate research in the last 15 y. Layers of IRD containing detrital carbonate (Heinrich events) were recognized at this site in the early stages of their correlation to the Greenland ice core record (e.g., Bond et al., 1993). The 1500 y cycle in petrologic characteristics such as hematite-stained grains and Icelandic glass has also been recognized at this site (Bond et al., 1999). Most of the recent work on DSDP Site 609 sediments has been conducted on the last glacial cycle due in part to uncertainties in the continuity of the section at greater depth. The objective of the reoccupation of DSDP Site 609 was to recover a demonstrably complete sedimentary section that could be used to establish the isotopic characteristics of NADW, monitor the detrital layer stratigraphy of the central Atlantic IRD belt, and place this record into a well-constrained chronostratigraphy. Several factors affected core quality at Site 1308. Sea swells reaching 6 m during drilling in Hole 1308A affected this hole as well as other holes at this site. In addition, sticky clay and other debris caught around the bit and in the BHA were believed to be the cause of loss of core from the base of core liners, and crushed liners in intervals from all holes. To obtain a complete, undisturbed stratigraphic record at Site 1308 required six holes consuming all the remaining operational time. The maximum penetration at Site U1308 was 341 mbsf to the upper Miocene at ~6 Ma (Fig. F4). However, the complete composite section is limited to the uppermost 247 mcd, extending well within the Gauss Chron at ~3.1 Ma, with the mean sedimentation rate since that time being ~8.3 cm/k.y (Fig. F5).

- *Site U1308 is a reoccupation of a classic site (DSDP Site 609) in the central Atlantic that has driven many of the most important advances in paleoceanography during the last 10–15 y. A demonstrably complete section was recovered back to 3.1 Ma, with almost continuous recovery back to about 3.5 Ma. The site will provide a record of central Atlantic detrital layer stratigraphy, as well as a means of monitoring NADW, within a well-constrained chronostratigraphy.*

The drilling and recovery phase of Expedition 303 has been an unqualified success due to the dedication of IODP staff, the Transocean employees, and members of the science party. The weather also played an important role in permitting the recovery of high-quality cores at all sites. A total of 4656 m of high-quality core was recovered from sites with mean sedimentation rates in the 5–18 cm/k.y. range. The sites were chosen to recover Pliocene and Quaternary records of millennial-scale environmental variability in terms of ice sheet–ocean interactions, deep circulation changes, or sea-surface conditions. The sites provide the requirements, including adequate sedimentation rates, for developing millennial-scale stratigraphies (through geomagnetic

paleointensity, oxygen isotopes, and regional environmental patterns). We expect research on these cores in the coming years to break new ground in the fields of paleoclimatology and paleoceanography.

## REFERENCES

- Alley, R.B., Clark, P.U., Keigwin, L.D., and Webb, R.S., 1999. Making sense of millennial-scale climate change. In Clark, P.U., Webb, R.S., and Keigwin, L.D. (Eds.), *Mechanisms of Global Climate Change at Millennial Time Scales*. Geophys. Monogr., 112:385–394.
- Baumgartner, S., Beer, J., Masarik, J., Wagner, G., Meynadier, L., and Synal, H.-A., 1998. Geomagnetic modulation of the  $^{36}\text{Cl}$  flux in the GRIP ice core. *Science*, 279:1330–1332.
- Bodén, P., and Backman, J., 1996. A laminated sediment sequence from northern North Atlantic Ocean and its climatic record. *Geology*, 24:507–510.
- Bond, G., Broecker, W., Johnsen, S., McManus, J., Labeyrie, L., Jouzel, J., and Bonani, G., 1993. Correlations between climate records from the North Atlantic sediments and Greenland ice. *Nature*, 365:143–147.
- Bond, G., Showers, W., Cheseby, M., Lotti, R., Almasi, P., deMenocal, P., Priore, P., Cullen, H., Hajdas, I., and Bonani, G., 1997. A pervasive millennial-scale cycle in North Atlantic Holocene and glacial climates. *Science*, 278(5341):1257–1266.
- Bond, G., Heinrich, H., Broecker, W., Labeyrie, L.D., McManus, J., Andrews, J., Huon, S., Jantschik, R., Clasen, S., Simet, C., Tedesco, K., Klas, M., Bonani, G., and Ivy, S., 1992. Evidence for massive discharges of icebergs into the North Atlantic Ocean during the last glacial period. *Nature*, 360:245–249.
- Bond, G., Kromer, B., Beer, J., Muscheler, R., Evans, M.N., Showers, W., Hoffmann, S., Lotti-Bond, R., Hajdas, I., and Bonani, G., 2001. Persistent solar influence on North Atlantic climate during the Holocene. *Science*, 294:2130–2136.
- Bond, G.C., Showers, W., Elliot, M., Evans, M., Lotti, R., Hajdas, I., Bonani, G., and Johnson, S., 1999. The North Atlantic's 1–2 kyr climate rhythm: relation to Heinrich events, Dansgaard/Oeschger cycles and the Little Ice Age. In Clark, P.U., Webb, R.S., and Keigwin, L.D. (Eds.), *Mechanisms of Global Climate Change at Millennial Time Scales*. Geophys. Monogr., 112:35–58.
- Campbell, I.D., Campbell, C., Apps, M.J., Rutter, N.W., and Bush, A.B.G., 1998. Late Holocene ~1500 yr climatic periodicities and their implications. *Geology*, 26:471–473.
- Carlut, J., and Courtillot, V., 1998. How complex is the time-averaged geomagnetic field over the past 5 Myr? *Geophys. J. Int.*, 134:527–544.
- Channell, J.E.T., Hodell, D.A., McManus, J., and Lehman, B., 1998. Orbital modulation of the Earth's magnetic field intensity. *Nature*, 394:464–468.
- Channell, J.E.T., and Lehman, B., 1997. The last two geomagnetic polarity reversals recorded in high-deposition-rate sediment drifts. *Nature*, 389:712–715.
- Channell, J.E.T., Mazaud, A., Sullivan, A., Turner, S., and Raymo, M.E., 2002. Geomagnetic excursions and paleointensities in the 0.9–2.15 Ma interval of the Matuyama Chron at ODP Site 983 and 984 (Iceland Basin). *J. Geophys. Res.*, 107:10.1029/2001JB000491.
- Channell, J.E.T., Stoner, J.S., Hodell, D.A., and Charles, C.D., 2000. Geomagnetic paleointensity for the last 100 kyr from the sub-antarctic South Atlantic: a tool for inter-hemispheric correlation. *Earth Planet. Sci. Lett.*, 175:145–160.
- Clark, P.U., Webb, R.S., and Keigwin, L.D. (Eds.), 1999. *Mechanisms of Global Climate Change at Millennial Time Scales*. Geophys. Monogr., Vol. 112.
- Coe, R.S., Hongre, L., and Glatzmaier, G.A., 2000. An examination of simulated geomagnetic reversals from a palaeomagnetic perspective. *Philos. Trans. R. Soc. London, Ser. A.*, 358(1768):1141–1170.
- Crowley, T.J., 1999. Correlating high-frequency climate variations. *Paleoceanography*, 14:271–272.

- De Menocal, P., Ortiz, J., Guilderson, T., and Sarnthein, M., 2000. Coherent high- and low-latitude climate variability during the Holocene warm period. *Science*, 288(5474):2198–2202.
- Flower, B.P., Oppo, D.W., McManus, J.F., Venz, K.A., Hodell, D.A., and Cullen, J., 2000. North Atlantic intermediate to deep water circulation and chemical stratification during the past 1 Myr. *Paleoceanography*, 15:388–403.
- Frank, M., Schwarz, B., Baumann, S., Kubik, P.W., Suter, M., and Mangini, A., 1997. A 200 kyr record of cosmogenic radionuclide production rate and geomagnetic field intensity from  $^{10}\text{Be}$  in globally stacked deep-sea sediments. *Earth Planet. Sci. Lett.*, 149:121–129.
- Glatzmaier, G.A., and Roberts, P.H., 1995. A 3-dimensional self-consistent computer-simulation of a geomagnetic-field reversal. *Nature*, 377:203–209.
- Gubbins, D., 1999. The distinction between geomagnetic excursions and reversals. *Geophys. J. Int.*, 137:F1–F3.
- Guyodo, Y., Gaillot, P., and Channell, J.E.T., 2000. Wavelet analysis of relative geomagnetic paleointensity at ODP Site 983. *Earth Planet. Sci. Lett.*, 184:109–123.
- Guyodo, Y., and Valet, J.-P., 1996. Relative variations in geomagnetic intensity from sedimentary records: the past 200,000 years. *Earth. Planet. Sci. Lett.*, 143:23–36.
- Hillaire-Marcel, C., De Vernal, A., Bilodeau, G., and Wu, G., 1994. Isotope stratigraphy, sedimentation rates, deep circulation, and carbonate events in the Labrador Sea during the last ~200 ka. *Can. J. Earth Sci.*, 31:63–89.
- Hiscott, R.N., Aksu, A.E., Mudie, P.J., and Parsons, D.F., 2001. A 340,000 year record of ice rafting, paleoclimatic fluctuations, and shelf-crossing glacial advances in the southwestern Labrador Sea. *Global Planet. Change*, 28:227–240.
- Hulot, G., and Le Mouél, J.-L., 1994. A statistical approach to the Earth's main magnetic field. *Phys. Earth Planet. Inter.*, 82:167–183.
- Hongre, L., Hulot, G., and Khokhlov, A., 1998. An analysis of the geomagnetic field over the past 2000 years. *Phys. Earth Planet. Inter.*, 106:311–335.
- Johnson, C.L., and Constable, C.G., 1997. The time-averaged geomagnetic field: global and regional biases for 0–5 Ma. *Geophys. J. Int.*, 131:643–666.
- Keigwin, L.D., Rio, D., Acton, G.D., et al., 1998. *Proc. ODP, Init. Repts.*, 172: College Station, TX (Ocean Drilling Program).
- Kelly, P., and Gubbins, D., 1997. The geomagnetic field over the past 5 million years. *Geophys. J. Int.*, 128:315–330.
- Kissel, C., Laj, C., Labeyrie, L., Dokken, T., Voelker, A., and Blamart, D., 1999. Rapid climatic variations during marine isotopic Stage 3: magnetic analysis of sediments from Nordic Seas and North Atlantic. *Earth Planet. Sci. Lett.*, 171:489–502.
- Kleiven, H.F., Jansen, E., Curry, W.B., Hodell, D.A., and Venz, K., 2003. Atlantic Ocean thermohaline circulation changes on orbital to suborbital timescales during the mid-Pleistocene. *Paleoceanography*, 18:10.1029/2001PA000629.
- Laj, C., Kissel, C., Mazaud, A., Channell, J.E.T., and Beer, J., 2000. North Atlantic paleointensity stack since 75 ka (NAPIS-75) and the duration of the Laschamp Event. *Phil. Trans. R. Soc. Lond.*, 358:1009–1025.
- Lund, S.P., Acton, G., Clement, B., Hastedt, M., Okada, M., and Williams, T., 1998. Geomagnetic field excursions occurred often during the last million years. *Eos, Trans. Am. Geophys. Union*, 79:178–179.
- Lund, S.P., Acton, G.D., Clement, B., Okada, M., and Williams, T., 2001a. Paleomagnetic records of Stage 3 excursions, Leg 172. In Keigwin, L.D., Rio, D., Acton, G.D., and Arnold, E. (Eds.), *Proc. ODP, Sci. Results*, 172, 1–20 [Online]. Available from World Wide Web: <[http://www.odp.tamu.edu/publications/172\\_SR/VOLUME/CHAPTERS/SR172\\_11.PDF](http://www.odp.tamu.edu/publications/172_SR/VOLUME/CHAPTERS/SR172_11.PDF)>.

- Lund, S.P., Williams, T., Acton, G., Clement, B., and Okada, M., 2001b. Brunhes Chron magnetic-field excursions recovered from Leg 172 sediments. *In* Keigwin, L.D., Rio, D., Acton, G.D., and Arnold, E. (Eds.), *Proc. ODP, Sci. Results*, 172, 1–18 [Online]. Available from World Wide Web: <[http://www\\_odp.tamu.edu/publications/172\\_SR/VOLUME/CHAPTERS/SR172\\_10.PDF](http://www_odp.tamu.edu/publications/172_SR/VOLUME/CHAPTERS/SR172_10.PDF)>.
- Mazaud, A., Laj, C., and Bender, M., 1994. A geomagnetic chronology for Antarctic ice accumulation. *Geophys. Res. Lett.*, 21:337–340.
- McManus, J., Bond, G., Broecker, W., Johnsen, S., Laybeyrie, L., and Higgins, S., 1994. High resolution climate records from the North Atlantic during the last interglacial. *Nature*, 371:326–329.
- McManus, J.F., Oppo, D.W., and Cullen, J.L., 1999. A 0.5 million year record of millennial-scale climate variability in the North Atlantic. *Science*, 283:971–975.
- Meynadier, L., Valet, J.-P., Weeks, R.J., Shackleton, N.J., and Hagee, V.L., 1992. Relative geomagnetic intensity of the field during the last 140 ka. *Earth Planet. Sci. Lett.*, 114:39–57.
- Oppo, D.W., McManus, J.F., and Cullen, J.L., 1998. Abrupt climate events 500,000 to 340,000 years ago: evidence from subpolar North Atlantic sediments. *Science*, 279:1335–1338.
- Poli, M.S., Thunell, R.C., and Rio, D., 2000. Millennial-scale changes in North Atlantic Deep Water circulation during marine isotope Stages 11 and 12: linkage to Antarctic climate. *Geology*, 28:807–810.
- Raisbeck, G.M., Yiou, F., Bourles, D., Lorius, C., Jouzel, J., and Barkov, N.I., 1987. Evidence for two intervals of enhanced  $^{10}\text{Be}$  deposition in Antarctic ice during the last glacial period. *Nature*, 326:273–277.
- Raymo, M., Ganley, K., Carter, S., Oppo, D.W., and McManus, J., 1998. Millennial-scale climate instability during the early Pleistocene epoch. *Nature*, 392:699–702.
- Raymo, M.E., 1999. Appendix. New insights into Earth's history: an introduction to Leg 162 postcruise research published in journals. *In* Raymo, M.E., Jansen, E., Blum, P., and Herbert, T.D. (Eds.), *Proc. ODP, Sci. Results*, 162: College Station, TX (Ocean Drilling Program), 273–275.
- Raymo, M.E., Oppo, D.W., Flower, B.P., Hodell, D.A., McManus, J.F., Venz, K.A., Kleiven, K.F., and McIntyre, K., 2004. Stability of North Atlantic water masses in face of pronounced climate variability during the Pleistocene. *Paleoceanography*, 19:10.1029/2003PA000921.
- Sarnthein, M., Statterger, K., Dreger, D., Erienkeuser, H., Grootes, P., Haupt, B.J., Jung, S., Kiefer, T., Kuhnt, W., Pflaumann, U., Schäfer-Neth, C., Schultz, H., Schultz, M., Seidov, D., Simstich, J., van Kreveld, S., Vogelsang, E., Völker, A., and Weinelt, M., 2001. Fundamental modes and abrupt changes in North Atlantic circulation and climate over the last 60 k.y.: concepts, reconstruction, and numerical modeling. *In* Schäfer, P., Ritzrau, W., Schlueter, M., and Thiede, J. (Eds.), *The Northern North Atlantic: A Changing Environment*: Berlin (Springer-Verlag), 365–410.
- Schmieder, F., von Dobeneck, T., and Bleil, U., 2000. The mid-Pleistocene climate transition as documented in the deep South Atlantic Ocean: initiation, interim state and terminal event. *Earth Planet. Sci. Lett.*, 179:539–549.
- Sirocko, F., Garbe-Schönberg, D., McIntyre, A., and Molino, B., 1996. Teleconnections between the subtropical monsoons and high-latitude climates during the last deglaciation. *Science*, 272:526–529.
- Stoner, J.S., Channell, J.E.T., and Hillaire-Marcel, C., 1995. Late Pleistocene relative geomagnetic paleointensity from the deep Labrador Sea: regional and global correlations. *Earth Planet. Sci. Lett.*, 134:237–252.
- Stoner, J.S., Channell, J.E.T., and Hillaire-Marcel, C., 1996. The magnetic signature of rapidly deposited detrital layers from the deep Labrador sea: relationship to North Atlantic Heinrich layers. *Paleoceanography*, 11:309–325.

- Stoner, J.S., Channell, J.E.T., and Hillaire-Marcel, C., 1998. A 200 ka geomagnetic chronostratigraphy for the Labrador Sea: indirect correlation of the sediment record to SPECMAP. *Earth Planet. Sci. Lett.*, 159:165–181.
- Stoner, J.S., Channell, J.E.T., Hillaire-Marcel, C., and Kissel, C., 2000. Geomagnetic paleointensity and environmental record from Labrador Sea Core MD95-2024: global marine sediment and ice core chronostratigraphy for the last 110 kyr. *Earth Planet. Sci. Lett.*, 183:161–177.
- Stoner, J.S., Channell, J.E.T., Hodell, D.A., and Charles, C.D., 2003. A ~580 kyr paleomagnetic record from the sub-Antarctic South Atlantic (ODP Site U1089). *J. Geophys. Res.*, 108:10.1029/2001JB001390.
- Stoner, J.S., Laj, C., Channell, J.E.T., and Kissel, C., 2002. South Atlantic (SAPIS) and North Atlantic (NAPIS) geomagnetic paleointensity stacks (0–80 ka): implications for inter-hemispheric correlation. *Quat. Sci. Rev.*, 21:1141–1151.
- Toews, M.W., and Piper, D.J.W., 2002. Recurrence intervals of seismically triggered mass-transport deposits at Orphan Knoll continental margin off Newfoundland and Labrador. *Curr. Res.—Geol. Surv. Can.*, E17:1–8.
- van Kreveld, S., Sarnthein, M., Erlenkeuser, H., Grootes, P., Jung, S., Nadeau, M.J., Pflaumann, U., and Voelker, A., 2000. Potential links between surging ice sheets, circulation changes, and the Dansgaard–Oeschger cycles in the Irminger Sea. *Paleoceanography*, 15:425–442.
- Voelker, A.H.L., Sarnthein, M., Grootes, P.M., Erlenkeuser, H., Laj, C., Mazaud, A., Nadeau, M.-J., and Schleicher, M., 1998. Correlation of marine  $^{14}\text{C}$  ages from the Nordic Seas with the GISP2 isotope record: implications for  $^{14}\text{C}$  calibration beyond 25 ka BP. *Radiocarbon*, 40:517–534.
- Yamazaki, T., 1999. Relative paleointensity of the geomagnetic field during Brunhes Chron recorded in North Pacific deep-sea sediment cores: orbital influence? *Earth Planet. Sci. Lett.*, 169:23–35.

---

Expedition 303 Preliminary Report

---

**Table T1.** Expedition 303 operations summary.

Hole	Latitude	Longitude	Water depth (mbsl)	Number of cores	Interval cored (m)	Core recovered (m)	Recovery (%)	Drilled interval (m)	Penetration (m)	Time on hole (h)	Time on site (days)
U1302A	50°9.985'N	45°38.271'W	3568.6	13	107.1	91.7	85.6	0.0	107.1	30.50	1.3
U1302B	50°9.995'N	45°38.290'W	3563.4	11	104.7	102.8	98.2	0.0	104.7	13.25	0.6
U1302C	50°10.007'N	45°38.309'W	3559.2	11	104.5	97.1	92.9	0.0	104.5	13.67	0.6
U1302D	50°10.019'N	45°38.324'W	3555.7	2	13.0	4.9	37.5	0.0	13.0	2.58	0.1
U1302E	50°10.030'N	45°38.343'W	3558.1	2	15.1	14.6	96.6	0.0	15.1	4.00	0.2
Site 1302 totals:				39	344.4	311.0	90.3	0.0	344.4	64.00	2.7
U1303A	50°12.401'N	45°41.220'W	3524.2	10	93.9	69.1	73.6	0.0	93.9	14.83	0.6
U1303B	50°12.383'N	45°41.197'W	3517.9	9	85.7	71.5	83.5	0.0	85.7	20.42	0.9
Site 1303 totals:				19	179.6	140.6	78.3	0.0	179.6	35.25	1.5
U1304A	53°3.401'N	33°31.781'W	3069.1	26	239.0	251.4	105.2	0.0	239.0	35.75	1.5
U1304B	53°3.393'N	33°31.768'W	3065.4	26	242.4	252.1	104.0	0.0	242.4	30.50	1.3
U1304C	53°3.384'N	33°31.751'W	3064.5	8	69.6	71.8	103.2	0.0	69.6	12.17	0.5
U1304D	53°3.378'N	33°31.741'W	3064.5	21	190.9	185.7	97.3	53.0	243.9	46.08	1.9
Site 1304 totals:				81	741.9	761.0	102.6	53.0	794.9	124.50	5.2
U1305A	57°28.507'N	48°31.842'W	3463.0	30	280.0	294.6	105.2	0.0	280.0	44.00	1.8
U1305B	57°28.507'N	48°31.813'W	3459.2	28	264.8	274.3	103.6	0.0	264.8	33.50	1.4
U1305C	57°28.509'N	48°31.783'W	3458.8	31	287.1	298.2	103.9	0.0	287.1	59.75	2.5
Site 1305 totals:				89	831.9	867.1	104.2	0.0	831.9	137.25	5.7
U1306A	58°14.228'N	45°38.588'W	2270.5	33	303.3	307.0	101.2	1.0	304.3	38.33	1.6
U1306B	58°14.227'N	45°38.557'W	2273.0	33	305.3	315.9	103.5	4.0	309.3	35.67	1.5
U1306C	58°14.228'N	45°38.527'W	2274.8	28	257.5	267.6	103.9	8.0	265.5	28.50	1.2
U1306D	58°14.227'N	45°38.500'W	2271.8	19	178.0	179.5	100.9	2.0	180.0	21.50	0.9
Site 1306 totals:				113	1044.1	1069.9	102.5	15.0	1059.1	124.00	5.2
U1307A	58°30.347'N	46°24.033'W	2575.1	19	156.6	160.5	102.5	6.0	162.6	27.42	1.1
U1307B	58°30.358'N	46°24.054'W	2575.3	17	154.6	157.0	101.5	0.0	154.6	25.08	1.0
Site 1307 totals:				36	311.2	317.4	102.0	6.0	317.2	52.50	2.2
U1308A	49°52.666'N	24°14.287'W	3871.0	36	341.1	323.8	94.9	0.0	341.1	67.92	2.8
U1308B	49°52.667'N	24°14.313'W	3871.1	22	198.3	186.2	93.9	0.0	198.3	52.83	2.2
U1308C	49°52.684'N	24°14.287'W	3872.7	30	279.9	271.1	96.9	0.0	279.9	49.50	2.1
U1308D	49°52.700'N	24°14.287'W	3873.8	1	6.7	6.7	100.3	0.0	6.7	1.83	0.1
U1308E	49°52.700'N	24°14.287'W	3871.0	21	193.0	172.5	89.4	7.5	200.5	28.92	1.2
U1308F	49°52.700'N	24°14.312'W	3872.1	24	227.0	228.6	100.7	0.0	227.0	41.00	1.7
Site 1308 totals:				134	1246.0	1188.9	95.4	7.5	1253.5	242.00	10.1
Expedition 303 totals:				511	4699.1	4656.1	99.1	81.5	4780.6	779.50	32.5

**Figure F1** Location of IODP Expedition 303 sites (red), and other DSDP and ODP sites mentioned in the text. Figure modified after Raymo et al. (2004). Arrows indicate major deepwater flows. DSOW = Denmark Strait Overflow Water; NGS = Norwegian Greenland Sea; ISOW = Iceland Sea Overflow Water; WTRO = Wyville Thomson Ridge Overflow; GFZ = Charlie Gibbs Fracture Zone; LSW = Labrador Sea Water; LDW = Lower Deep Water.

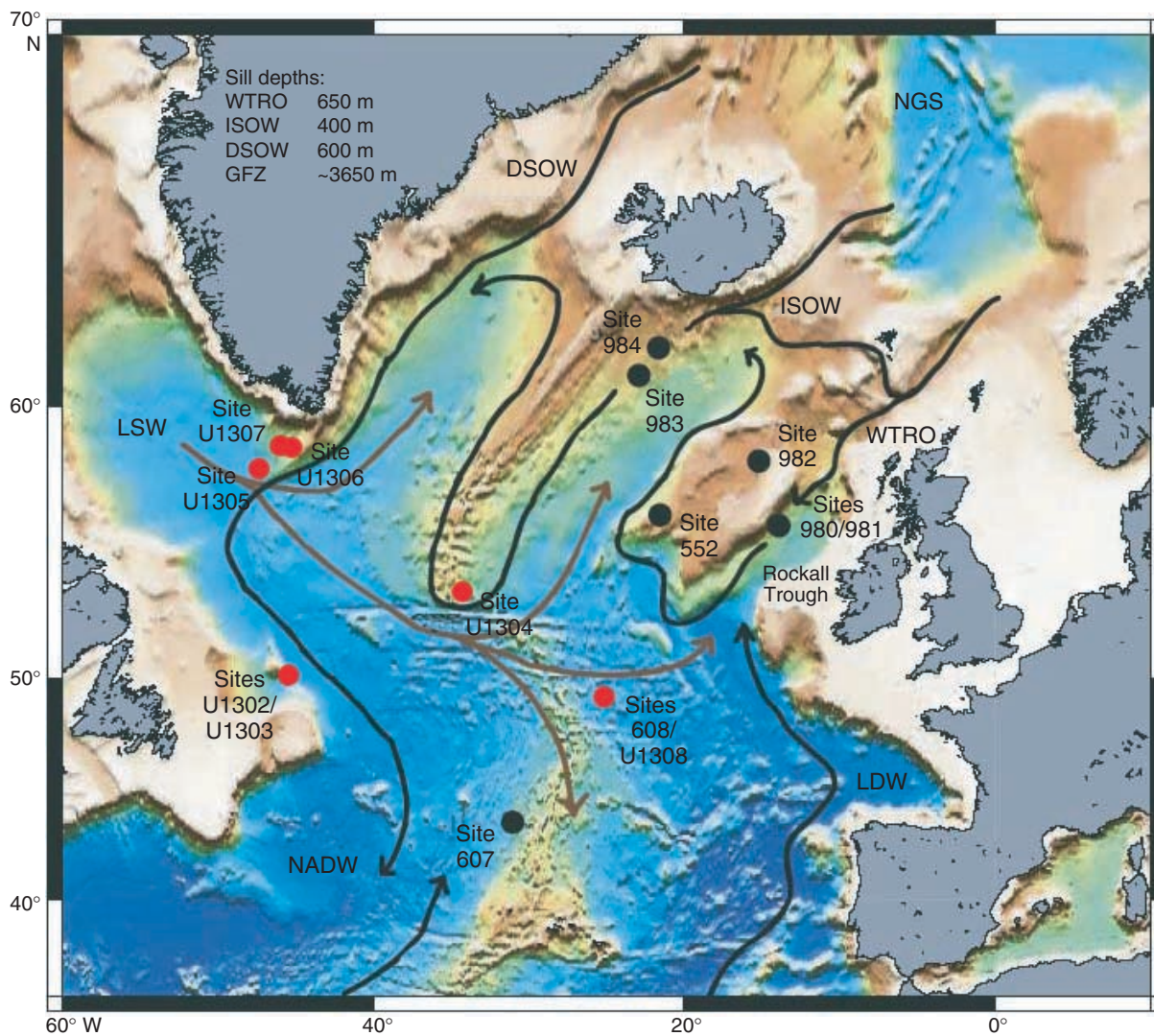




**Figure F2.** Composite digital image scan of Core 303-U1303B-1H indicating detrital layers delineated by magnetic susceptibility (MS) (red line) and gamma ray attenuation (GRA) density (yellow line). Detrital layer labels follow Stoner et al. (2000) for Core MD95-2024 collected at the same location. The detrital layer H6 (Heinrich Layer 6) has an age of ~60 ka, indicating a mean sedimentation rate in this core of 15 cm/k.y.

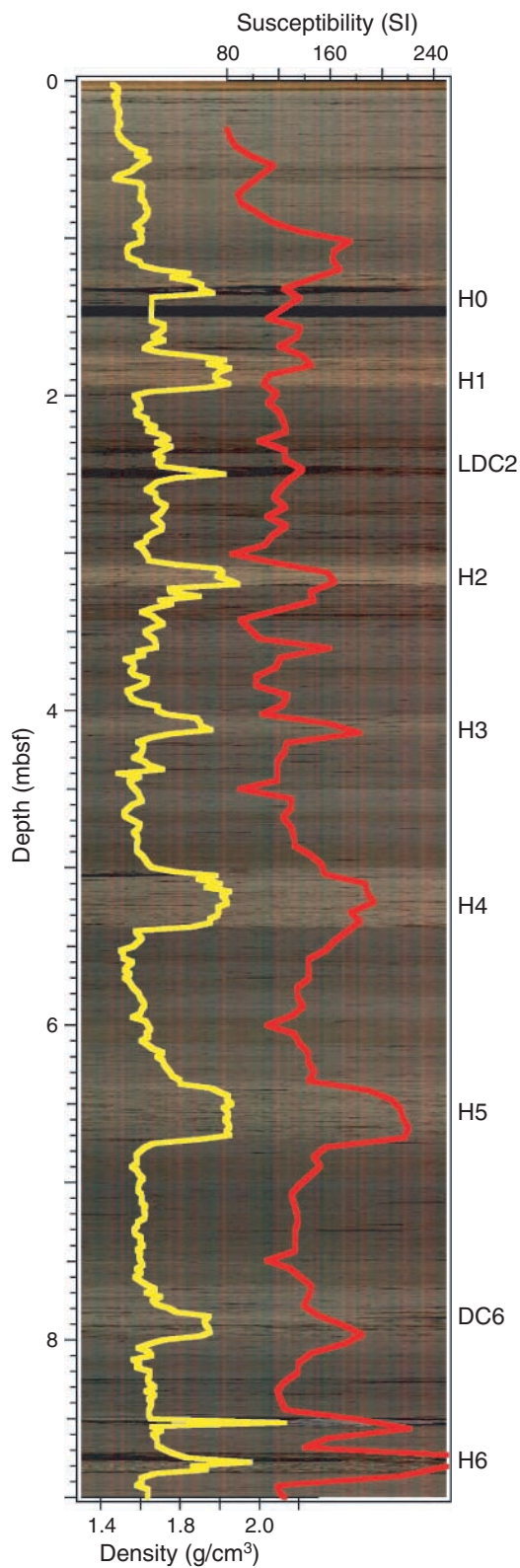


**Figure F3.** Recovery record at Sites U1302 and U1303 with natural gamma ray (NGR), magnetic susceptibility (MS), gamma ray attenuation (GRA) density, and lightness (L\*) for the composite section (mcd).

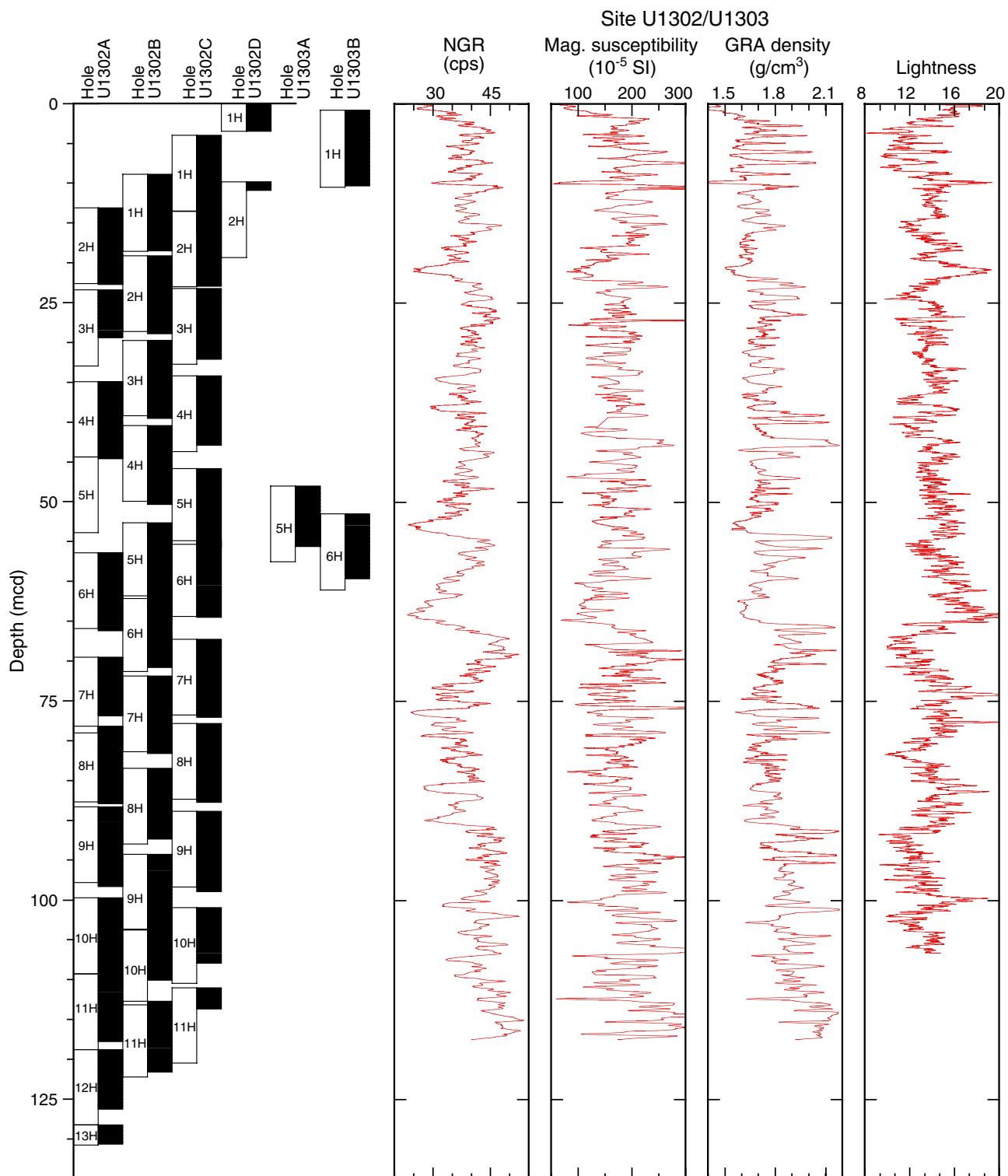


**Figure F4.** Schematic stratigraphy at the seven sites drilled during Expedition 303. The geomagnetic polarity timescale is shown on the right. The normal and reversed polarity zones are indicated in black and white, respectively. Hatched intervals indicate uncertain polarity in the debris flow of Sites U1302 and U1303. Blue tie lines indicate biostratigraphic datums and correlations. Red tie lines indicate magnetostratigraphic correlations.

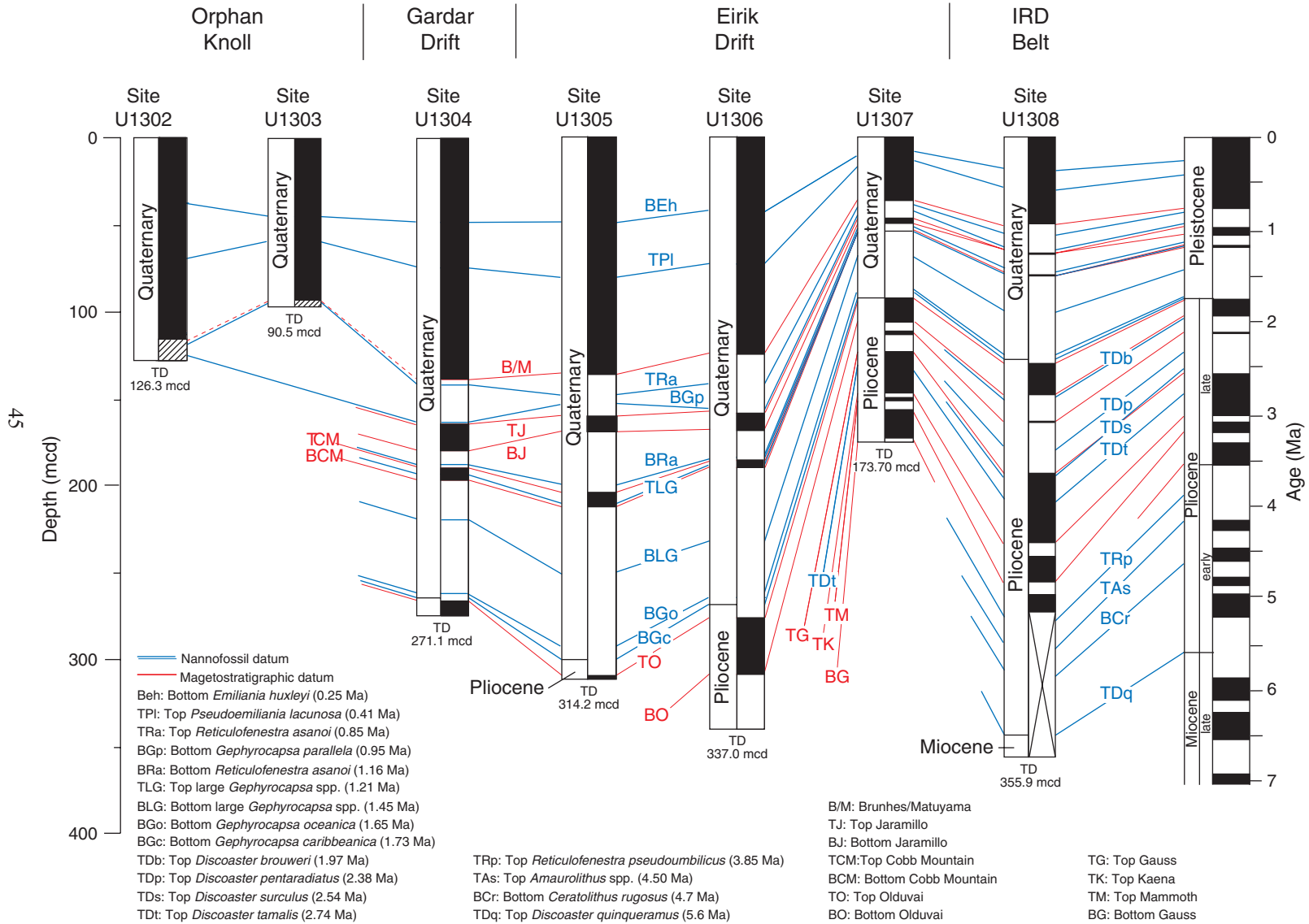


**Figure F5.** Sedimentation rates at the sites drilled during Expedition 303. Solid circles = magnetostratigraphy-based ages, open circles = nannofossil-based ages, open squares = diatom-based ages, open triangles = foraminiferal-based ages. Mean sedimentation rates are calculated from straight-line segments.

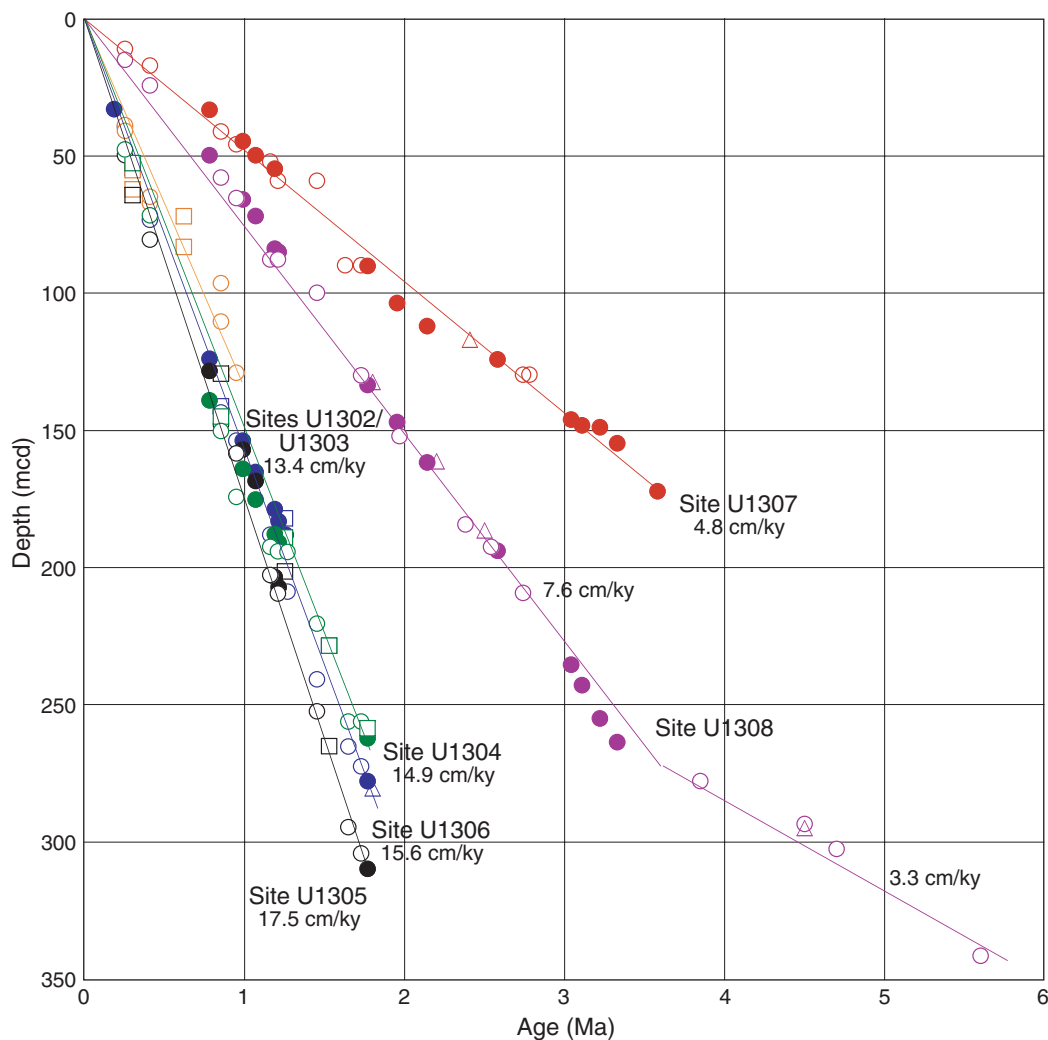


**Figure F6.** Recovery record at Site U1304 with natural gamma ray (NGR), magnetic susceptibility (MS), gamma ray attenuation (GRA) density, and lightness for the composite section (mcd).

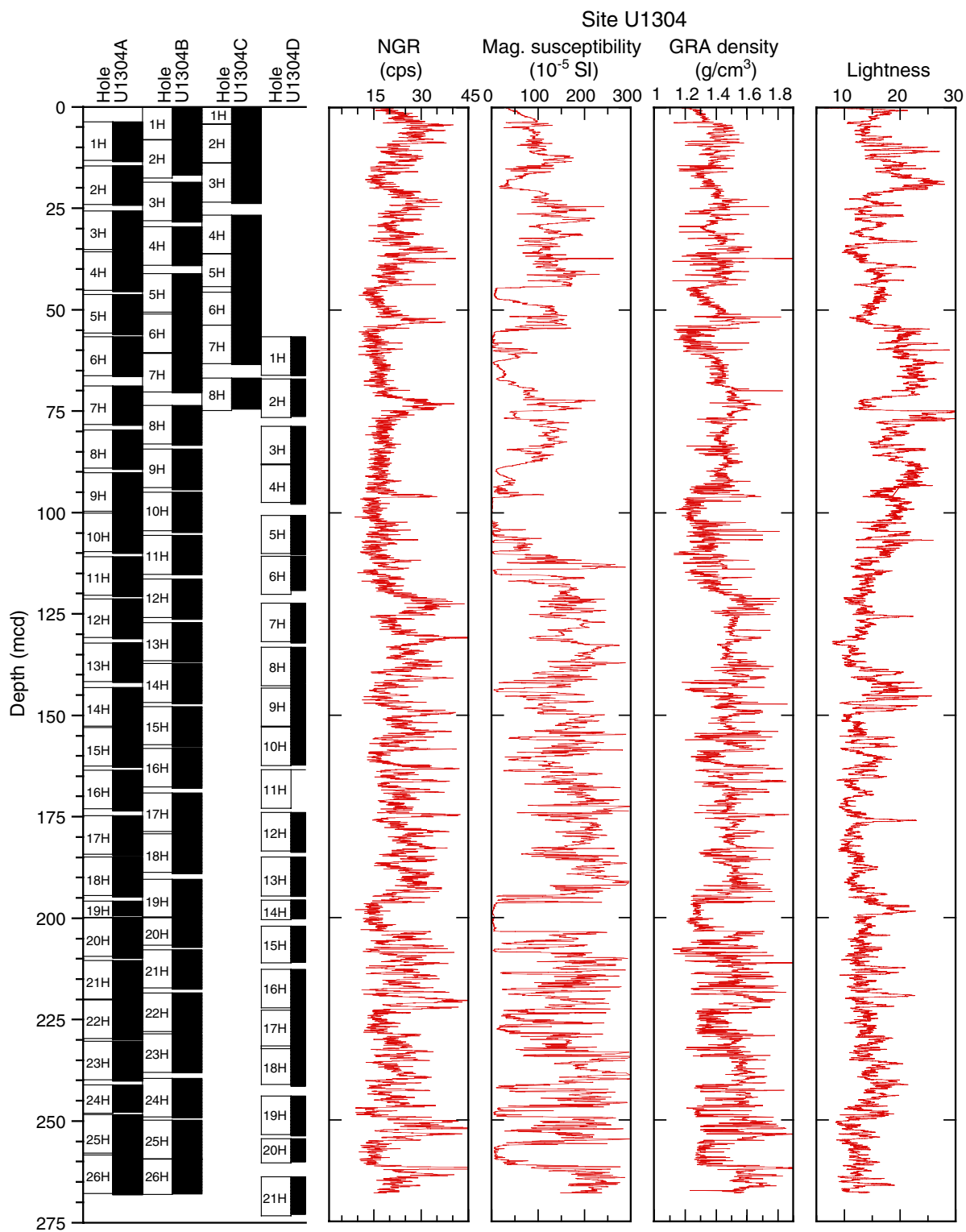


**Figure F7.** Recovery record at Site U1305 with natural gamma ray (NGR), magnetic susceptibility (MS), gamma ray attenuation (GRA) density, and lightness for the composite section (mcd).

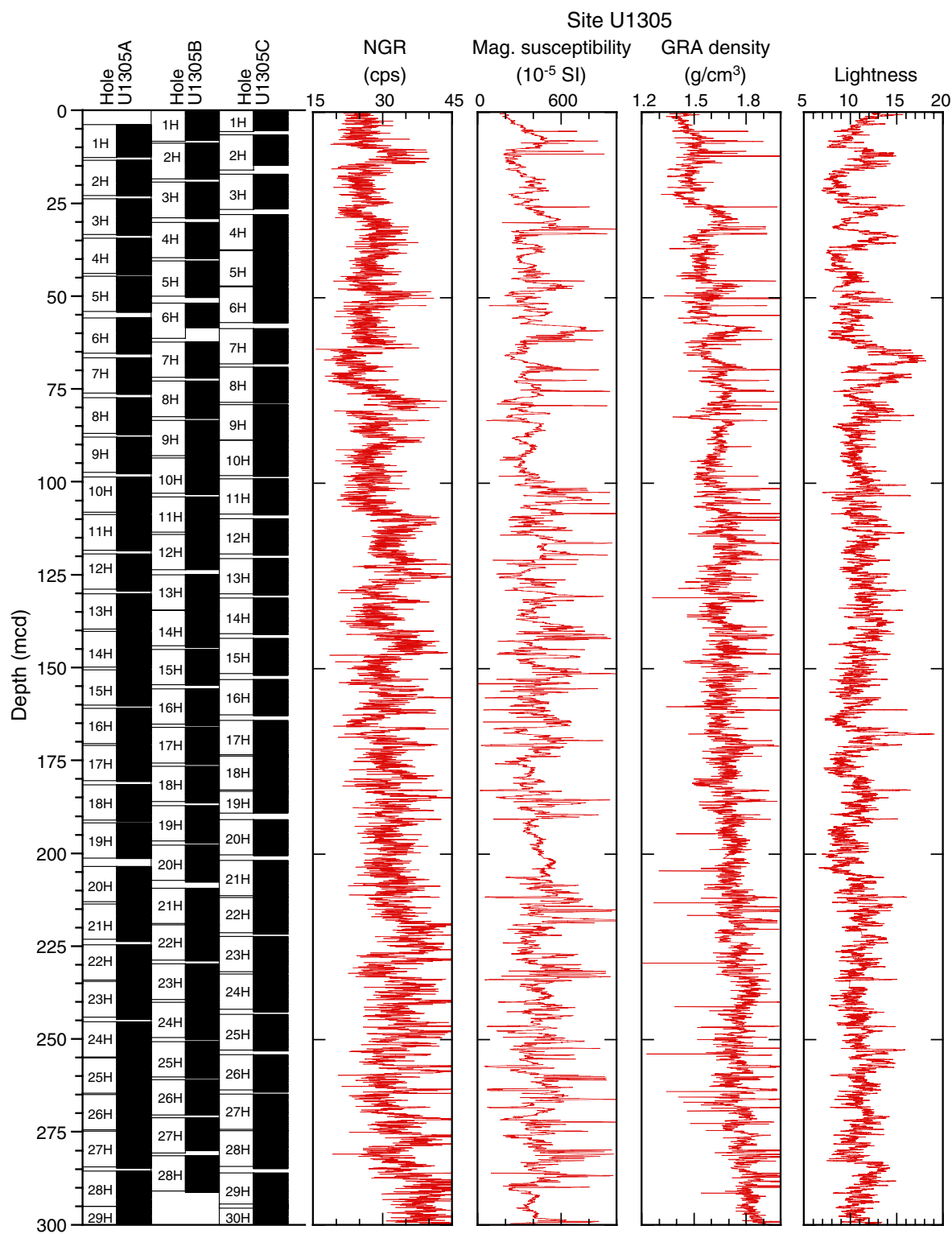


**Figure F8.** Recovery record at Site U1306 with natural gamma ray (NGR), magnetic susceptibility (MS), gamma ray attenuation (GRA) density, and lightness for the composite section (mcd).

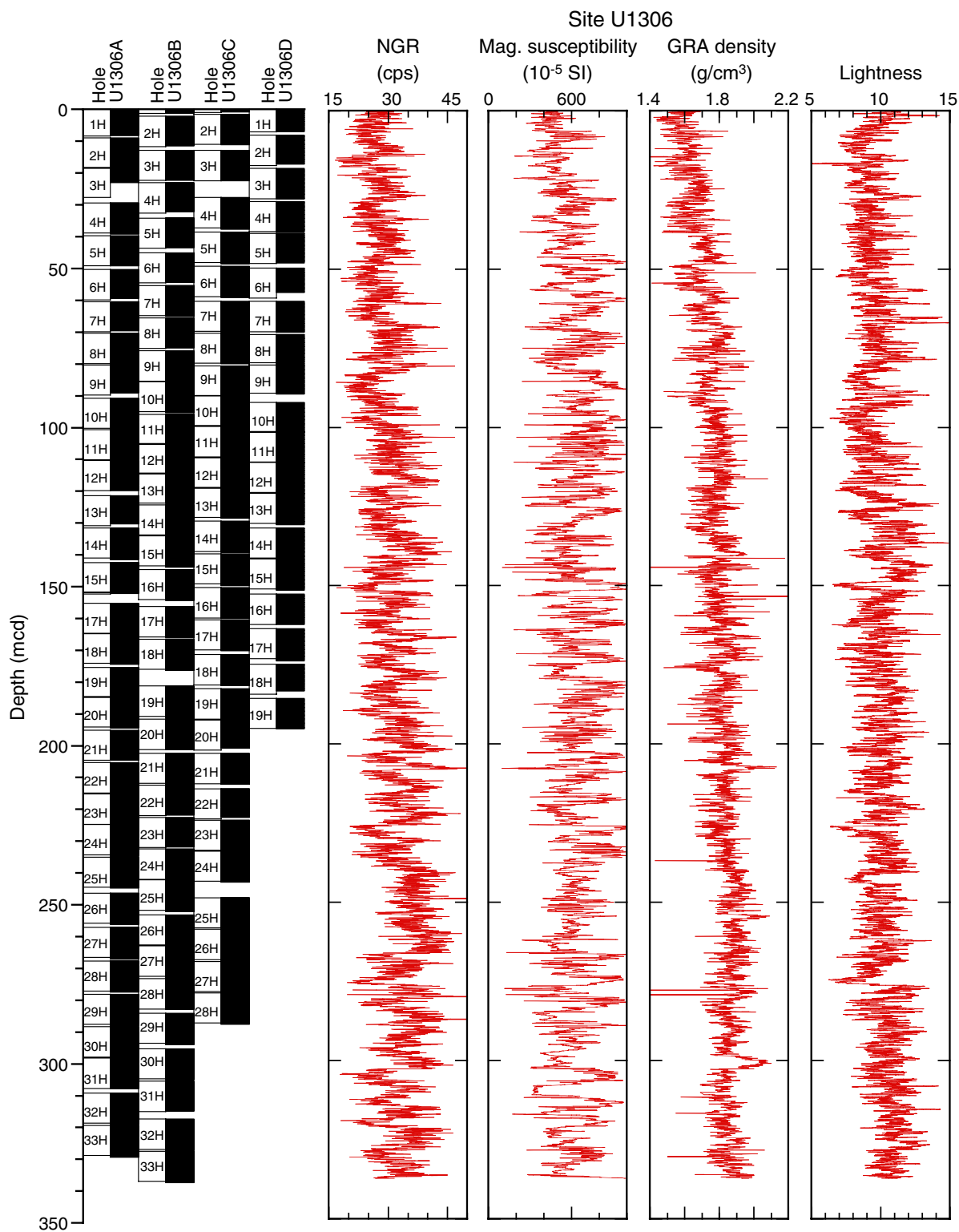


**Figure F9.** Recovery record at Site U1307 with natural gamma ray (NGR), magnetic susceptibility (MS), gamma ray attenuation (GRA) density, and lightness for the composite section (mcd).

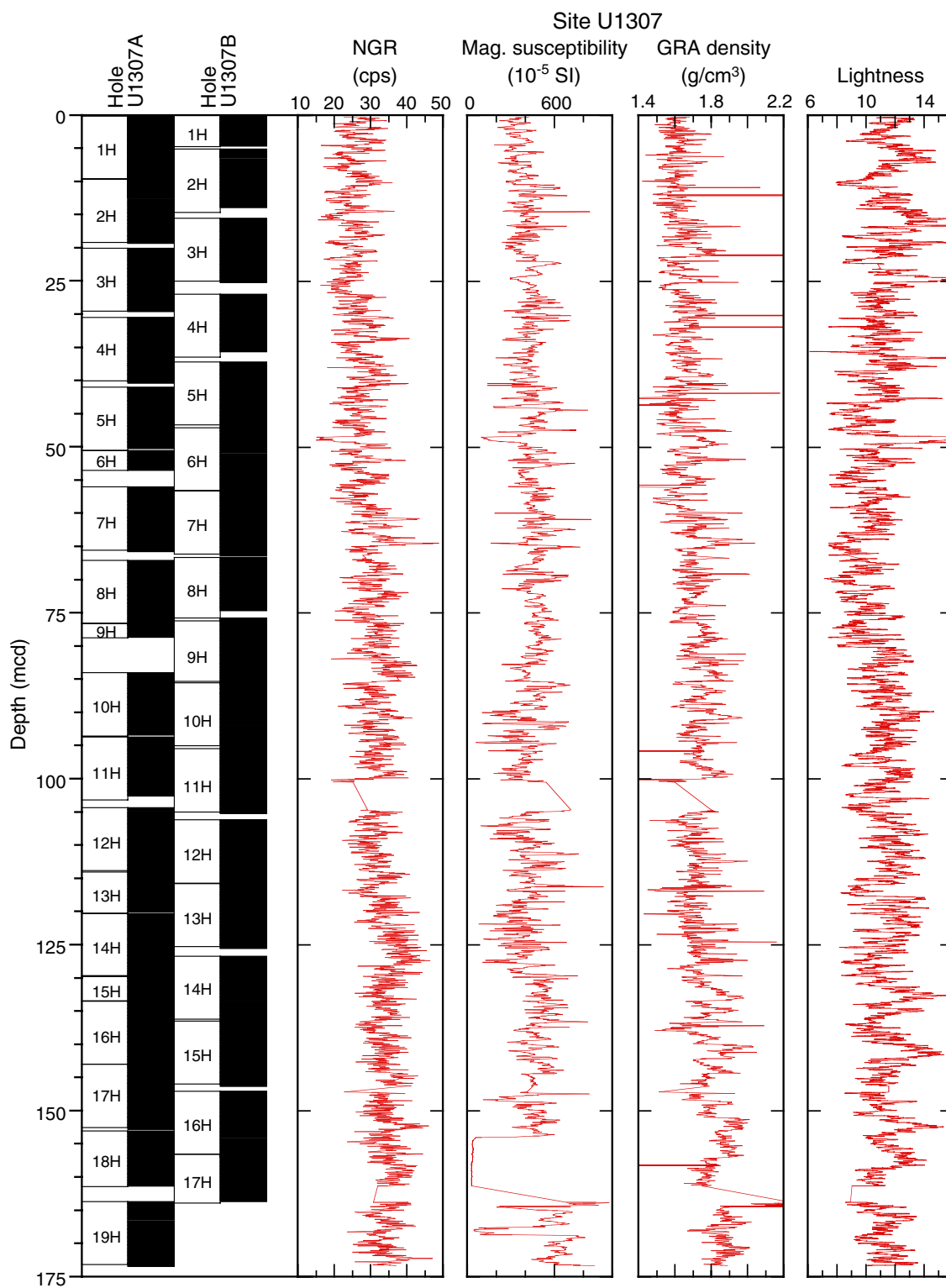
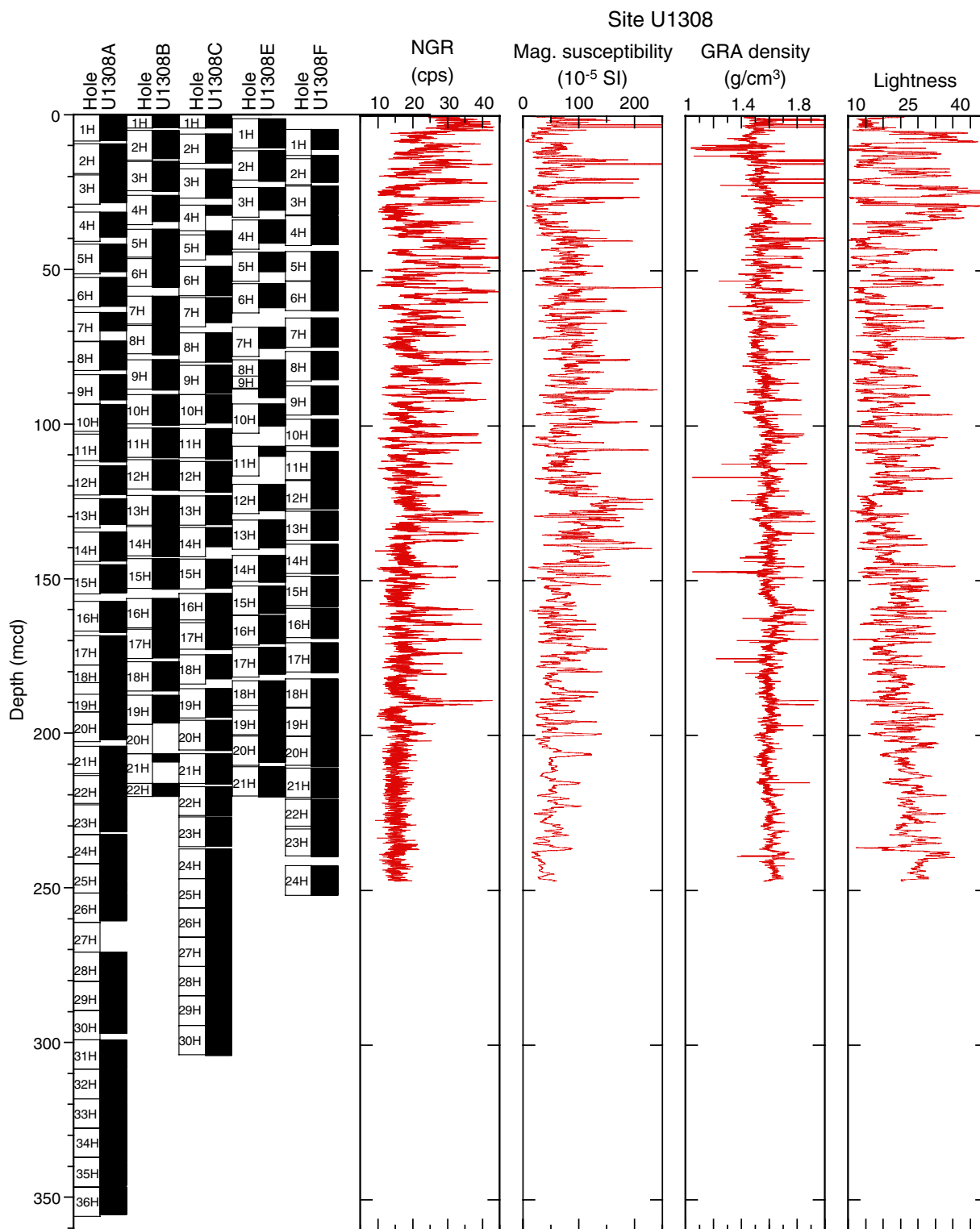




**Figure F10.** Recovery record at Site U1308 with natural gamma ray (NGR), magnetic susceptibility (MS), gamma ray attenuation (GRA) density, and lightness for the composite section (mcd).





## Chapter 8

### INTEGRATED OCEAN DRILLING PROGRAM

### EXPEDITION 303: Northern Atlantic climate I

*IODP/ICDP joint colloquium Potsdam 2005, extended abstract*

G. Bartoli<sup>(1)</sup> and O. E. Romero<sup>(2)</sup>

(1) Institute for Geosciences, Christian-Albrechts-Universität zu Kiel, Ludewig-Meyn-Str.10, 24118 Kiel. [gb@gpi.uni-kiel.de](mailto:gb@gpi.uni-kiel.de)

(2) Dept. of Geosciences, Universität Bremen, POBox 33 04 40, 28334 Bremen.  
oromero@uni-bremen.de

The North Atlantic Ocean is undoubtedly one of the most climatically sensitive regions on Earth because the ocean-atmosphere-cryosphere system is prone to mode jumps that are triggered by changes in freshwater delivery to source areas of deepwater formation. During the last glaciation, these abrupt jumps in climate state are manifest by Dansgaard/Oeschger (D/O) cycles and Heinrich Events in ice and marine sediment cores, respectively. Determining the long-term evolution of millennial-scale variability in surface temperature, ice sheet dynamics, and thermohaline circulation can provide clues to the mechanisms responsible for abrupt climate change. For example, the average climate state evolved toward generally colder conditions with larger ice sheets during the Pliocene–Pleistocene. This shift was accompanied by a change in the spectral character of climate proxies, from dominantly 41- to 100-k.y. periods between ~920 and 640 ka (Schmieder et al., 2000).

The overall objectives of Expedition 303 were to establish late Neogene-Quaternary inter-calibration of geomagnetic paleointensity, isotope stratigraphies and regional environmental stratigraphies, and in so-doing develop a millennial-scale stratigraphic template. Such a template is required for understanding the relative phasing of atmospheric, cryospheric and oceanic changes that are central to our understanding of the mechanisms of global climate change on orbital to millennial timescales. The common overall objective of Expeditions 303 and 306 (scheduled for March-April, 2005) provided more flexibility to occupy sites as weather conditions allowed than is usual for an individual expedition. The October–November window in the North Atlantic ensured that this flexibility would be utilized.

The overall objective at **Sites 1302 and 1303** is to explore the record of Laurentide Ice Sheet (LIS) instability at this location, close to Orphan Knoll (Fig. 1, Table 1). Piston cores collected previously at or near Sites 1302 and 1303 show the presence of numerous detrital layers (*e.g.* Hillaire-Marcel et al., 1994; Stoner et al., 1995, 2000). Isotopic data from planktonic foraminifers indicate that these detrital layers are associated with low-productivity meltwater pulses. The objective at Sites 1302 and 1303 is to document this manifestation of LIS instability further back in time, to the base of the recovered section (approximately MIS 17). The mean sedimentation rates are estimated to be ~13 cm/ky, ensuring a high-resolution record.

**Table 1.** Expedition 303 operations summary.

Hole	Latitude	Longitude	Water Depth (mbsl)	Core Recovered (m)	Recovery %	Penetration (m)	Time on Hole (hours)	Time on Site (days)
1302A	50 9.985°N	45 38.271°W	3568.6	91.7	85.6	107.1	30.50	1.3
1302B	50 9.995°N	45 38.290°W	3563.4	102.8	98.2	104.7	13.25	0.6
1302C	50 10.007°N	45 38.309°W	3559.2	97.1	92.9	104.5	13.67	0.6
1302D	50 10.019°N	45 38.324°W	3555.7	4.9	37.5	13	2.58	0.1
1302E	50 10.030°N	45 38.343°W	3558.1	14.6	96.6	15.1	4.00	0.2
Site 1302 Totals:				311	90.3	344.4	64.00	2.7
1303A	50 12.401°N	45 41.220°W	3524.2	69.1	73.6	93.9	14.83	0.6
1303B	50 12.383°N	45 41.197°W	3517.9	71.5	83.5	85.7	20.42	0.9
Site 1303 Totals:				140.6	78.3	179.6	35.25	1.5
1304A	53 3.401°N	33 31.781°W	3069.1	251.4	105.2	239	35.75	1.5
1304B	53 3.393°N	33 31.768°W	3065.4	252.1	104	242.4	30.50	1.3
1304C	53 3.384°N	33 31.751°W	3064.5	71.8	103.2	69.6	12.17	0.5
1304D	53 3.378°N	33 31.741°W	3064.5	185.7	97.3	243.9	46.08	1.9
Site 1304 Totals:				761	102.6	794.9	124.50	5.2
1305A	57 28.507°N	48 31.842°W	3463.0	294.6	105.2	280	44.00	1.8
1305B	57 28.507°N	48 31.813°W	3459.2	274.3	103.6	264.8	33.50	1.4
1305C	57 28.509°N	48 31.783°W	3458.8	298.2	103.9	287.1	59.75	2.5
Site 1305 Totals:				867.1	104.2	831.9	137.25	5.7
1306A	58 14.228°N	45 38.588°W	2270.5	307	101.2	304.3	38.33	1.6
1306B	58 14.227°N	45 38.557°W	2273.0	315.9	103.5	309.3	35.67	1.5
1306C	58 14.228°N	45 38.527°W	2274.8	267.6	103.9	265.5	28.50	1.2
1306D	58 14.227°N	45 38.500°W	2271.8	179.5	100.9	180	21.50	0.9
Site 1306 Totals:				1069.9	102.5	1059.1	124.00	5.2
1307A	58 30.347°N	46 24.033°W	2575.1	160.5	102.5	162.6	27.42	1.1
1307B	58 30.358°N	46 24.054°W	2575.3	157	101.5	154.6	25.08	1.0
Site 1307 Totals:				317.4	102	317.2	52.50	2.2
1308A	49 52.666°N	24 14.287°W	3871.0	323.8	94.9	341.1	67.92	2.8
1308B	49 52.667°N	24 14.313°W	3871.1	186.2	93.9	198.3	52.83	2.2
1308C	49 52.684°N	24 14.287°W	3872.7	271.1	96.9	279.9	49.50	2.1
1308D	49 52.700°N	24 14.287°W	3873.8	6.7	100.3	6.7	1.83	0.1
1308E	49 52.700°N	24 14.287°W	3871.0	172.5	89.4	200.5	28.92	1.2
1308F	49 52.700°N	24 14.312°W	3872.1	228.6	100.7	227	41.00	1.7
Site 1308 Totals:				1188.9	95.4	1253.5	242.00	10.1
Expedition 303 Totals:				4656.1	99.1	4780.6	779.50	32.5

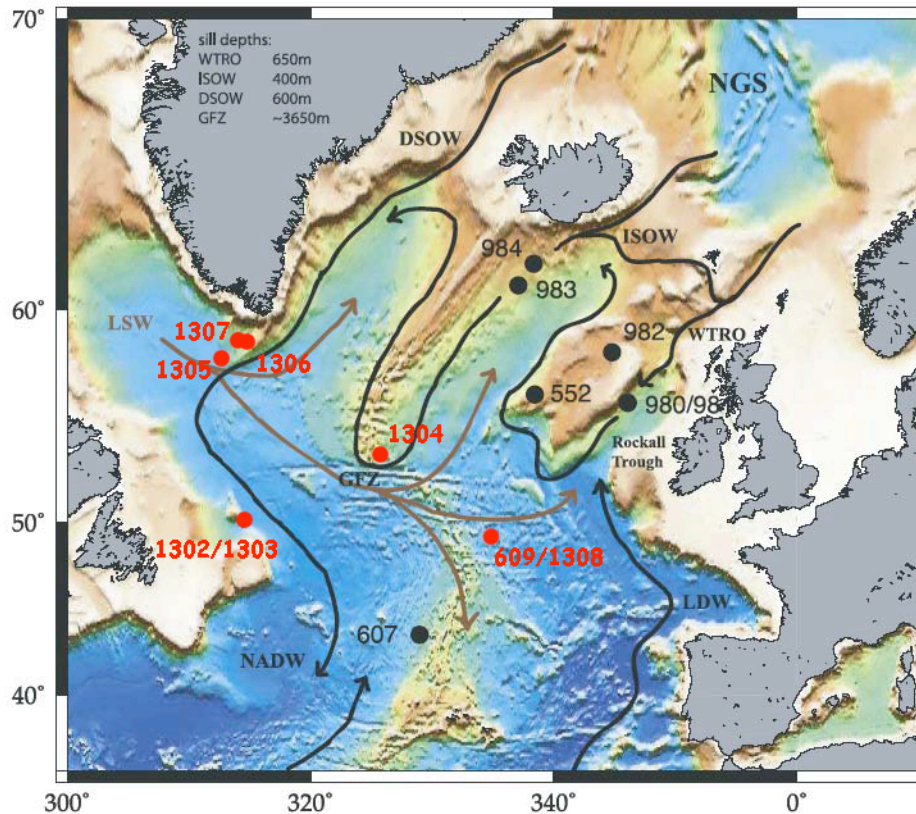


**Fig. 1.** Location of IODP Expedition 303 sites (red), and other DSDP and ODP sites. Arrows indicate major deep-water flows. Abbreviations: DSOW: Denmark Strait Overflow Water; NGS: Norwegian Greenland Sea; ISOW: Iceland Sea Overflow Water; WTRO: Wyville Thomson Ridge Overflow; GFZ: Charlie Gibbs Fracture Zone; LSW: Labrador Sea Water. LDW: Lower Deep Water. (Figure modified after Raymo et al., 2004).

At Site 1302, the first site to be drilled off Orphan Knoll, a debris flow was encountered at ~105 mcd that was not recognized in seismic data (Toews and Piper, 2002). The top of the debris flow appears to be within the Brunhes Chronozone at about 700 ka, and the base of the section is estimated, from nannofossil stratigraphy, to be at about 950 ka. In an attempt to avoid the debris flow, we traversed in dynamic positioning mode, with the base of the drill-string lifted a few hundred meters above the seafloor, to **Site 1303**, located 5.68 km NW of Site 1302. The debris flow was again encountered at Site 1303 at approximately the same depth, drilling was again discontinued. Sites 1302 and 1303 can be easily correlated using a range of MST data, and it is clear that essentially the same section was recovered at the two sites.

The sediments at **Site 1304** comprise interbedded diatom (Fig. 2) and nannofossil oozes with clay and silty clay. The lithologies are generally interbedded on a centimeter or decimeter scale. The site is located within the central Atlantic IRD belt (Fig. 1, Table 1) and therefore provides a distal record (relative to that at Sites 1302/1303) of the ice-sheet instability. Site 1304 provides a high sedimentation rate record (15.3 cm/ky) at a water depth (3065 m) sufficient to determine the stable isotopic composition of North Atlantic Deep Water (NADW). The diatom-rich sedimentary section extends back into the uppermost Pliocene at 258 mcd. The stratigraphy implies that the site has been located at the sub-arctic convergence between the surface Labrador Current and the North Atlantic Current (Bodén and Backman, 1996).



**Fig. 2.** Site 1304. Example of laminated diatom ooze in core split with saw showing the fine laminae characteristic of these sediments (Interval 1304A-24H-4, 59-80 cm).

Three sites (**Sites 1305, 1306 and 1307**) were drilled on the Eirik Drift (Fig. 1, Table 1). The first of these was the designated the “deep-water” site (Site 1305) in 3459 m water depth at the western extremity of the Eirik Drift. The primary “shallow-water” site (Site 1306) in 2273 m water depth is located 191 km NE of Site 1305. The two sites were chosen by maximizing the thickness of the Quaternary sedimentary section in the multichannel seismic network obtained over the Eirik Drift during Cruise KN-166 (R/V Knorr, PI: Greg Mountain).

Conventional piston cores have shown that the sedimentation history on the Eirik Drift during the last glacial cycle is strongly affected by the Western Boundary Undercurrent (WBUC) that sweeps along east Greenland and into the Labrador Sea (Hillaire-Marcel et al., 1994; Stoner et al., 1998). Based on two conventional piston cores (HU90-013-013P and HU90-013-012) from the Eirik Drift at similar water depths, the “deep-water” site (Site 1305) is expected to display relatively expanded interglacials and relatively condensed glacial intervals, and the converse is true for the “shallow-water” site (Site 1306). The base of the section at both sites lies within the Olduvai Subchronozone at ~300 mcd, and the mean sedimentation rates are 17-18 cm/ky. Sites 1305 and 1306 will provide complementary high-resolution records of the history of the WBUC, detrital layer stratigraphy signifying instability of the surrounding ice sheets, and the attributes for well-constrained age models using stable isotopes, biostratigraphy and geomagnetic paleointensity.

**Site 1307** was not in the initial plan for Expedition 303, but was occupied when a storm moving northeastward across the North Atlantic blocked our passage to our intended next site (Site 1308). Site 1307 was placed at a location on the Eirik Drift (Fig. 1, Table 1) where the Quaternary sedimentary section appears to be thinned relative to its thickness at Site 1306, providing APC access to the underlying Pliocene section. Two holes were drilled at Site 1307 reaching a maximum depth of 162 mcd in the uppermost Gilbert Chronozone (~3.6 Ma). The mean sedimentation rate for the recovered section was 4.9 cm/ky. Poor weather and excessive shipheave curtailed drilling at this site, and the two holes were insufficient to generate a complete composite section. The site did, however, establish the feasibility of recovering the Pliocene sedimentary section on the Eirik Drift using the APC. The site extends the environmental record back to ~3.6 Ma.

The final site of Expedition 303 was **Site 1308**, a re-occupation of DSDP Site 609 (Fig. 1, Table 1). Shipboard and shore-based analytical techniques have changed considerably in the 21 years since this site was originally drilled (in 1983). DSDP Site 609 has been the focus of some of the most important developments in paleoclimate research in the last 15 years. Layers of ice rafted debris containing detrital carbonate (Heinrich events) were recognized at this site in the

early stages of their correlation to the Greenland ice core record (Bond et al., 1993). The 1500-y cycle in petrologic characteristics such as hematite stained grains and Icelandic glass has also been recognized at this site (Bond et al., 1999). The objective of the re-occupation of DSDP Site 609 was to recover a demonstrably complete sedimentary section that could be used to establish the isotopic characteristics of NADW, monitor the detrital layer stratigraphy of the central Atlantic IRD belt, and place this record into a well-constrained chronostratigraphy. The maximum penetration at Site 1308 was 341 mbsf, to the Upper Miocene at about 6 Ma. However, the complete composite section is limited to the top 190 mbsf, extending down to the Gauss Chronozone at ~2.6 Ma, the mean sedimentation rate since that time being ~7 cm/ky.

A total of 4656 m of high quality core were recovered from sites with mean sedimentation rates in the 5-18 cm/ky range. The sites were chosen in order to recover Pliocene and Quaternary records of millennial-scale environmental variability in terms of ice sheet-ocean interactions, deep circulation changes or sea surface conditions. The sites provide the requirements, including adequate sedimentation rates, for developing millennial-scale stratigraphies (through geomagnetic paleointensity, oxygen isotopes and regional environmental patterns).

## References

- Bodén, P. and J. Backman, 1996. A laminated sediment sequence from the northern North Atlantic Ocean and its climatic record. *Geology*, 24: 507-510.
- Bond, G., W. Broecker, S. Johnsen, J. McManus, L. Laberyie, J. Jouzel, and G. Bonani. 1993. Correlations between climate records from North Atlantic sediments and Greenland ice. *Nature*, 365: 143-147.
- Bond, G., W. Showers, M. Elliot, M. Evans, R. Lotti, I. Hajdas, G. Bonani, and S. Johnson. 1999. The North Atlantic's 1-2 kyr climate rhythm: relation to Heinrich Events, Dansgaard/Oeschger cycles and the Little Ice Age. In: *Mechanisms of millennial-scale global climate change.* (Webb et al., ed.) Geoph. Monograph Series, 112, 35-58.
- Hillaire-Marcel, C., A. De Vernal, G. Bilodeau, and G. Wu. 1994. Isotope stratigraphy, sedimentation rates, deep circulation, and carbonate events in the Labrador Sea during the last ~200 ka. *Can. J. Earth Sci.*, 31: 63-89.
- Raymo, M.E., D.W. Oppo, B.P. Flower, D.A. Hodell, J.F. McManus, K.A. Venz, K.F. Kleiven. 2004. McIntyre, Stability of North Atlantic water masses in face of pronounced climate variability during the Pleistocene. *Paleoceanography*, 19, PA2008, doi:10.1029/2003PA000921.
- Schmieder, F., T. von Dobeneck and U. Bleil. 2000. The Mid-Pleistocene climate transition as documented in the deep South Atlantic Ocean: Initiation, interim state and terminal event. *Earth and Planetary Science Letters*, 179: 539-549.
- Stoner, J.S., J.E.T. Channell and C. Hillaire-Marcel. 1995. Late Pleistocene relative geomagnetic paleointensity from the deep Labrador Sea: regional and global correlations. *Earth Planet. Sci. Lett.*, 134: 237-252.
- Stoner, J. S, J.E.T. Channell and C. Hillaire-Marcel. 1998. A 200 kyr geomagnetic stratigraphy for the Labrador Sea: Indirect correlation of the sediment record to SPECMAP. *Earth Planet. Sci. Lett.*, 159: 165-181.
- Stoner, J.S., J.E.T. Channell, C. Hillaire-Marcel, and C. Kissel. 2000. Geomagnetic paleo-intensity and environmental record from Labrador Sea Core MD95-2024: global marine sediment and ice core chronostratigraphy for the last 110 kyr. *Earth Planet. Sci. Lett.*, 183: 161-177.
- Toews, M.W. and D.J.W. Piper. 2002. Recurrence intervals of seismically triggered mass-transport deposits at Orphan Knoll continental margin off Newfoundland and Labrador. *Curr. Res. - Geol. Surv. Can.*, E17: 1-8.





## Chapter 9

# Summary and Conclusions

Paleoclimatic records (i.e., IRD, SST, DWT,  $\delta^{18}\text{O}$  records of global ice volume, paleoproductivity, and of deepwater ventilation) at North Atlantic Sites ODP 984 and DSDP 609 were generated with multicentennial-scale resolution for the Late Pliocene time interval 2.5-3.3 Ma and supplemented by evidence from neighbor Sites 907 and 610.

In testing the scenario of the onset of NHG, we find clear evidence for an interglacial intensification of North Atlantic THC from 2.95 to 2.82 Ma (MIS G17-G11), depicted by a 0.2-0.3‰ increase in benthic  $\delta^{13}\text{C}$ . The intensification of THC follows immediately an increase in the SSS gradient between Caribbean and East Pacific, reaching up to 0.9‰ and marking the final restriction of the CAS starting at 3 Ma. This process has warmed the northern North Atlantic by 2-3°C thus promoted the poleward heat transport to high latitudes by 2-3°C between 2.95-2.82 Ma, thus probably enhancing evaporation and moisture transport from to northern high latitude continents as proposed by the “snow-gun hypothesis” (Driscoll & Haug, 1998). The subsequent build-up of sea ice in the Arctic Ocean and of the Greenland ice-sheet resulted in a ~90-m sea-level drop during glacial stages MIS G16-G10 and G6, which has probably accentuated the final closure of the CAS.

Over the time period 2.5-3.1 Ma short-term climate variability displayed dominating 1300-, 950-, and 450-yr periodicities that come close to solar cycles characteristic of Holocene climate change. The same applies to selected interglacial stages prior and after the onset of NHG. However, the onset of NHG has led to a clear increase in *glacial* millennial-scale climate variability, and most interesting to a first occurrence of DO-style cycles. This result supports models of Paillard & Labeyrie (1994) and Rahmstorf (1996) suggesting a causal link between DO cycles and continental ice breakouts.

A major benthic faunal “turnover” occurred in the northern North Atlantic around 2.73 Ma. In particular, it includes a switch from benthic foraminifera taxa characteristic for high-nutrient fluxes to taxa characteristic for low and unstable nutrient input. This faunal change is interpreted as result in changes in the nutrient flux and/or increase in surface water stratification and seasonality.

During IODP Expedition 303, high-quality sediment cores were retrieved from the northern North Atlantic. Off the southern tip of Greenland, sediments at Site U1307 have sedimentation rates averaging 4.6 cm/kyr and contain a climatic record back to ~3.58 Ma. This sediment section will serve for future studies that may provide a first paleoclimatic record with 300-yr time resolution to unravel the role of Labrador Sea paleoceanography for the Late Pliocene onset of NHG.

## References

- Driscoll, N.W., and G.H. Haug, A short circuit in thermohaline circulation: A cause for Northern Hemisphere Glaciation?, *Science*, 282, 436-438, 1998.
- Paillard, D., and L. Labeyrie, Role of the thermohaline circulation in the abrupt warming after Heinrich events, *Nature*, 372, 162-164, 1994.
- Rahmstorf, S., On the freshwater forcing and transport of the Atlantic thermohaline circulation., *Climate dynamics*, 12, 799-811, 1996.



## Appendices



**Gretta BARTOLI**

Citizenship: French  
 Born on 22/12/77 at Montpellier  
 (France)

Christian-Albrechts-Universität  
 Institut für Geowissenschaften  
 Ludewig-Meyn-Str. 10  
 D-24118 Kiel

☎ +0049 (0) 431-880-2884

e-mail: gb@gpi.uni-kiel.de

**Present position:**

Since January 2002, PhD student at Kiel University, working on “*Short-term climate variability in the North Atlantic during the onset of northern hemisphere glaciation and the final closure of the Panamanian seaways, 3.3-2.5 Ma*”, supervised by Prof. M. Sarnthein and Dr M. Weinelt in the frame of the Research Unit “Ocean Gateways”.

**Research interests:**

- Foraminiferal Mg/Ca-paleothermometry
- Late Pliocene long-term and short-term climate variability
- Stable Isotope Stratigraphy
- Late Neogene paleoceanography in northern North Atlantic
- Variations in the strength of the Irminger Current and related poleward heat transport
- Impact of the closure of the Panama Isthmus on the climate evolution

**International conferences:**

- **EGS-EGU joint assembly**, Vienna, April 2005.

Poster: *Gateway-controlled paleoceanography of the subpolar North Atlantic and intensification of Northern Hemisphere Glaciation*, Weinelt, M., Bartoli, G., Sarnthein, M, Garbe-Schönberg, D., Steph, S., Erlenkeuser, H.

- **IODP/ICDP joint Colloquium**, Potsdam, March 2005.

Poster: *Millennial-scale Late Pliocene climate variability in the northern North Atlantic prior and after the onset of northern hemisphere glaciation*, Bartoli, G., Sarnthein, M., Weinelt, M., and Andersen, N.

- **ICP-VIII**, Biarritz, September 2004.

Poster: *Enhanced North Atlantic heat transport, Late Pliocene build-up of Greenland ice-sheet, and the final closure of Panama*, Bartoli, G., Weinelt, M., Sarnthein, M Garbe-Schönberg, D. Erlenkeuser, H, Lea D., and Kleiven, K. **Student poster Award** (13 winners out of 250).

- **ICP-VIII**, Biarritz, September 2004.

Poster: *Ca isotopes as a new SST-proxy for high northern latitudes: A multi-proxy comparison*, Kozdon, R., Eisenhauer, A., Sarnthein, M., Weinelt, M., Hippler, D., Millo, C. and Bartoli, G.

- **EU - Conference “Paleoclimate: reducing the uncertainties”**, July 2004, Utrecht.

Poster: *Assessment of Diagenetic Effects on Primary Isotopic Signals preserved in Foraminifera from a Paleo-Venting Site*, L. Lembke-Jene, R. Tiedemann, D. Nuernberg, G. Bartoli, B. Bader, W.-Chr. Dullo, N. Biebow, A. Derkachev.

- **37ème Congrès de la CIESM**, Barcelona, Spain, June 2004.

Talk: *Atmospheric inputs of dissolved inorganic phosphorus and silicium to NW Mediterranean oligotrophic coastal waters: theoretical impact on phytoplankton dynamics*, Migon, C., Bartoli, G., and Sandroni, V.

• **XVIe Rencontres de Blois “Challenges in Climate Sciences”**, Blois, France, May 2004.

Talk: *Late Pliocene climate crash and the final closure of Panama*, Bartoli, G., Sarnthein, M., Weinelt, M., Garbe-Schönberg, D. Erlenkeuser, H, and D. Lea.

- **Euroforum for Scientific Earth Drilling**, Bremen, March 2004.

Poster: *Enhanced North Atlantic Heat Transport, Late Pliocene Build-up of Greenland Ice Sheet, and the Final Closure of Panama*, Bartoli, G., Sarnthein, M., Weinelt, M., Garbe-Schönberg, D., Erlenkeuser, H., and D. Lea. **Third Place at the poster Award** (out of 133 posters presented).

- **EURESCO Conference 2003 “Achieving Climate Predictability using Paleoclimate Data”**, San Feliu de Guixols, Spain, October 2003.

Poster: *Late Pliocene increase in North Atlantic heat pump matches build-up of Greenland Ice Sheet*, Bartoli, G., Sarnthein, M., Weinelt, M., Garbe-Schönberg, D., and Erlenkeuser, H.

- **DMG Annual Meeting 2003**, Bochum, September 2003.

Poster: *Evolution of Late Pliocene heat transport to the high latitudes: High-Resolution  $\delta^{18}O$  and Mg/Ca-derived Temperature Records of ODP Core 984 (Bjorn Drift)*, Bartoli, G., Weinelt, M., Sarnthein, M., Lea, D., and Erlenkeuser, H.

- **EGS-AGU-EUG Joint Assembly**, Nice, April 2003.

Poster: *Evolution of Late Pliocene Heat Transport to High Latitudes: Centennial-Scale  $\delta^{18}O$  and Mg/Ca-based Temperature Records from ODP Site 984 (Bjorn Drift)*, Bartoli, G., Sarnthein, M., Weinelt, M., Lea, D., and Erlenkeuser, H.

Poster: *Late Pliocene Norwegian Greenland Overflow based on Benthic Stable Isotopes, Mg/Ca, and Foraminifera Assemblages at ODP Site 984*, Weinelt, M., Bartoli, G., and Erlenkeuser, H.

### List of publications:

- *Late Pliocene millennial-scale climate variability in the northern North Atlantic prior and after the onset of northern hemisphere glaciation*, Bartoli, G., Sarnthein, M., Weinelt, M. **submitted to Paleceanography.**

- *Abrupt reorganization of northern North Atlantic productivity provinces during the initiation of NHG*, Weinelt, M., Bartoli, G., Sarnthein, M., Erlenkeuser, H., **submitted to Mar. Micropal.**

- *High-precision Mg/Ca and Sr/Ca ratios of biogenic carbonate and seawater by simultaneous ICP-OES*, Garbe-Schönberg, D., Groeneveld, J., Bartoli, G., Sarnthein, M., and Dullo, C., **submitted to Geophys. Geochem. Geosys.**

- *Final closure of Panama and the onset of northern hemisphere glaciation*, Bartoli G., Sarnthein, M., Weinelt, M., Erlenkeuser, H., Garbe-Schönberg, D., Lea, D. W. **Earth and Planet. Sci. Lett.** in press.

- *IODP Expedition 303:North Atlantic Climate I*, Bartoli, G. and Romero, O. IODP/ICDP joint Colloquium, Potsdam 2005, **extended abstract in the conference Book of Abstract.**

- *North Atlantic climate: ice sheet–ocean atmosphere interactions on millennial timescales during the late Neogene–Quaternary using a paleointensity-assisted chronology for the North Atlantic*, Shipboard Scientific Party, 2005, **IODP Prel. Rept., 303.** <http://iodp.tamu.edu/publications/PR/303PR/303PR.PDF>.

- *Global Impact of the Panamanian Seaway Closure*, Schmittner, A., M. Sarnthein, H. Kinkel, G. Bartoli, T. Bickert, M. Crucifix, D. Crudeli, J. Groeneveld, F. Kösters, U. Mikolajewicz, C. Millo, J. Reimer, P. Schäfer, D. Schmidt, B. Schneider, M. Schulz, S. Steph, R. Tiedemann (2004) **EOS**, 85, 526.

- Cruise report: *The expedition ARKTIS XVIII/1 a, b of the Research Vessel “Polarstern” in 2002*, Lemke, P. and participants. **Berichte zur Polar und Meeresforschung 446 (2003).**

- *Atmospheric inputs of dissolved inorganic phosphorus and silicon to the coastal northwestern Mediterranean Sea: fluxes, variability and possible impact on phytoplankton dynamics*, Bartoli G., Migon, C., Lono, R., **Deep Sea Res. I**, in press.

- *Theoretical impact of atmospheric input of nutrients on the phytoplankton dynamic in North-Western Mediterranean Sea*, Bartoli, G., Master thesis at LOV, France, 2001.

### Research skills:

- Selection of Pliocene foraminifera species for analyses
- Stable isotopes for paleoceanographic use
- ICP-AES analyses for Mg, Sr and trace elements in marine carbonates
- Time series analysis: SPECTRUM and REDFIT, ANALYSERIES

- Spectrophotometry for analysis of phosphorus and silicium.
- Introduction to modeling of marine and freshwater ecosystems.

**Cruises experiences:**

- IODP Expedition 303, *Joides resolution*.
- PRV *Polarstern* RV ARK XVIII/1a.

**Academic career:**

- Since January 2002: PhD student at Kiel University.
- February-September 2001: Master degree thesis at the L.O.V (Laboratory of Oceanography of Villefranche-sur-mer) with Christophe MIGON, associate professor (migon@obs-vlfr.fr). Rainwaters and aerosols sampling at the coastal site of Cap Ferrat (France). Phosphorus and silicon analysis with a spectrophotometer and aerosol carbon and nitrogen analysis with a CHN analyser.
- 2000/2001: "DEA" (Diploma in advanced studies, equivalent to master degree) in "Environmental Marine Sciences" option **Biogeochemistry** at the University of Aix-Marseille (France), with distinction.
- 1995-2000: Studies of **Marine Biology** at the University of Caen (France).

**Professional / Research experience:**

- End 2002: set-up of a laboratory for sample preparation for minor and trace elements analysis in marine carbonates at the Leibniz-Labor (Kiel university).
- Spring 2002: guest student at University of California, Santa Barbara, by David Lea, for learning the sample preparation technique for minor and trace elements analysis in foraminifera tests.
- Summer 2000: Realization of a steady-state planktonic food web model of the Lake Biwa applying the inverse analysis method (LBEM of La Rochelle).
- April-May 2000: training course at the Natural Regional Park of Lorraine (France). Fauna and flora inventory, GIS mapping, trophic-state study, and ecological analysis.
- October-December 1999: chemistry teaching to first-year Biology students at Caen University.

**Spoken languages:** French (mother tongue), English (good working knowledge), German (basic knowledge).





## **Eidesstattliche Erklärung**

Hiermit erkläre ich, daß die Abhandlung – abgesehen von der Beratung durch meine Betreuer Prof. Michael Sarnthein und Dr. Mara Weinelt – nach Inhalt und Form meine eigene Arbeit ist.

Ich habe diese Arbeit, ganz oder zum Teil, an keiner anderen Stelle im Rahmen eines Prüfungsverfahrens vorgelegt, veröffentlicht oder zur Veröffentlichung eingereicht.

Kiel, den 25 Mai 2005,

Gretta Bartoli